The Regulation of Cardiac Cell Proliferation and Survival During Vertebrate Development

Sarah Catherine Goetz

A dissertation submitted to the faculty of the University of North Carolina at Chapel Hill in partial fulfillment of the requirements for the degree of Doctor of Philosophy in the Department of Biology

Chapel Hill
2007

Approved by:

Frank L. Conlon

Robert Goldstein

Victoria Bautch

Stephen Crews

Suk-Won Jin

ABSTRACT

SARAH C. GOETZ: The Regulation of Cardiac Cell Proliferation and Survival During Vertebrate Development
(Under the direction of Frank L. Conlon)

The formation of organs during development requires that cell proliferation occur in a coordinated fashion. Furthermore, mis-regulation of the cell cycle during adulthood is associated with cancer and other human diseases. The molecular pathways that govern the eukaryotic cell cycle have been extensively studied, however the mechanisms by which the cell cycle is regulated in a tissue specific manner during development are not well understood. In this work, we explore the regulation of cell proliferation within the developing heart, as well as the maintenance of proliferating cardiac progenitor cells.

The T-box transcription factor TBX5 is expressed within the developing heart and is required for heart morphogenesis in vertebrates. Additionally, mutations to TBX5 have been associated with the human congenital heart defect Holt-Oram syndrome. Despite the evolutionarily conserved role for TBX5 in heart development, the precise cellular requirement for TBX5 has not been defined. We show that one of the earliest defects in the TBX5-depleted *Xenopus* embryos is a reduction in cardiac cell number due to a decrease in mitotic index. We have further demonstrated that TBX5 is both necessary and sufficient to control cardiac cell cycle progression, and that depleting TBX5 leads to arrest in late G1 or

early S-phase of the cell cycle. In this way, TBX5 is required to establish cardiac morphology during development.

Finally we have identified a requirement for the tyrosine phosphatase SHP-2 in the maintenance of proliferating cardiac progenitor cells downstream of FGF signaling. These studies show that SHP-2 is required for the maintenance of cardiac precursors, and that in the absence of SHP-2 activity, there is an increase in programmed cell death specifically in the cardiac precursor cells and pharyngeal mesoderm. When SHP-2 activity is inhibited at a later stage, when many cells have exited the cell cycle, cardiac differentation is able to proceed, however the number of proliferating cells within the heart is substantially reduced. These data suggest a specific requirement for SHP-2 in the survival of proliferating cardiac progenitor cells.

ACKNOWLEDGEMENTS

There are a number of people who have made the process of getting a Ph.D. both rewarding and enjoyable. First, I'd like to thank the current members of the Conlon lab: Yvette Langdon, Elizabeth Mandel, Kathleen Christine, Erika Paden, Chris Showell, and Jackie Swanik. They have been a wonderful group of people to work with both personally and scientifically. I feel truly lucky to have had such terrific lab mates to work with. In addition, former lab members Daniel Brown and Shauna Vasilatos made important contributions to the work with TBX5. Two former undergraduates who worked with me, Morgan Von Drehle and Shruti Nagaraj, both made important contributions to my work by helping to characterize the drug inhibitors and the heart field explants.

I would also like to thank the members of my committee: Bob Goldstein, Vicki Bautch, Steve Crews, and Suk-Won Jin for the years of constructive feedback they have given me that tremendously improved the quality of my work. In addition, I thank Bob Duronio, Larysa Pevny, Da-Zhi Wang, Mark Majesky, and Mark Peifer for sharing expertise and reagents, as well as for their critical feedback throughout this project.

My parents, Michael and Suzanne Goetz have also given me a tremendous amount of support over the years, and have made many sacrifices for me to be where I am. They have always given me their love and encoragement, and taught me the value of hard work.

I also owe a big thank you to my husband, David Christian. David has been my best friend and my biggest supporter since our sophomore year in college. Over the years, he has

shown an incredible amount of patience and flexibility, and always seems to know what to say or do to make me feel better when I'm having a tough time. I can't imagine having gotten through all of this without him.

Finally, the person to whom I probably owe the most thanks is my advisor, Frank Conlon. Frank has an impressive ability to be optimistic and positive the vast majority of the time. This quality has been very gratifying during the times when experiments have gone well and we produced interesting data, but has really proven crucial during the times when my project has run into difficulties. Frank's ability to be encouraging and to help me find a way forward in the face of problems and obstacles has made a huge difference in my ability to succeed in graduate school.

TABLE OF CONTENTS

LIST OF FIGURES

ABBREVIATIONS

ANF	Atrial naturitic factor
ARID	A-rich interacting domain
AVC	Atrio-ventricular canal
BMP	Bone morphogenic protein
CDK	Cyclin-dependent kinase
DMSO	Dimethyl sulfoxide
E	Mouse embryonic day
FGF	Fibroblast growth factor
G1	Gap phase 1
G2	Gap phase 2
GST	Glutathione S transferase
HH	Hamberger-Hamilton stage
HOS	Holt-Oram Syndrome
M	Mitosis
MAPK	Mitogen activated protein kinase
MCM	Mini-chromosome maintenance
MHC	Myosin heavy chain
MO	Morpholino
OFT	Outflow tract
ORC	Origin recognition complex
PCNA	Proliferating cell nuclear antigen

PTP	Protein tyrosine phosphatase
RB	Retinoblastoma protein
RC	Replication complex
RTK	Receptor tyrosine kinase
RT-PCR	Reverse transcriptase polymerase chain reaction
S	DNA synthesis phase
SHP	Src-homology containing protein tyrosine phosphatase
SV	Sinus venosus
TBX	T-box
TEM	Transmission electron microscopy
TMY	Tropomyosin
TNIC	Cardiac troponin I
XBRA	Xenopus brachyury

CHAPTER 1

Introduction

During development, numerous processes, such as cell fate specification, proliferation, migration, and cell death, must occur in a coordinated fashion. The failure of any of these processes during embryogenesis can lead to developmental abnormalities, while the mis-regulation of many of the same pathways in adulthood is associated with disorders such as cancer. Thus, understanding the cellular and molecular mechanisms of development provides crucial insight for human health.

The mechanisms by which cell proliferation is regulated have been extensively studied in single celled eukaryotes such as yeast, as well as in cultured cells. These studies have provided numerous valuable insights into how the different stages of the cell cycle are regulated, as well as the mechanisms by which cells exit the cell cycle and cease proliferating. Comparatively less is known about developmental regulation of cell proliferation, and especially about how this is achieved in a tissue-specific manner. A primary focus of my work has been on characterizing factors that promote cell cycle progression and cell survival specifically within the developing heart.

General Mechanisms of Cell Cycle Control

The eukaryotic cell cycle is divided into four basic stages: M-phase in which mitosis occurs, S-phase in which DNA is synthesized for the next round of cell division, and two gap phases- G1, which proceeds S-phase, and G2, between S-phase and M-phase (Fig. 1.1). The gap phases play regulatory roles, with the G1 restriction point acting to limit the rate at which cells proceed through the cell cycle, and ensure that cells have undergone cytokinesis prior to the initiation of DNA synthesis in S phase, while the G2 checkpoint assures that DNA is fully replicated prior to the onset of M-phase (Nurse, 1997).

The progression from one phase of the cell cycle to another is regulated primarily by the activity of cyclins and associated cyclin dependent kinases (CDK) (Sherr, 1993). Cdks regulate the major transitions of the cell cycle by phosphorylation of their target proteins. The activity of Cdks is regulated in turn through their association with cyclins, which are present only at specific stages of the cell cycle. To become catalytically active, Cdks first associate with a cyclin. This in turn enables phosphorylation of the Cdk, which allows for the activation of its catalytic domain through conformational changes induced by the addition of the phosphate group (De Bondt et al., 1993; Russo et al., 1996). During G1, progression of cells to S phase is mediated primarily by D, E, and A cyclins and their associated Cdks (Ekholm and Reed, 2000; Sherr, 1993). Cyclin D/Cdk4/6 and Cyclin E/Cdk2 promote progression through the cell cycle primarily by acting sequentially to phosphorylate and inactivate retinoblastoma protein (Rb) (Harbour et al., 1999). Active Rb acts as a transcriptional repressor, inhibiting expression of other factors required for cell cycle progression (Zhang et al., 2000). In addition, Rb also binds to and sequesters members of the E2F family of transcription factors, and prevents their activating downstream targets that

function to promote cell cycle progression (Bagchi et al., 1991; Chellappan et al., 1991; Hiebert et al., 1992) (Fig. 1.2).

In addition to promoting entry into S-phase by inhibiting Rb, the G1 cyclin/Cdk complexes also promote the synthesis and activation of the licensing factors required for replication of the DNA during S-phase (Blow, 2001; D'Urso et al., 1990). Licensing occurs when the pre-replication complexes (RC) consisting of the origin recognition complex (ORC), Cdc6, Cdt1, and mini chromosome maintenance (MCM) proteins are loading onto the DNA. The complexes are then activated by G1 cyclin/Cdk complexes including Cyclin E/Cdk2, allowing S phase of the cell cycle to begin (Blow, 2001; Takisawa et al., 2000). Replication of the DNA once and only once during each S phase is assured by the displacement of the MCM proteins from the pre-RC after origin firing, and also by subsequent activity of S-phase CDKs in mediating the displacement and degradation of the other pre-RC components (Nguyen et al., 2001).

In order to assure that faithful replication of the DNA has occurred prior to mitosis, cells undergo a DNA damage checkpoint in G1 prior to entry into S phase, and again in G2 prior to M phase of the cell cycle (Elledge, 1996). In this way, the gap phases of the cell cycle provide critical mechanisms for regulating both the length of the cell cycle and the frequency with which cells proliferate, and also assure that both daughter cells receive an intact genome. Cyclin/CDK complexes also play key roles in these DNA replication checkpoints. In response to DNA damage detected during G1, p53 is activated, and in turn activates transcription of p21, a cyclin dependent kinase inhibitor (CKI), which binds to CDKs, including Cdk4, and inhibits their activity (Elledge, 1996). Thus cells are prevented from entering S phase in the presence of DNA damage (Fig. 1.2). During S phase, DNA

replication can be slowed or stopped in response to DNA damage to allow time for repair to take place. A final checkpoint during M phase assures that chromosomes are properly segregated to daughter cells prior to cytokinesis (Reviewed by (Rudner and Murray, 1996)).

Cell Cycle Regulation During Development

Much of what is known about the regulation of the cell cycle and DNA synthesis has been studied primarily in yeast, mammalian cell culture, or in cell-free systems using *Xenopus* oocyte extracts (Chellappan et al., 1991; Cross, 1988; Lohka et al., 1988; Murray and Kirschner, 1989; Murray et al., 1989; Nurse, 1975). During embryonic development, however, the cell cycle is modified by extracellular signaling events, with some cell types exiting the cell cycle early in development, while others proliferate extensively up to adulthood. Studies to address the *in vivo* requirements for important cell cycle regulators during development have initially been carried out in *Drosophila* (Follette and O'Farrell, 1997; Lehner and O'Farrell, 1990). *Drosophila* provides and excellent model system for studying the developmental requirements for cell cycle regulators, as the *Drosophila* embryo initially undergoes synchronous rounds of DNA replication followed by nuclear cleavage, while the cytoplasm remains as a syncytium. A G2 phase is then added once the embryo begins to cellularize after 13 rounds of replication, and later in development, a G1 phase is added (Orr-Weaver, 1994). This increasing complexity of the cell cycle over the course of development made it possible to assess how cyclin/Cdk complexes are differentially regulated with the addition of the gap phases.

Cyclins A and E, which were shown to promote cell cycle progression in yeast and in *Xenopus* oocyte extracts (Booher et al., 1989; Koff et al., 1991; Murray and Kirschner, 1989;

Murray et al., 1989), are both necessary and sufficient to trigger S phase in *Drosophila* embryos, and are thereby essential for embryonic development (Knoblich et al., 1994; Lehner and O'Farrell, 1990). Both Cyclin A and E are regulated differently at distinct stages of development. Cyclin A is expressed at fairly low levels at syncytial stages, with expression increasing with the addition of the G2 phase (Whitfield et al., 1990). Cyclin E is expressed constitutively during the early stages of *Drosophila* development, when the embryo undergoes alternating rounds of S phase followed by nuclear cleavage without intervening gap phases (Richardson et al., 1993). Upon the addition of G1 phase following cellularization, Cyclin E expression is downregulated (Duronio and O'Farrell, 1994; Knoblich et al., 1994), and its activity is further restricted by the expression of cell cycle inhibitors such as *Decapo*, the *Drosophila* homolog of vertebrate p27 (de Nooij et al., 1996; Lane et al., 1996). Collectively, these early studies of cell cycle control in *Drosophila* demonstrated the critical role of cell proliferation in normal embryogenesis.

More recently, studies have been undertaken in the mouse to determine the requirements for various cell cycle regulators during vertebrate embryonic development (Reviewed by (Sherr and Roberts, 2004)). Surprisingly, despite the key role that cyclin/CDK complexes play during cell cycle progression, individual cyclins and CDKs largely do not appear to be required for embryonic development in mammals and other vertebrates (Berthet et al., 2003; Geng et al., 2003; Kozar et al., 2004; Malumbres et al., 2004). Targeted deletion in mice of Cyclin A2, which is required for both G1/S and G2/M transition, does result in early embryonic lethality. Embryos are able to develop until mouse embryonic day (E) 5.5-6.5, however this is most likely due to the presence of cyclin A2

protein translated from maternal mRNA stores, which is depleted by E6.5 (Murphy et al., 1997).

In contrast to Cyclin A2, deletion of the G1 cyclins, Cyclin E1 and E2, does not result in early embryonic lethality or impaired cell cycle progression (Geng et al., 2003). This is in contrast to *Drosophila*, where Cyclin E was required for progression to S phase, and its absence results in embryonic lethality. Additionally, knockout of all three mammalian D Cyclins, Cyclins D1, D2, and D3, failed to cause widespread proliferation defects in mouse embryos (Kozar et al., 2004). Triple knockout formed most tissues normally, and cells derived from these embryos were able to enter S phase. The embryos display cardiac abnormalities, however, which likely results in the observed lethality between E13.5 and E15.5 (Kozar et al., 2004). Similarly, mice lacking both Cdk4 and Cdk6, which partner with the D Cyclins to promote the initial phosphorylation of Rb, are viable until late stages of gestation. Additionally, deletion of Cdk2 the binding partner of the E and A cyclins, does not result in major cell cycle defects *in vivo* (Ortega et al., 2003). Only the combined knockout of Cdk2 and Cdk4 has been shown to result in defects in cell cycle progression and loss of Rb phosphorylation *in vivo*. However, these embryos survive until E15, and die primarily due to cardiac defects (Berthet et al., 2006).

Together, these data suggest that a high level of functional compensation can occur between the different Cyclins and Cdks. The lack of a severe phenotype in the Cdk4/Cdk6 double knockout or the Cyclin D triple knockout suggests that Cdk2/Cyclin E can compensate for Cdk4/6/Cyclin D complexes to promote S phase entry, and vice versa. Functional redundancy between the G1 Cyclin/Cdks is further supported by the finding that a knock-in of Cyclin E into the Cyclin D1 locus is able to rescue the tissue-specific defects

resulting from the Cyclin D1 knockout (Geng et al., 1999). The functional redundancy between the various cyclin/Cdk complexes is not total, however, as other complexes cannot fully compensate for the loss of both Cdk2 and Cdk4. However, the fact that the embryos survive until E15, and there are fairly high levels of mitosis and Rb phosphorylation until mid-gestation, suggests that some degree of compensation occurs (Berthet et al., 2006).

The unexpected degree of functional redundancy between the Cyclin/Cdk complexes *in vivo* compared with what has been observed in cell culture underscores the importance of understanding how the cell cycle is regulated during development. Of particular interest is that, while knockouts of individual or various combinations of Cyclins and Cdks do not cause massive defects in cell proliferation throughout the embryo, deletion of each of these genes results in subtle and tissue specific defects. For example, deletion of Cdk4 affects primarily pancreatic islet cells (Rane et al., 1999), while the loss of Cyclin E results in a failure of endoreplication in trophoblast giant cells (Geng et al., 2003), and deletion of Cyclins D1, D2, and D3 primarily affects heart and hematopoetic development (Kozar et al., 2004). This suggests that the relative roles of these cyclin/Cdk complexes, despite their broad expression patterns, might be somewhat tissue specific. Thus, the examination of how the cell cycle is regulated in a tissue specific manner during development can provide important insights into organogenesis and is in need of further study.

Overview of Vertebrate Heart Formation

In order to explore the regulation of cell proliferation during cardiac development, and the role of this process in ensuring the proper formation of the heart, it is necessary to give a brief overview of heart development in vertebrates. In all vertebrate species, the heart is

among the first organs to form, and the basic processes of cardiac development are largely conserved across vertebrate species (Fishman and Chien, 1997). Two bilateral populations of cells on either side of the midline of the embryo are induced into the cardiac lineage during gastrulation by signals emanating from the anterior endoderm underlying the anterior lateral plate mesoderm, and from the organizer (Jacobson and Duncan, 1968; Nascone and Mercola, 1995; Sater and Jacobson, 1989; Schultheiss et al., 1995). The position of cardiac cells along the anterior-posterior axis, which will ultimately determine which cardiac chamber they contribute to, is determined in part by the order in which they pass through the blastopore or primitive streak (Garcia-Martinez and Schoenwolf, 1993). Additionally, the anterior portions of the heart tube, including the outflow tract and right ventricle, are contributed by the anterior heart field (Cai et al., 2003; Waldo et al., 2001). The cells of the anterior heart field reside in the splanchic mesoderm anterior to the primary cardiac mesoderm, and express the marker *islet1 (isl1*) (Cai et al., 2003).

Following induction, the two populations of cardiac precursors migrate to the midline of the embryo where they fuse and form the linear heart tube composed of both an outer myocardial layer which will form the beating heart muscle, and an inner endocardial layer, which will form the endothelial layer of the heart contiguous with the vasculature (Reviewed by (Fishman and Chien, 1997; Harvey, 2002)). Once the bilaminar heart tube has formed, the heart begins the process of rightward looping, which will ultimately generate the distinct chambers of the heart (Taber et al., 1995)- two atria and two ventricles in mammals and birds, while amphibians have a three chambered heart with a single ventricle (Fig. 1.3).

During cardiac looping, the ventral portion of the heart tube rotates to form the outer curvature of the heart, with the dorsal side becoming the inner curvature (Christoffels et al.,

2000a). The chambers of the myocardium form out of the outer curvature through a process of rapid cell proliferation and increase in cell size (Soufan et al., 2006), while the cells of the inner curvature become the non chamber myocardium of the atrio-ventricular canal (AVC) and outflow tract (OFT), which will play a role in the alignment and septation of the cardiac chambers (Christoffels et al., 2000a).

The early patterning of the myocardium (ie, the formation of the chamber vs. non chamber myocardium) is established, in part, by differential expression of cardiac transcription factors. The T-box transcription factor *Tbx5* is expressed in the atria, and left ventricle of mammals, and in the common ventricle of amphibians (Bruneau et al., 1999; Chapman et al., 1996). TBX5 and the homeobox transcription factor NKX2.5 have been shown to synergistically interact to activate transcription of *Atrial naturitic factor (ANF)* (Bruneau et al., 2001b; Hiroi et al., 2001), and each of these transcription factors is required for expression of *ANF in vivo* (Bruneau et al., 2001b; Lyons et al., 1995; Tanaka et al., 1999). *ANF* marks the future chamber myocardium during embryonic development, and is excluded from non-chamber myocardium, such as the AVC (Christoffels et al., 2000a). ANF expression in the AVC is specifically inhibited by the transcriptional repressor TBX2, which competes with TBX5 to bind the T-Box- binding-element in the ANF promoter (Habets et al., 2002). *Tbx2* is expressed in a pattern complementary to that of ANF- expressed in the AVC and OFT, and is excluded from the chamber myocardium (Habets et al., 2002). Within the chamber myocardium, *Tbx2* is repressed by TBX20 (Cai et al., 2005; Singh et al., 2005; Stennard et al., 2005), another T-box transcription factor that promotes formation of cardiac chambers (Fig. 1.4).

Other chamber restricted cardiac transcription factors include Hand1 and Hand2 (also known as eHand and dHand, respectively). In mammals, Hand1 and Hand2 are restricted to the left and right ventricles, respectively but are expressed ubiquitously in avian and amphibian hearts (Srivastava et al., 1995; Srivastava et al., 1997). The Iroquois homeobox genes (*Irx*) are also expressed in specific cardiac chamber primoridia (Christoffels et al., 2000b). The mechanisms by which these chamber-specific transcription factors promote cardiac morphogenesis are just beginning to be understood. Hand1, Hand2, and Irx4 have all been shown to be required for proper heart development, and for the expression of chamber-specific markers (Bruneau et al., 2001a; Riley et al., 1998; Yamagishi et al., 2001). However their precise cellular functions remain unknown. The polarity of the heart tube seen through the differential expression patterns of these and other cardiac genes is later reinforced by changes in cell proliferation, polarity, and size (Christoffels et al., 2000b). The roles of some of these transcription factors in cell proliferation will be further explored below.

Regulation of Cell Proliferation During Early Cardiac Development

Cell proliferation plays a key role in heart formation. Following the initial induction of cardiac precursor cells in vertebrate embryos, these cells undergo a period of rapid proliferation, corresponding with E8 in the mouse (Alsan and Schultheiss, 2002; Pasumarthi and Field, 2002; Schultheiss et al., 1995). Proliferation within the heart field then transiently slows, followed by a second peak in proliferation at E11 (Pasumarthi and Field, 2002). However, the molecular mechanisms regulating these waves of proliferation within the precardiac mesoderm are poorly understood.

This early period of proliferation in the precardiac mesoderm corresponds with the close association between the endoderm and the cardiac progenitor population. During this time, cardiac cells continue to be exposed to a variety of growth factors, including fibroblast growth factors (FGFs) and bone morphogenic proteins (BMPs). In particular, *Fgf8*, expressed in the endoderm contacting the precardiac mesoderm in chicks, is required for the maintenance of *Nkx2.5* and *Mef2c* expression (Alsan and Schultheiss, 2002). FGF signaling has also been implicated in cardiac cell proliferation specifically during this developmental window, with several studies demonstrating that FGFs 1, 2 and 4, which are expressed beginning at gastrulation (Hamberger-Hamilton stage 5 in chick) in the endoderm underlying the heart-forming field, are required for cardiac cell proliferation in explants of the precardiac mesoderm (Sugi et al., 1993; Zhu et al., 1999; Zhu et al., 1996). Moreover, a retroviral vector encoding a dominant negative form of FGF receptor 1 (FGFR1) resulted in reduced cardiac cell proliferation when infected at day 3 and assessed at day 7 of chick development, demonstrating a requirement for FGF signaling in cardiac cell proliferation *in vivo* later in heart development. In contrast, no effect on cardiac cell proliferation was observed when hearts were infected at day 7 and observed at day 14 (Mima et al., 1995). Together these data suggest a role for FGF signaling in regulating the high levels of cardiac cell proliferation observed during the early stages of cardiac migration, heart tube formation, and cardiac looping (Pasumarthi and Field, 2002). Moreover, the reduction in cardiac proliferation that occurs after stage 24 in chick (approx. E12 in mouse), corresponds closely with reduced expression of FGFs within the myocardium (Zhu et al., 1996).

BMPs are also present in the early heart field and myocardium during the same developmental window as FGFs. Together with FGF signaling, BMP signaling also plays a

role in the induction and maintenance of early cardiac progenitor cells (Lough and Sugi, 2000). BMP2, expressed in the anterior endoderm, is required for the induction of cardiac progenitors in early heartfield explants (Schultheiss et al., 1997), and together with FGF4, is sufficient to induce non-cardiac mesoderm to produce heart tissue (Lough et al., 1996). Recent evidence also suggests that FGF/MAPK signaling may counterbalance BMP signaling *in vivo*. Smad1 is a key effector of the BMP pathway that is activated by phosphorylation in response to BMP signaling. Smad1 then translocates to the nucleus where it activates transcription of downstream targets of the BMP pathway. Smad1 is also phophorylated by MAPK within the linker domain connecting the DNA binding and membrane receptor binding domains. This MAPK-mediated phosphorylation restricts Smad1 activity by promoting its recognition by the ubiquitin ligase Smurf1. Subsequently, Smad1 is prevented from entering the nucleus, and targeted for degradation by the proteasome (Sapkota et al., 2007). Thus, FGF/MAPK signaling can act to negatively regulate BMP signaling in certain cellular contexts.

BMP signaling downstream of *Gata6* also appears to be required after the initial induction of cardiac progenitors for the maintenance of early cardiac genes, including *Nkx2.5* (Peterkin et al., 2003). Later in development, BMPs function to promote the proliferation of the myocardium, as mice lacking BMP receptor 1A exhibit a thin myocardial wall (Gaussin et al., 2002), while mice lacking the BMP antagonist *Noggin* display hyperplastic growth of the ventricular myocardium (Choi et al., 2007).

Proliferation and Cardiac Morphogenesis

In spite of the reduction in cell proliferation that occurs during cardiac chamber formation and remodeling, cell proliferation plays a critical role throughout the process of heart morphogenesis. The initially high levels of DNA synthesis observed in the early pre-cardiac mesoderm and myocardium are thought to be important both for the expansion and segmentation of the heart tube along its anterior-posterior axis, as well as for the formation of the cardiac chambers (Christoffels et al., 2000a; Soufan et al., 2006).

Recent studies of the basic-helix-loop-helix transcription factor Hand1 underscore the importance of proper regulation of the cardiac cell cycle in heart morphogenesis. Loss of function and over-expression studies support a role for Hand 1 in promoting the proliferation of cardiac progenitor cells prior to terminal differentiation (McFadden et al., 2005; Riley et al., 1998; Risebro et al., 2006). Deletion of Hand1 from the developing heart results in shortening of the outflow tract as well as hypoplasia of the right ventricle, resulting in the formation of an unlooped heart tube (Riley et al., 1998). In contrast, over-expression of Hand1 within the developing heart tube has the opposite effect where the outflow tract is lengthened due to increased cell proliferation, resulting in abnormal cardiac looping (Risebro et al., 2006). Thus, the proliferation of cardiac precursor cells plays a role in establishing the correct length of the early heart tube, thereby contributing to the process of cardiac looping.

In addition to playing a crucial role in establishing the length of the heart tube, increased levels of cell proliferation are observed in the presumptive chamber myocardium of the atria and ventricles, as compared with the non-chamber myocardium of the OFT and AVC (Christoffels et al., 2000a). The mechanisms by which cell proliferation is

differentially regulated between the chamber myocardium and non-chamber myocardium are not well characterized, however some recent studies have begun to elucidate this process.

The early cardiac chambers of the vertebrate heart are initially formed by increased levels of proliferation in the presumptive chamber myocardium compared with non-chamber myocardium of the heart tube. This results in the "ballooning" out of the chamber myocardium (Christoffels et al., 2000a; Soufan et al., 2006). Prior to this expansion, chambers are specified in part by the activity of cardiac T-Box transcription factors. *Tbx5* exhibits a graded expression pattern within the heart tube, with the highest levels of expression seen in the future atria and left ventricle (common ventricle in amphibians) (Christoffels et al., 2000a; Horb and Thomsen, 1999), while *Tbx20* is expressed throughout the developing myocardium (Brown et al., 2003; Iio et al., 2001; Kraus et al., 2001). These two transcription factors promote the formation of the chamber myocardium in concert with NKX2.5 by promoting expression of chamber-specific genes. In the non-chamber myocardium, the activity of TBX5 and TBX20 is opposed by the transcriptional repressors TBX2 and TBX3 (Christoffels et al., 2004), which are thought to compete for binding to NKX2.5 (Habets et al., 2002). Furthermore, TBX20 has been shown to repress *Tbx2* expression within the chamber myocardium: in the absence of TBX20, *Tbx2* expression is increased throughout the heart tube (Cai et al., 2005). Interestingly, TBX2 has been shown to repress transcription of *N-myc*, a protein required for G1/S transition in cardiac and other cell types (Moens et al., 1993). Deletion of *Tbx20* thereby results in decreased expression of *N-myc* and hypoplasia of the heart and a failure of cardiac morphogenesis (Cai et al., 2005). These data support a model of chamber formation wherein, cell proliferation is maintained at low levels in the non-chamber myocardium, while high levels of proliferation are promoted

in the chamber myocardium, either by repressing the activity of factors that inhibit cell cycle progression, or by directly promoting cell cycle progression (Fig. 1.4).

In addition to a role in chamber formation, cardiac cell proliferation is also important for the remodeling of the ventricles to distinguish the compact and trabecular myocardium. Remodeling of the ventricles begins at the end of the cardiac looping stage (E10.5 in mouse, HH stage 18 in chick, and Niewkoop and Faber stage 37 in *Xenopus*). The trabeculae of the ventricle are finger-like bundles of cardiomyoctyes that project into the chamber of the ventricle by about E10.5 in mouse. In contrast, the compact myocardium consists of cardiac myocytes that are more densely organized. In early embryonic heart function, the trabecular myocardium provides most of the contractile force, while later in heart development this role shifts to the compact myocardium (Sedmera and Thomas, 1996). In addition to distinct cellular organization, the two myocardial layers also differ in their mitotic activity, with the compact myocardium being more highly proliferative, thereby driving the growth of the embryonic heart, and the trabecular myocardium proliferating at a much lower rate. The mitotic index (MI) of the trabecular layer peaks at mouse E10.5, while in the compact layer, the MI peaks between E9.5 and E11.5 and gradually declines (Toyoda et al., 2003).

The fate of ventricular cardiomyocytes to become either compact or trabecular myocardium appears to be governed, at least in part, by signals emanating from the epicardium (Kang and Sucov, 2005; Lavine et al., 2005; Pennisi et al., 2003) and endocardium respectively (Gassmann et al., 1995; Kang and Sucov, 2005; Lee et al., 1995; Meyer and Birchmeier, 1995). While the exact nature of the signal from the epicardium that patterns the compact myocardium is unknown (Kang and Sucov, 2005), the growth factor neuregulin plays a critical role in the outgrowth of the trabecular myocardium (Gassmann et

al., 1995; Lee et al., 1995; Meyer and Birchmeier, 1995). Once this patterning is established, it is reinforced by the differential levels of proliferation observed between the compact and trabecular myocardium. Proliferation in the compact myocardium is promoted primarily through FGF signaling downstream of retinoic acid from the epicardium (Lavine et al., 2005). Recently, several transcription factors have been identified that play crucial roles in cardiac morphogenesis by negatively regulating proliferation in the trabecular myocardium.

The gene *jumonji* (jmj), which encodes a member of the AT-rich interaction domain (ARID) family of transcription factors, was found to negatively regulate the cell cycle with over proliferation observed in hearts of embryos lacking *jmj* (Takeuchi et al., 1999). The timing of *jmj* expression in trabecular and compact myocardium of the ventricle matches the time points when each begin to reduce their respective MI (Toyoda et al., 2003). JMJ has been shown to function in part by repressing cyclin D1 expression in the trabecular myocardium (Toyoda et al., 2003). JMJ also physically interacts both with NKX2.5 and GATA4. This results in repression of *ANF* in the AVC (Kim et al., 2004), suggesting that JMJ plays a role in chamber formation beyond its function in regulating cell cycle progression.

Other transcription factors that act to restrict cardiac cell proliferation within the ventricular trabeculae include FoxP1, a member of the winged helix family of transcription factors (Wang et al., 2004), and HOP1, an unusual homeobox-containing protein (Chen et al., 2002; Shin et al., 2002). An increase in cell proliferation in the trabecular zone of *Foxp1* null embryos has been observed, however, *Foxp1* is expressed primarily in the compact myocardium and the mechanism by which Foxp1 acts to restrict proliferation in the trabeculae has not been established (Wang et al., 2004). The hearts of HOP1 null mice

exhibit thickened ventricular walls in comparison with wild-type littermates, due primarily to an increase in cell number. HOP1 appears to be expressed primarily within the trabecular myocardium of the ventricle, and was shown to physically interact with Serum Response Factor (SRF). One molecular function of HOP1 is to antagonize the activity of SRF (Chen et al., 2002; Shin et al., 2002). Again, the exact molecular mechanism by which HOP1 acts to inhibit cardiac cell cycle progression is not yet known. Thus, analysis of how tissue-specific transcription factors interact with, and regulate the cell cycle machinery during development is crucial to our understanding of how specific organs are patterned, and achieve their required size and function.

In addition to differential rates of proliferation within the myocardium, recent analysis suggests that the orientation of cell divisions plays an important role in cardiac morphogenesis. Retrospective clonal analysis of the developing mammalian heart has revealed two distinct phases of myocardial proliferation. In the first phase, which corresponds to the formation and elongation of the heart tube earlier in development (prior to E8.5), descendents of individual labeled cells are observed to disperse over fairly long ranges, and always in along the arterio-venous axis. Thus, this phase is termed the dispersive phase (Meilhac et al., 2003). In the second phase, which begins at or around E8.5, clonal cells form larger clusters and remain adjacent. This latter phase has been termed the coherent phase of growth, and further analysis revealed that coherent clones have a distinct orientation of growth that corresponds with the chamber in which they reside (Meilhac et al., 2003). For example, clones in the outflow tract take on a linear anterior-posterior orientation, while clones in the left ventricle tend to radiate out away from the AVC (Meilhac et al., 2004; Meilhac et al., 2003). This work provides evidence that the orientation of cell proliferation,

as well as the rate of proliferation, plays a critical role in cardiac morphogenesis. In further support of this, several zebrafish mutants have been identified that have severe cardiac abnormalities due to the failure of cardiac cells to divide along the proper axis. The mutants *Santa*, *Valentine*, and *heart of glass* each have a very similar phenotype wherein the hearts are enlarged, and exhibit a thin ventricular wall due to the failure to add concentric layers to the myocardium. These concentric layers are added when cardiac cells shift their orientation of cell division to divide along the transmural axis (from the epicardium to the endocardium). Failure of this process results in expansion of the myocardium only along the initial axis (Mably et al., 2006; Mably et al., 2003). Thus, cell proliferation within the heart plays a critical role in generating proper morphology and function of this organ.

The Relationship Between Proliferation and Cardiac Differentiation

In many tissues, such as muscle, and the nervous system, the withdrawal of cells from the cell cycle is tightly associated with the onset of terminal differentiation (Alexiades and Cepko, 1996; Dyer and Cepko, 2001; Lathrop et al., 1985; Walsh and Perlman, 1997). In contrast, relatively little is know about the relationship between the cell cycle progression and terminal differentiation in the heart. Cardiac cells continue to proliferate until just after birth in mammals, when they finally exit the cell cycle. As a result of this cell cycle exit, cardiomyocytes in the adult heart are very limited in their regenerative capacity. In skeletal muscle, in contrast, associated muscle progenitor cells, satellite cells, retain the ability to proliferate and differentiate into mature muscle upon injury (Charge and Rudnicki, 2004).

Mutations to a number of genes that are required for cell cycle progression in the heart also result in defects in cardiac differentiation. Hand1 is required, primarily in the OFT

and left ventricle, for cell cycle progression at the G1/S transition by promoting transcription of cyclin D2 and Cdk4 (Risebro et al., 2006). Over-expression of Hand 1 in the developing heart results in increased cardiac cell proliferation as well as delayed and reduced expression of cardiac differentiation markers (Risebro et al., 2006). In addition, deletion of *Jumonji*, a transcription factor that promotes cell cycle exit by repressing cyclin D1 expression (Toyoda et al., 2003), results in reduced expression of cardiac differentiation markers as well as increased proliferation within the heart (Takeuchi et al., 1999). These experiments would lend support to a model where cardiac cell cycle exit and terminal differentiation are closely associated, inter-regulated processes, as has been demonstrated for other cell types. However, the consequences of disrupting the cell cycle upon cardiomyocyte differentiation during development have never been directly examined, leaving open the possibility that cell cycle exit is not directly linked with terminal differentiation with in the heart. Supporting this possibility is the fact that cell proliferation continues within the heart even after the fully differentiated, beating heart has formed (Pasumarthi and Field, 2002).

During development, cell proliferation in the heart continues at fairly high levels, even as cardiomyocytes begin undergoing terminal differentiation (Pasumarthi and Field, 2002). It is not clear, however, whether differentiated cardiomyocytes (ie, those that are expressing contractile proteins organized into sarcomeric structures) continue to proliferate, or whether a separate population of cells within the heart, such as undifferentiated progenitor cells or less differentiated cardiomyocytes, proliferate while terminally differentiated cardiomyocytes exit the cell cycle.

Recently, several reports have indicated that rare cardiac progenitor cells exist within the mammalian myocardium. These progenitor populations are positive for distinct sets of

markers, and were isolated from hearts at different stages, including embryonic, neonatal, and adult hearts (Beltrami et al., 2003; Laugwitz et al., 2005; Moretti et al., 2006; Oh et al., 2004; Wu et al., 2006). One population of progenitor cells isolated from embryonic hearts and positive for *islet1*, a marker of progenitor cells originating from the secondary heart field during embryonic development, is capable of forming fully differentiated cardiomyocytes in culture (Laugwitz et al., 2005), and these cells are also capable of differentiating into endothelial and smooth muscle cells (Moretti et al., 2006). cKit+ cells with the ability to differentiate into cardiac cells have been identified both in adult (Beltrami et al., 2003) and embryonic (Wu et al., 2006) hearts. Finally, a Sca1+ population of cells in the adult myocardium are also capable of differentiating into cardiomyocytes when isolated from the heart and cultured *in vitro*, and also when injected back into mice with ischemia/reprofusion injuries (Oh et al., 2004). Thus, despite the fact that cardiomyocytes begin to exit the cell cycle during embryonic development following the onset of differentiation, and that most cardiac exit the cell cycle shortly after birth, one or more populations of undifferentiated cardiac progenitor cells exist in both the embryonic and adult myocardium. However, the molecular pathways by which these cells are specified and maintained within the heart during development are largely unknown.

The fact that there are sub-populations of undifferentiated progenitor cells within the adult heart potentially lends support to a model wherein a separate population of cells within the heart continues proliferating during embryonic development as other cardiac cells undergo terminal differentiation. It remains possible, however that this population of progenitor cells, which potentially represents an adult cardiac stem cell population, is set aside later in development, and is therefore distinct from the cardiac precursor cells during

embryonic development. Therefore, a model wherein cardiac cells continue to proliferate as they proceed to differentiate cannot be excluded. It has been demonstrated, for example, that differentiated cardiomyoctyes continue to undergo DNA replication, as shown by incorporation of BrDU (Armstrong et al., 2000). However, this may be indicative of the round of endoreplication that is known to occur in post-mitotic cardiomyocytes (Armstrong et al., 2000; Pasumarthi and Field, 2002).

Thesis Goals

Understanding the mechanisms by which the cardiac cell cycle is regulated during development can provide crucial insights into the molecular basis of congenital heart disease. In this work, I explore the requirements for the T-Box transcription factors TBX5 and TBX20 in heart development in the frog *Xenopus laevis*. In particular, I describe the role of TBX5 in promoting cell cycle progression within the heart during the developmental period corresponding with cardiac looping and chamber formation. Finally, I will describe the requirement for the protein tyrosine phosphatase SHP-2 down stream of FGF signaling in the survival of proliferating cardiac progenitor cells. In this way, we have gained a further understanding of how cardiac cell proliferation and survival are regulated and coordinated during vertebrate heart development.

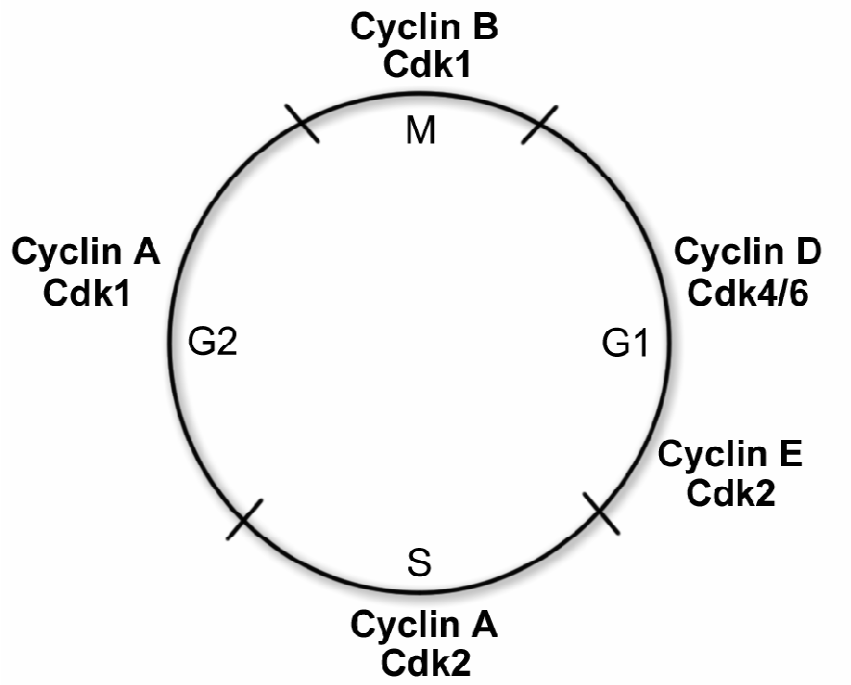

Figure 1.1. The stages of the eukaryotic cell cycle.

The schematic depictes the stages of the cell cycle, mitosis (M), the first gap phase (G1), DNA synthesis phase (S), and the second gap phase (G2). The predominant cyclin/Cdk complexes associated with each phase are also shown.

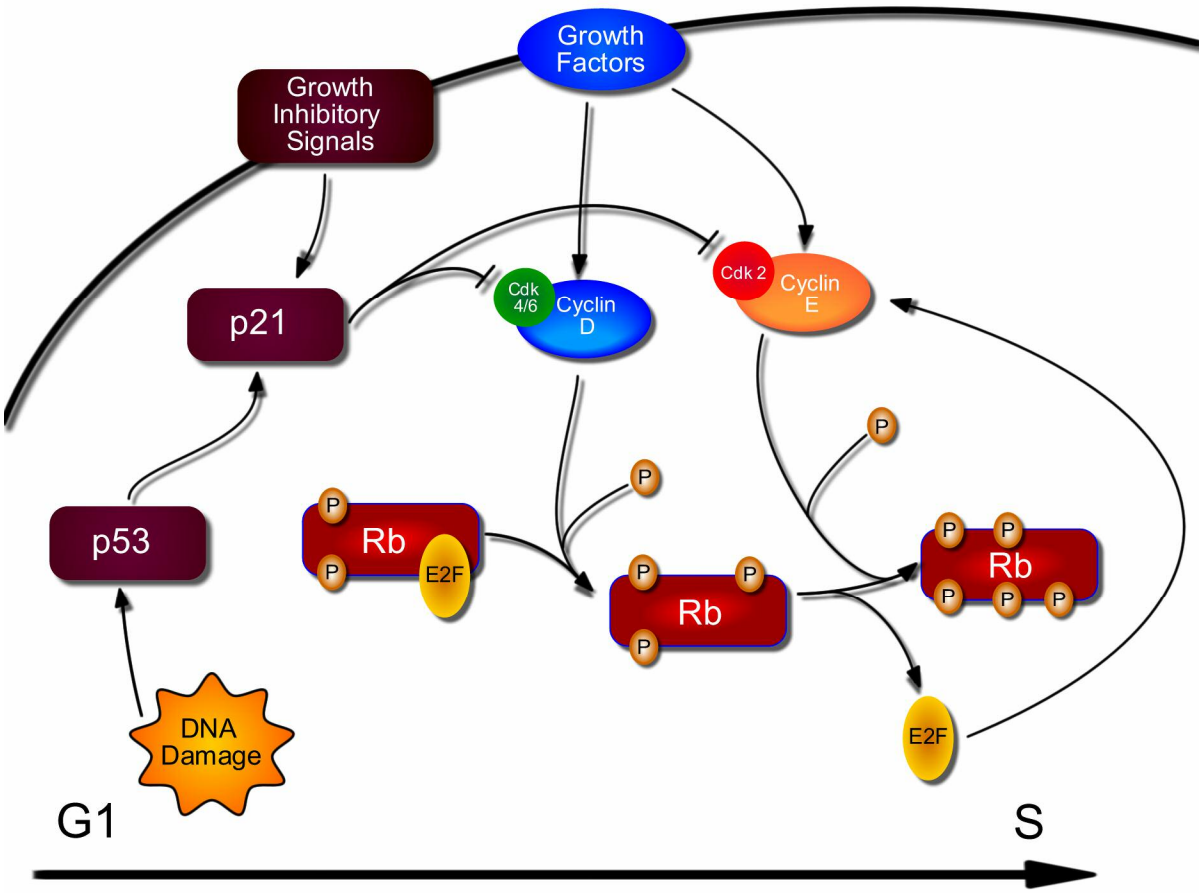

Figure 1.2. *Molecular mechanism of the G1/S transition.*

A schematic of the major molecular pathways both promoting and inhibiting the progression to S phase of the cell cycle. Growth factors promote entry into S phase by inducing expression and activity of Cyclin D, Cyclin E, and their associated Cdks. These complexes in turn phosphorylate and inactivate the retinoblastoma protein (Rb), which then releases E2F, a transcription factor upstream of many other cell cycle promoting factors, as well as DNA replication factors. Cell cycle progression can be inhibited by growth inhibitory signals, or by DNA damage, which results in p53 expression. Both of these pathways result

in increased expression of Cdk inhibitors such as p21 and p27, which antagonize activity of the Cyclin/Cdk complexes, inhibiting entry into S-phase.

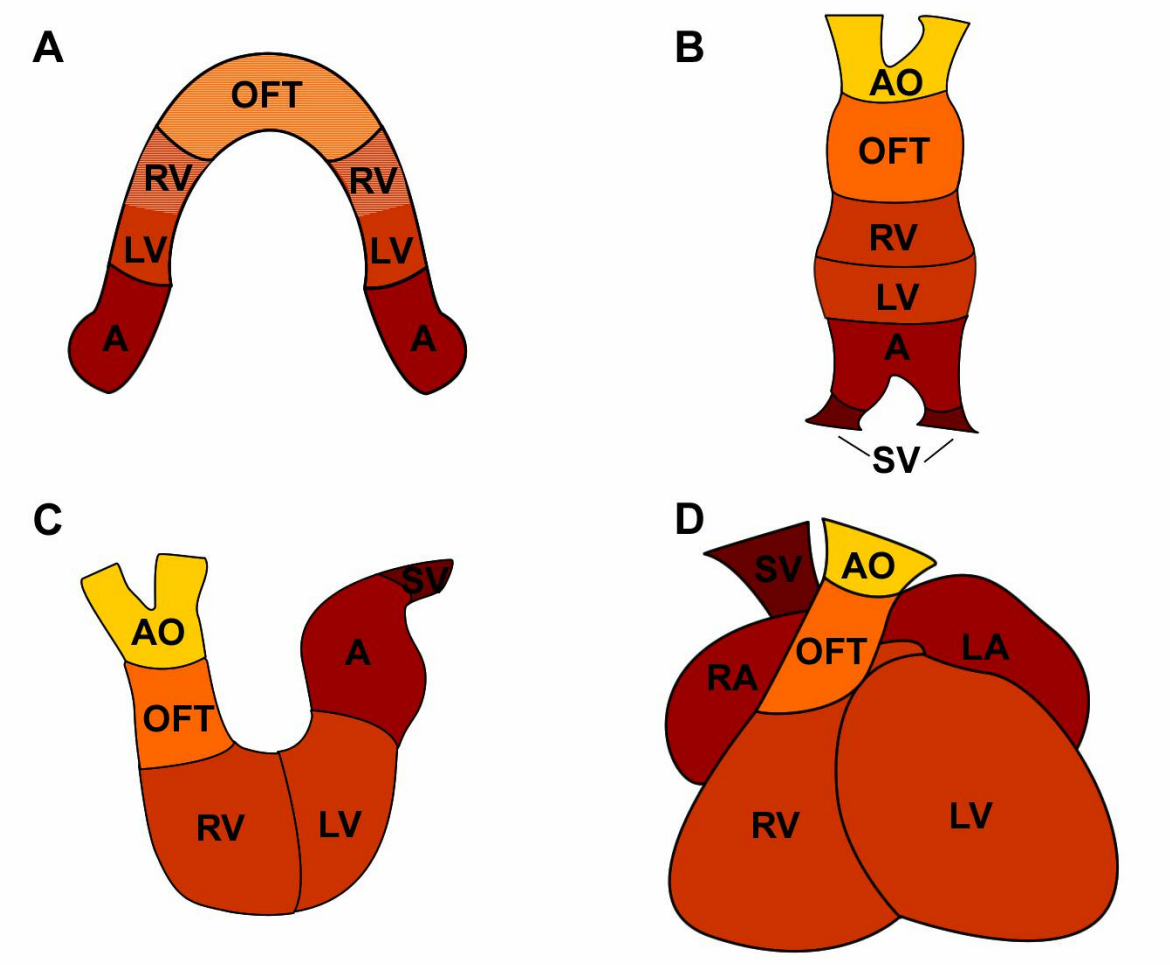

Figure 1.3. *Development of the vertebrate heart.*

A schematic depiction of the vertebrate heart morphogenesis (based on the mouse) at the equivalent of mouse E7.5 (A), E8.5 (B), E9.5 (C), and E11.5 (D). The shaded regions in A are contributed by the anterior heart field in mammals and birds. OFT = outflow tract, RV = right ventricle, LV= left ventricle, A = atria, AO = aorta, SV = sinus venosus, RA = right atrium, LA = left atrium.

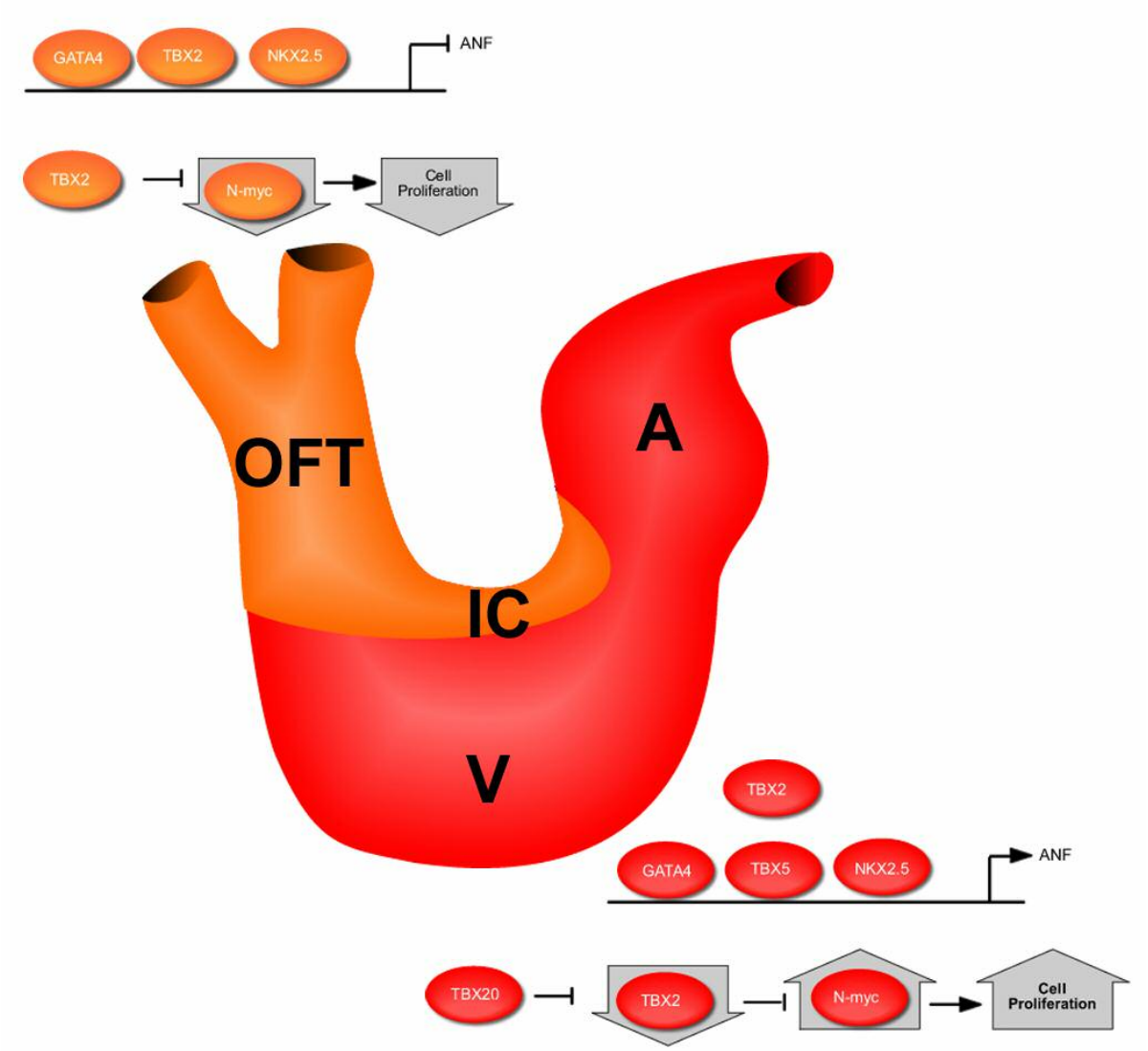

Figure 1.4. T-box transcription factors and the development of the chamber and non-chamber myocardium.

In the non-chamber myocardium (orange), TBX2 represses transcription of ANF and other genes specific to the chamber myocardium. TBX2 also represses N-myc, a transcription factor that promotes cell proliferation, keeping proliferation levels low in the non-chamber myocardium. In the chamber myocardium (red), TBX2 is displaced from binding to NKX2.5 by TBX5, which in turn binds to the *ANF* promoter and promotes its transcription. In addition, expression of TBX2 is repressed by TBX20, thus relieving repression of N-myc.

This leads to higher levels of cell proliferation within the chamber myocardium. OFT = outflow tract, IC = inner curvature, V = ventricles, A = atria.

References

Alexiades, M. R. and Cepko, C. (1996). Quantitative analysis of proliferation and cell cycle length during development of the rat retina. *Dev Dyn* **205**, 293-307.

Alsan, B. H. and Schultheiss, T. M. (2002). Regulation of avian cardiogenesis by Fgf8 signaling. *Development* **129**, 1935-43.

Armstrong, M. T., Lee, D. Y. and Armstrong, P. B. (2000). Regulation of proliferation of the fetal myocardium. *Dev Dyn* **219**, 226-36.

Bagchi, S., Weinmann, R. and Raychaudhuri, P. (1991). The retinoblastoma protein copurifies with E2F-I, an E1A-regulated inhibitor of the transcription factor E2F. *Cell* **65**, 1063-72.

Beltrami, A. P., Barlucchi, L., Torella, D., Baker, M., Limana, F., Chimenti, S., Kasahara, H., Rota, M., Musso, E., Urbanek, K. et al. (2003). Adult cardiac stem cells are multipotent and support myocardial regeneration. *Cell* **114**, 763-76.

Berthet, C., Aleem, E., Coppola, V., Tessarollo, L. and Kaldis, P. (2003). Cdk2 knockout mice are viable. *Curr Biol* **13**, 1775-85.

Berthet, C., Klarmann, K. D., Hilton, M. B., Suh, H. C., Keller, J. R., Kiyokawa, H. and Kaldis, P. (2006). Combined loss of Cdk2 and Cdk4 results in embryonic lethality and Rb hypophosphorylation. *Dev Cell* **10**, 563-73.

Blow, J. J. (2001). Control of chromosomal DNA replication in the early Xenopus embryo. *Embo J* **20**, 3293-7.

Booher, R. N., Alfa, C. E., Hyams, J. S. and Beach, D. H. (1989). The fission yeast cdc2/cdc13/suc1 protein kinase: regulation of catalytic activity and nuclear localization. *Cell* **58**, 485-97.

Brown, D. D., Binder, O., Pagratis, M., Parr, B. A. and Conlon, F. L. (2003). Developmental expression of the Xenopus laevis Tbx20 orthologue. *Dev Genes Evol* **212**, 604-7.

Bruneau, B. G., Bao, Z. Z., Fatkin, D., Xavier-Neto, J., Georgakopoulos, D., Maguire, C. T., Berul, C. I., Kass, D. A., Kuroski-de Bold, M. L., de Bold, A. J. et al. (2001a). Cardiomyopathy in Irx4-deficient mice is preceded by abnormal ventricular gene expression. *Mol Cell Biol* **21**, 1730-6.

Bruneau, B. G., Logan, M., Davis, N., Levi, T., Tabin, C. J., Seidman, J. G. and Seidman, C. E. (1999). Chamber-specific cardiac expression of Tbx5 and heart defects in Holt-Oram syndrome. *Dev Biol* **211**, 100-8.

Bruneau, B. G., Nemer, G., Schmitt, J. P., Charron, F., Robitaille, L., Caron, S., Conner, D. A., Gessler, M., Nemer, M., Seidman, C. E. et al. (2001b). A murine model of Holt-Oram syndrome defines roles of the T-box transcription factor Tbx5 in cardiogenesis and disease. *Cell* **106**, 709-21.

Cai, C. L., Liang, X., Shi, Y., Chu, P. H., Pfaff, S. L., Chen, J. and Evans, S. (2003). Isl1 identifies a cardiac progenitor population that proliferates prior to differentiation and contributes a majority of cells to the heart. *Dev Cell* **5**, 877-89.

Cai, C. L., Zhou, W., Yang, L., Bu, L., Qyang, Y., Zhang, X., Li, X., Rosenfeld, M. G., Chen, J. and Evans, S. (2005). T-box genes coordinate regional rates of proliferation and regional specification during cardiogenesis. *Development* **132**, 2475-87.

Chapman, D. L., Garvey, N., Hancock, S., Alexiou, M., Agulnik, S. I., Gibson-Brown, J. J., Cebra-Thomas, J., Bollag, R. J., Silver, L. M. and Papaioannou, V. E. (1996). Expression of the T-box family genes, Tbx1-Tbx5, during early mouse development. *Dev Dyn* **206**, 379-90.

Charge, S. B. and Rudnicki, M. A. (2004). Cellular and molecular regulation of muscle regeneration. *Physiol Rev* **84**, 209-38.

Chellappan, S. P., Hiebert, S., Mudryj, M., Horowitz, J. M. and Nevins, J. R. (1991). The E2F transcription factor is a cellular target for the RB protein. *Cell* **65**, 1053-61.

Chen, F., Kook, H., Milewski, R., Gitler, A. D., Lu, M. M., Li, J., Nazarian, R., Schnepp, R., Jen, K., Biben, C. et al. (2002). Hop is an unusual homeobox gene that modulates cardiac development. *Cell* **110**, 713-23.

Choi, M., Stottmann, R. W., Yang, Y. P., Meyers, E. N. and Klingensmith, J. (2007). The Bone Morphogenetic Protein Antagonist Noggin Regulates Mammalian Cardiac Morphogenesis. *Circ Res*.

Christoffels, V. M., Habets, P. E., Franco, D., Campione, M., de Jong, F., Lamers, W. H., Bao, Z. Z., Palmer, S., Biben, C., Harvey, R. P. et al. (2000a). Chamber formation and morphogenesis in the developing mammalian heart. *Dev Biol* **223**, 266-78.

Christoffels, V. M., Hoogaars, W. M., Tessari, A., Clout, D. E., Moorman, A. F. and Campione, M. (2004). T-box transcription factor Tbx2 represses differentiation and formation of the cardiac chambers. *Dev Dyn* **229**, 763-70.

Christoffels, V. M., Keijser, A. G., Houweling, A. C., Clout, D. E. and Moorman, A. F. (2000b). Patterning the embryonic heart: identification of five mouse Iroquois homeobox genes in the developing heart. *Dev Biol* **224**, 263-74.

Cross, F. R. (1988). DAF1, a mutant gene affecting size control, pheromone arrest, and cell cycle kinetics of Saccharomyces cerevisiae. *Mol Cell Biol* **8**, 4675-84.

D'Urso, G., Marraccino, R. L., Marshak, D. R. and Roberts, J. M. (1990). Cell cycle control of DNA replication by a homologue from human cells of the p34cdc2 protein kinase. *Science* **250**, 786-91.

De Bondt, H. L., Rosenblatt, J., Jancarik, J., Jones, H. D., Morgan, D. O. and Kim, S. H. (1993). Crystal structure of cyclin-dependent kinase 2. *Nature* **363**, 595-602.

de Nooij, J. C., Letendre, M. A. and Hariharan, I. K. (1996). A cyclin-dependent kinase inhibitor, Dacapo, is necessary for timely exit from the cell cycle during Drosophila embryogenesis. *Cell* **87**, 1237-47.

Duronio, R. J. and O'Farrell, P. H. (1994). Developmental control of a G1-S transcriptional program in Drosophila. *Development* **120**, 1503-15.

Dyer, M. A. and Cepko, C. L. (2001). Regulating proliferation during retinal development. *Nat Rev Neurosci* **2**, 333-42.

Ekholm, S. V. and Reed, S. I. (2000). Regulation of G(1) cyclin-dependent kinases in the mammalian cell cycle. *Curr Opin Cell Biol* **12**, 676-84.

Elledge, S. J. (1996). Cell cycle checkpoints: preventing an identity crisis. *Science* **274**, 1664-72.

Fishman, M. C. and Chien, K. R. (1997). Fashioning the vertebrate heart: earliest embryonic decisions. *Development* **124**, 2099-117.

Follette, P. J. and O'Farrell, P. H. (1997). Cdks and the Drosophila cell cycle. *Curr Opin Genet Dev* **7**, 17-22.

Garcia-Martinez, V. and Schoenwolf, G. C. (1993). Primitive-streak origin of the cardiovascular system in avian embryos. *Dev Biol* **159**, 706-19.

Gassmann, M., Casagranda, F., Orioli, D., Simon, H., Lai, C., Klein, R. and Lemke, G. (1995). Aberrant neural and cardiac development in mice lacking the ErbB4 neuregulin receptor. *Nature* **378**, 390-4.

Gaussin, V., Van de Putte, T., Mishina, Y., Hanks, M. C., Zwijsen, A., Huylebroeck, D., Behringer, R. R. and Schneider, M. D. (2002). Endocardial cushion and myocardial defects after cardiac myocyte-specific conditional deletion of the bone morphogenetic protein receptor ALK3. *Proc Natl Acad Sci U S A* **99**, 2878-83.

Geng, Y., Whoriskey, W., Park, M. Y., Bronson, R. T., Medema, R. H., Li, T., Weinberg, R. A. and Sicinski, P. (1999). Rescue of cyclin D1 deficiency by knockin cyclin E. *Cell* **97**, 767-77.

Geng, Y., Yu, Q., Sicinska, E., Das, M., Schneider, J. E., Bhattacharya, S., Rideout, W. M., Bronson, R. T., Gardner, H. and Sicinski, P. (2003). Cyclin E ablation in the mouse. *Cell* **114**, 431-43.

Habets, P. E., Moorman, A. F., Clout, D. E., van Roon, M. A., Lingbeek, M., van Lohuizen, M., Campione, M. and Christoffels, V. M. (2002). Cooperative action of Tbx2 and Nkx2.5 inhibits ANF expression in the atrioventricular canal: implications for cardiac chamber formation. *Genes Dev* **16**, 1234-46.

Harbour, J. W., Luo, R. X., Dei Santi, A., Postigo, A. A. and Dean, D. C. (1999). Cdk phosphorylation triggers sequential intramolecular interactions that progressively block Rb functions as cells move through G1. *Cell* **98**, 859-69.

Harvey, R. P. (2002). Patterning the vertebrate heart. *Nat Rev Genet* **3**, 544-56.

Hiebert, S. W., Chellappan, S. P., Horowitz, J. M. and Nevins, J. R. (1992). The interaction of RB with E2F coincides with an inhibition of the transcriptional activity of E2F. *Genes Dev* **6**, 177-85.

Hiroi, Y., Kudoh, S., Monzen, K., Ikeda, Y., Yazaki, Y., Nagai, R. and Komuro, I. (2001). Tbx5 associates with Nkx2-5 and synergistically promotes cardiomyocyte differentiation. *Nat Genet* **28**, 276-80.

Horb, M. E. and Thomsen, G. H. (1999). Tbx5 is essential for heart development. *Development* **126**, 1739-51.

Iio, A., Koide, M., Hidaka, K. and Morisaki, T. (2001). Expression pattern of novel chick T-box gene, Tbx20. *Dev Genes Evol* **211**, 559-62.

Jacobson, A. G. and Duncan, J. T. (1968). Heart induction in salamanders. *J Exp Zool* **167**, 79-103.

Kang, J. O. and Sucov, H. M. (2005). Convergent proliferative response and divergent morphogenic pathways induced by epicardial and endocardial signaling in fetal heart development. *Mech Dev* **122**, 57-65.

Kim, T. G., Chen, J., Sadoshima, J. and Lee, Y. (2004). Jumonji represses atrial natriuretic factor gene expression by inhibiting transcriptional activities of cardiac transcription factors. *Mol Cell Biol* **24**, 10151-60.

Knoblich, J. A., Sauer, K., Jones, L., Richardson, H., Saint, R. and Lehner, C. F. (1994). Cyclin E controls S phase progression and its down-regulation during Drosophila embryogenesis is required for the arrest of cell proliferation. *Cell* **77**, 107-20.

Koff, A., Cross, F., Fisher, A., Schumacher, J., Leguellec, K., Philippe, M. and Roberts, J. M. (1991). Human cyclin E, a new cyclin that interacts with two members of the CDC2 gene family. *Cell* **66**, 1217-28.

Kozar, K., Ciemerych, M. A., Rebel, V. I., Shigematsu, H., Zagozdzon, A., Sicinska, E., Geng, Y., Yu, Q., Bhattacharya, S., Bronson, R. T. et al. (2004). Mouse development and cell proliferation in the absence of D-cyclins. *Cell* **118**, 477-91.

Kraus, F., Haenig, B. and Kispert, A. (2001). Cloning and expression analysis of the mouse T-box gene tbx20. *Mech Dev* **100**, 87-91.

Lane, M. E., Sauer, K., Wallace, K., Jan, Y. N., Lehner, C. F. and Vaessin, H. (1996). Dacapo, a cyclin-dependent kinase inhibitor, stops cell proliferation during Drosophila development. *Cell* **87**, 1225-35.

Lathrop, B., Thomas, K. and Glaser, L. (1985). Control of myogenic differentiation by fibroblast growth factor is mediated by position in the G1 phase of the cell cycle. *J Cell Biol* **101**, 2194-8.

Laugwitz, K. L., Moretti, A., Lam, J., Gruber, P., Chen, Y., Woodard, S., Lin, L. Z., Cai, C. L., Lu, M. M., Reth, M. et al. (2005). Postnatal isl1+ cardioblasts enter fully differentiated cardiomyocyte lineages. *Nature* **433**, 647-53.

Lavine, K. J., Yu, K., White, A. C., Zhang, X., Smith, C., Partanen, J. and Ornitz, D. M. (2005). Endocardial and epicardial derived FGF signals regulate myocardial proliferation and differentiation in vivo. *Dev Cell* **8**, 85-95.

Lee, K. F., Simon, H., Chen, H., Bates, B., Hung, M. C. and Hauser, C. (1995). Requirement for neuregulin receptor erbB2 in neural and cardiac development. *Nature* **378**, 394-8.

Lehner, C. F. and O'Farrell, P. H. (1990). The roles of Drosophila cyclins A and B in mitotic control. *Cell* **61**, 535-47.

Lohka, M. J., Hayes, M. K. and Maller, J. L. (1988). Purification of maturation-promoting factor, an intracellular regulator of early mitotic events. *Proc Natl Acad Sci U S A* **85**, 3009-13.

Lough, J., Barron, M., Brogley, M., Sugi, Y., Bolender, D. L. and Zhu, X. (1996). Combined BMP-2 and FGF-4, but neither factor alone, induces cardiogenesis in non-precardiac embryonic mesoderm. *Dev Biol* **178**, 198-202.

Lough, J. and Sugi, Y. (2000). Endoderm and heart development. *Dev Dyn* **217**, 327-42.

Lyons, I., Parsons, L. M., Hartley, L., Li, R., Andrews, J. E., Robb, L. and Harvey, R. P. (1995). Myogenic and morphogenetic defects in the heart tubes of murine embryos lacking the homeo box gene Nkx2-5. *Genes Dev* **9**, 1654-66.

Mably, J. D., Chuang, L. P., Serluca, F. C., Mohideen, M. A., Chen, J. N. and Fishman, M. C. (2006). santa and valentine pattern concentric growth of cardiac myocardium in the zebrafish. *Development* **133**, 3139-46.

Mably, J. D., Mohideen, M. A., Burns, C. G., Chen, J. N. and Fishman, M. C. (2003). heart of glass regulates the concentric growth of the heart in zebrafish. *Curr Biol* **13**, 2138-47.

Malumbres, M., Sotillo, R., Santamaria, D., Galan, J., Cerezo, A., Ortega, S., Dubus, P. and Barbacid, M. (2004). Mammalian cells cycle without the D-type cyclin-dependent kinases Cdk4 and Cdk6. *Cell* **118**, 493-504.

McFadden, D. G., Barbosa, A. C., Richardson, J. A., Schneider, M. D., Srivastava, D. and Olson, E. N. (2005). The Hand1 and Hand2 transcription factors regulate expansion of the embryonic cardiac ventricles in a gene dosage-dependent manner. *Development* **132**, 189-201.

Meilhac, S. M., Esner, M., Kerszberg, M., Moss, J. E. and Buckingham, M. E. (2004). Oriented clonal cell growth in the developing mouse myocardium underlies cardiac morphogenesis. *J Cell Biol* **164**, 97-109.

Meilhac, S. M., Kelly, R. G., Rocancourt, D., Eloy-Trinquet, S., Nicolas, J. F. and Buckingham, M. E. (2003). A retrospective clonal analysis of the myocardium reveals two phases of clonal growth in the developing mouse heart. *Development* **130**, 3877-89.

Meyer, D. and Birchmeier, C. (1995). Multiple essential functions of neuregulin in development. *Nature* **378**, 386-90.

Mima, T., Ueno, H., Fischman, D. A., Williams, L. T. and Mikawa, T. (1995). Fibroblast growth factor receptor is required for in vivo cardiac myocyte proliferation at early embryonic stages of heart development. *Proc Natl Acad Sci U S A* **92**, 467-71.

Moens, C. B., Stanton, B. R., Parada, L. F. and Rossant, J. (1993). Defects in heart and lung development in compound heterozygotes for two different targeted mutations at the N-myc locus. *Development* **119**, 485-99.

Moretti, A., Caron, L., Nakano, A., Lam, J. T., Bernshausen, A., Chen, Y., Qyang, Y., Bu, L., Sasaki, M., Martin-Puig, S. et al. (2006). Multipotent embryonic isl1+ progenitor cells lead to cardiac, smooth muscle, and endothelial cell diversification. *Cell* **127**, 1151-65.

Murphy, M., Stinnakre, M. G., Senamaud-Beaufort, C., Winston, N. J., Sweeney, C., Kubelka, M., Carrington, M., Brechot, C. and Sobczak-Thepot, J. (1997). Delayed early embryonic lethality following disruption of the murine cyclin A2 gene. *Nat Genet* **15**, 83-6.

Murray, A. W. and Kirschner, M. W. (1989). Cyclin synthesis drives the early embryonic cell cycle. *Nature* **339**, 275-80.

Murray, A. W., Solomon, M. J. and Kirschner, M. W. (1989). The role of cyclin synthesis and degradation in the control of maturation promoting factor activity. *Nature* **339**, 280-6.

Nascone, N. and Mercola, M. (1995). An inductive role for the endoderm in Xenopus cardiogenesis. *Development* **121**, 515-23.

Nguyen, V. Q., Co, C. and Li, J. J. (2001). Cyclin-dependent kinases prevent DNA re-replication through multiple mechanisms. *Nature* **411**, 1068-73.

Nurse, P. (1975). Genetic control of cell size at cell division in yeast. *Nature* **256**, 547-51.

Nurse, P. (1997). Regulation of the eukaryotic cell cycle. *Eur J Cancer* **33**, 1002-4.

Oh, H., Chi, X., Bradfute, S. B., Mishina, Y., Pocius, J., Michael, L. H., Behringer, R. R., Schwartz, R. J., Entman, M. L. and Schneider, M. D. (2004). Cardiac muscle plasticity in adult and embryo by heart-derived progenitor cells. *Ann N Y Acad Sci* **1015**, 182-9.

Orr-Weaver, T. L. (1994). Developmental modification of the Drosophila cell cycle. *Trends Genet* **10**, 321-7.

Ortega, S., Prieto, I., Odajima, J., Martin, A., Dubus, P., Sotillo, R., Barbero, J. L., Malumbres, M. and Barbacid, M. (2003). Cyclin-dependent kinase 2 is essential for meiosis but not for mitotic cell division in mice. *Nat Genet* **35**, 25-31.

Pasumarthi, K. B. and Field, L. J. (2002). Cardiomyocyte cell cycle regulation. *Circ Res* **90**, 1044-54.

Pennisi, D. J., Ballard, V. L. and Mikawa, T. (2003). Epicardium is required for the full rate of myocyte proliferation and levels of expression of myocyte mitogenic factors FGF2 and its receptor, FGFR-1, but not for transmural myocardial patterning in the embryonic chick heart. *Dev Dyn* **228**, 161-72.

Peterkin, T., Gibson, A. and Patient, R. (2003). GATA-6 maintains BMP-4 and Nkx2 expression during cardiomyocyte precursor maturation. *Embo J* **22**, 4260-73.

Rane, S. G., Dubus, P., Mettus, R. V., Galbreath, E. J., Boden, G., Reddy, E. P. and Barbacid, M. (1999). Loss of Cdk4 expression causes insulin-deficient diabetes and Cdk4 activation results in beta-islet cell hyperplasia. *Nat Genet* **22**, 44-52.

Richardson, H. E., O'Keefe, L. V., Reed, S. I. and Saint, R. (1993). A Drosophila G1-specific cyclin E homolog exhibits different modes of expression during embryogenesis. *Development* **119**, 673-90.

Riley, P., Anson-Cartwright, L. and Cross, J. C. (1998). The Hand1 bHLH transcription factor is essential for placentation and cardiac morphogenesis. *Nat Genet* **18**, 271-5.

Risebro, C. A., Smart, N., Dupays, L., Breckenridge, R., Mohun, T. J. and Riley, P. R. (2006). Hand1 regulates cardiomyocyte proliferation versus differentiation in the developing heart. *Development* **133**, 4595-606.

Rudner, A. D. and Murray, A. W. (1996). The spindle assembly checkpoint. *Curr Opin Cell Biol* **8**, 773-80.

Russo, A. A., Jeffrey, P. D. and Pavletich, N. P. (1996). Structural basis of cyclin-dependent kinase activation by phosphorylation. *Nat Struct Biol* **3**, 696-700.

Sapkota, G., Alarcon, C., Spagnoli, F. M., Brivanlou, A. H. and Massague, J. (2007). Balancing BMP signaling through integrated inputs into the Smad1 linker. *Mol Cell* **25**, 441-54.

Sater, A. K. and Jacobson, A. G. (1989). The specification of heart mesoderm occurs during gastrulation in Xenopus laevis. *Development* **105**, 821-30.

Schultheiss, T. M., Burch, J. B. and Lassar, A. B. (1997). A role for bone morphogenetic proteins in the induction of cardiac myogenesis. *Genes Dev* **11**, 451-62.

Schultheiss, T. M., Xydas, S. and Lassar, A. B. (1995). Induction of avian cardiac myogenesis by anterior endoderm. *Development* **121**, 4203-14.

Sedmera, D. and Thomas, P. S. (1996). Trabeculation in the embryonic heart. *Bioessays* **18**, 607.

Sherr, C. J. (1993). Mammalian G1 cyclins. *Cell* **73**, 1059-65.

Sherr, C. J. and Roberts, J. M. (2004). Living with or without cyclins and cyclin-dependent kinases. *Genes Dev* **18**, 2699-711.

Shin, C. H., Liu, Z. P., Passier, R., Zhang, C. L., Wang, D. Z., Harris, T. M., Yamagishi, H., Richardson, J. A., Childs, G. and Olson, E. N. (2002). Modulation of cardiac growth and development by HOP, an unusual homeodomain protein. *Cell* **110**, 725-35.

Singh, M. K., Christoffels, V. M., Dias, J. M., Trowe, M. O., Petry, M., Schuster-Gossler, K., Burger, A., Ericson, J. and Kispert, A. (2005). Tbx20 is essential for cardiac chamber differentiation and repression of Tbx2. *Development* **132**, 2697-707.

Soufan, A. T., van den Berg, G., Ruijter, J. M., de Boer, P. A., van den Hoff, M. J. and Moorman, A. F. (2006). Regionalized sequence of myocardial cell growth and proliferation characterizes early chamber formation. *Circ Res* **99**, 545-52.

Srivastava, D., Cserjesi, P. and Olson, E. N. (1995). A subclass of bHLH proteins required for cardiac morphogenesis. *Science* **270**, 1995-9.

Srivastava, D., Thomas, T., Lin, Q., Kirby, M. L., Brown, D. and Olson, E. N. (1997). Regulation of cardiac mesodermal and neural crest development by the bHLH transcription factor, dHAND. *Nat Genet* **16**, 154-60.

Stennard, F. A., Costa, M. W., Lai, D., Biben, C., Furtado, M. B., Solloway, M. J., McCulley, D. J., Leimena, C., Preis, J. I., Dunwoodie, S. L. et al. (2005). Murine T-box transcription factor Tbx20 acts as a repressor during heart development, and is essential for adult heart integrity, function and adaptation. *Development* **132**, 2451-62.

Sugi, Y., Sasse, J. and Lough, J. (1993). Inhibition of precardiac mesoderm cell proliferation by antisense oligodeoxynucleotide complementary to fibroblast growth factor-2 (FGF-2). *Dev Biol* **157**, 28-37.

Taber, L. A., Lin, I. E. and Clark, E. B. (1995). Mechanics of cardiac looping. *Dev Dyn* **203**, 42-50.

Takeuchi, T., Kojima, M., Nakajima, K. and Kondo, S. (1999). jumonji gene is essential for the neurulation and cardiac development of mouse embryos with a C3H/He background. *Mech Dev* **86**, 29-38.

Takisawa, H., Mimura, S. and Kubota, Y. (2000). Eukaryotic DNA replication: from pre-replication complex to initiation complex. *Curr Opin Cell Biol* **12**, 690-6.

Tanaka, M., Chen, Z., Bartunkova, S., Yamasaki, N. and Izumo, S. (1999). The cardiac homeobox gene Csx/Nkx2.5 lies genetically upstream of multiple genes essential for heart development. *Development* **126**, 1269-80.

Toyoda, M., Shirato, H., Nakajima, K., Kojima, M., Takahashi, M., Kubota, M., Suzuki-Migishima, R., Motegi, Y., Yokoyama, M. and Takeuchi, T. (2003). jumonji downregulates cardiac cell proliferation by repressing cyclin D1 expression. *Dev Cell* **5**, 85-97.

Waldo, K. L., Kumiski, D. H., Wallis, K. T., Stadt, H. A., Hutson, M. R., Platt, D. H. and Kirby, M. L. (2001). Conotruncal myocardium arises from a secondary heart field. *Development* **128**, 3179-88.

Walsh, K. and Perlman, H. (1997). Cell cycle exit upon myogenic differentiation. *Curr Opin Genet Dev* **7**, 597-602.

Wang, B., Weidenfeld, J., Lu, M. M., Maika, S., Kuziel, W. A., Morrisey, E. E. and Tucker, P. W. (2004). Foxp1 regulates cardiac outflow tract, endocardial cushion morphogenesis and myocyte proliferation and maturation. *Development* **131**, 4477-87.

Whitfield, W. G., Gonzalez, C., Maldonado-Codina, G. and Glover, D. M. (1990). The A- and B-type cyclins of Drosophila are accumulated and destroyed in temporally distinct events that define separable phases of the G2-M transition. *Embo J* **9**, 2563-72.

Wu, S. M., Fujiwara, Y., Cibulsky, S. M., Clapham, D. E., Lien, C. L., Schultheiss, T. M. and Orkin, S. H. (2006). Developmental origin of a bipotential myocardial and smooth muscle cell precursor in the mammalian heart. *Cell* **127**, 1137-50.

Yamagishi, H., Yamagishi, C., Nakagawa, O., Harvey, R. P., Olson, E. N. and Srivastava, D. (2001). The combinatorial activities of Nkx2.5 and dHAND are essential for cardiac ventricle formation. *Dev Biol* **239**, 190-203.

Zhang, H. S., Gavin, M., Dahiya, A., Postigo, A. A., Ma, D., Luo, R. X., Harbour, J. W. and Dean, D. C. (2000). Exit from G1 and S phase of the cell cycle is regulated by repressor complexes containing HDAC-Rb-hSWI/SNF and Rb-hSWI/SNF. *Cell* **101**, 79-89.

Zhu, X., Sasse, J. and Lough, J. (1999). Evidence that FGF receptor signaling is necessary for endoderm-regulated development of precardiac mesoderm. *Mech Ageing Dev* **108**, 77-85.

Zhu, X., Sasse, J., McAllister, D. and Lough, J. (1996). Evidence that fibroblast growth factors 1 and 4 participate in regulation of cardiogenesis. *Dev Dyn* **207**, 429-38.

CHAPTER 2

Tbx5 and *Tbx20* Act Synergistically to Control Vertebrate Heart Morphogenesis

PREFACE TO CHAPTER 2

Chapter 2 describes the requirement for the T-Box transcription factor TBX20 during vertebrate heart development, as well as providing evidence for a synergistic interaction between TBX20 and TBX5. TBX20 had been previously shown to be expressed throughout the developing heart in mouse, avian, and Xenopus embryos (Iio et al., 2001; Kraus et al., 2001; Brown et al., 2003), however a requirement for TBX20 in heart formation had not been demonstrated.

This work was published in *Development* in 2005 and produced in collaboration with Daniel Brown, Shauna Martz, Olav Binder, Brenda Price, and Jim Smith. I performed the analysis of total cardiac cell number in embryos depleted of TBX5 and TBX20 by morpholinos. The finding that there are fewer cells in the hearts of TBX5 and TBX20-depleted embryos also lead to the hypothesis that these transcription factors might be required for proliferation in the embryonic heart. We test this hypothesis with respect to TBX5 in Chapter 4.

SUMMARY

Members of the T-box family of proteins play a fundamental role in patterning the developing vertebrate heart; however, the precise cellular requirements for any one family member and the mechanism by which individual T-box genes function remains largely unknown. In this study, we investigate the cellular and molecular relationship between two T-box genes, *Tbx5* and *Tbx20*. We demonstrate that blocking *Tbx5* or *Tbx20* gives phenotypes that display a high degree of similarity as judged by overall gross morphology, molecular marker analysis, and cardiac physiology, implying that the two genes are required for and have non-redundant functions in early heart development. In addition, we demonstrate that although coexpressed, *Tbx5* and *Tbx20* are not dependent on one another's expression, but rather have a synergistic role during early heart development. Consistent with this proposal, we show that TBX5 and TBX20 can physically interact, map the interaction domains, show a cellular interaction for the two proteins in cardiac development and therefore, provide the first evidence for direct interaction between members of the T-box gene family.

INTRODUCTION

The vertebrate heart constitutes the earliest functional organ in the developing embryo and about 1% of all live births exhibit congenital heart disease (Hoffman, 1995a; Hoffman, 1995b; Payne et al., 1995). It is becoming increasingly clear that a complex molecular regulatory network is required to initiate and complete the formation of a functional heart. The proteins implicated in this process include a number of transcription factors from a range of transcription factor families, including the T-box, basic helix-loop-helix homeodomain,

zinc finger, and MADS domain families (Cripps and Olson, 2002; Harvey, 2002; Zaffran and Frasch, 2002).

The T-box family of transcription factors is a large family of proteins involved in determining early cell fate decisions and controlling differentiation and organogenesis. Two sets of clinical data have provided direct evidence for the involvement of T-box genes in human heart development (for review see Packham and Brook, 2003; Ryan and Chin, 2003). Deletions of *Tbx1* have been found in patients with DiGeorge syndrome (Baldini, 2004; Chieffo et al., 1997; Jerome and Papaioannou, 2001; Lindsey et al., 2001; Merscher et al., 2001; Yagi et al., 2003), and mutations in *Tbx5* are associated with Holt-Oram Syndrome (HOS), a congenital heart disease characterized by defects in heart formation and upper limb development (Basson et al., 1997; Li et al., 1997). Clinical studies of HOS patients have demonstrated a fundamental role for *Tbx5* in heart development. HOS is a highly penetrant autosomal dominant condition associated with skeletal and cardiac malformations (Newbury-Ecob et al., 1996). Patients with HOS often carry mutations within the coding region of the T-box transcription factor *Tbx5* (Basson et al., 1997; Basson et al., 1999; Benson et al., 1996; Li et al., 1997). The role of *Tbx5* in heart development, and in the HOS disease state, is further supported by recent gene-targeting experiments in mouse. These studies demonstrate that mice heterozygous for mutations in *Tbx5* display many of the phenotypic abnormalities of HOS patients (Bruneau et al., 2001) and show that TBX5 is required for growth and differentiation of the left ventricle and atria as well as for proper development of the cardiac conduction system. Similar defects are seen in the zebrafish *Tbx5* mutant *heartstrings*, suggesting that the expression and function of TBX5 is conserved throughout vertebrate evolution (Garrity et al., 2002).

Previously, we described the cloning and expression of the *Xenopus laevis* (*X. laevis*) *Tbx20* orthologue, *Tbx20* (Brown et al., 2003). Studies of *Tbx20* have demonstrated that along with *Tbx5*, *Tbx20* is one of the first genes expressed in the vertebrate cardiac lineage. Moreover, *Tbx20* is expressed at the same time and in many of the same regions of the heart that also express the heart markers *Tbx5*, *Nkx2-5*, and *Gata4* (Horb and Thomsen, 1999; Laverriere et al., 1994; Serbedzija et al., 1998; Tonissen et al., 1994).

Despite our knowledge of the expression pattern of *Tbx20*, little is known of *Tbx20* function in heart development. In the zebrafish, it has recently been observed that eliminating endogenous TBX20 (HrT) via morpholinos leads to cardiac defects (Szeto et al., 2002). Specifically, TBX20 knockdown in zebrafish leads to dysmorphic hearts and a loss of blood circulation. The morphological defects are not apparent until the cardiac looping stage, despite high levels of *Tbx20* during the earlier stages of specification and development suggesting that other T-box genes may act redundantly with *Tbx20* during early heart development.

In this study we investigate the cellular and molecular relationship between *Tbx5* and *Tbx20* in *X. laevis*. We show that the phenotypes of knocking down TBX5 and TBX20 are highly similar, with embryos derived from either *Tbx5* or *Tbx20* morpholino injections displaying profound morphological defects including pericardial edema, reduced cardiac mass, and loss of circulation. In addition, we show that the morphological phenotype is not a reflection of alterations in the specification, commitment, or differentiation of cardiac tissue. Thus, in addition to sharing a number of molecular properties, we show that *Tbx5* and *Tbx20* function in a non-redundant fashion and are essential for cardiac morphogenesis. However, despite the similarities in phenotype and shared molecular properties, *Tbx5* and *Tbx20* also have independent roles in heart development.

Given the similarity in TBX5 and TBX20 morphant phenotypes, we investigated the pathways by which *Tbx5* and *Tbx20* function. We show that TBX5 and TBX20 do not function in a linear pathway (i.e. *Tbx20* does not act downstream of *Tbx5*, and vice versa), but rather imply a synergistic role for these two proteins during early heart development. Consistent with this proposal, we show that TBX5 and TBX20 can physically interact, map the interaction domains, and show an interaction for the two proteins in cardiac development, therefore providing the first evidence for interaction between members of the T-box gene family.

MATERIALS AND METHODS

DNA Constructs

XANF was generously provided by Paul Krieg (p*XANF*) (Small and Krieg, 2000), and the *cardiac troponin I* (p*XTnIc*) plasmid was generously provided by Tim Mohun (Logan and Mohun, 1993). *Nkx*2-5 was cloned by degenerate PCR from a ventral-anterior *X. laevis* cDNA library (generous gift of Tim Mohun). Sequence analysis revealed that the clone shows extensive homology to a partial sequence of the second *X. laevis* allele of *Nkx2-5* (accession AF283102). The clone is predicted to be full-length and in vitro translation of the protein gave a band of the correct size. The clone is referred to as pCRNkx-2.5B (accession number AY644403). To construct the pBS-*Nkx2-5* hybridization probe, *Nkx2-5* was subcloned into pBLUESCRIPT II KS+. Details of X*Tbx20* and X*Tbx5*, respective deletions and GST fusions, cell transfections and nuclear localization protocols can be obtained at: www.unc.edu/~fconlon/SuppMat.pdf.

Transient Transfections

293T cells were plated at 1 X 10^6 cells/well in six-well tissue culture plates 24 hours prior to transfection. Plasmids used in transients are: the *Nppa* promoter-luciferase reporter (Hiroi et al., 2001), p*Tbx5*-V5, p*Tbx20*-V5, pCMV-*LacZ*; pBS/KS. The amount of luciferase reporter plasmid DNA was kept constant at 100 ng for *Tbx5*, while titering in *Tbx20* (25 ng-100 ng). Expression vector plasmid DNA was kept constant at 100 ng total and 50 ng of *LacZ* reporter plasmid was used. Total amount of DNA was kept constant at 2 µg and transfected using Lipofectamine 2000 (Invitrogen). Plasmid DNA was diluted in OPTI-MEM (GibcoBRL) and complexes were allowed to form for 25 minutes at RT and added to each well. 48 hours post-transfection, cells were harvested using M-PER (Pierce) with gentle shaking. Luciferase activity was normalized to ß-galactosidase activity. All assays were done three independent times in triplicate. Results were graphed using normalized Relative Luciferase Units (RLUs).

Embryo Injections

Preparation and injection of *X. laevis* embryos was carried out as previously described (Wilson and Hemmati-Brivanlou, 1995). Embryos were staged according to Nieuwkoop and Faber (Nieuwkoop and Faber, 1967). Equal amounts of both *Tbx5* morpholinos were used in all injections. This combination is referred to in the text and figures as "TBX5MO". *Tbx20* morpholinos were also injected in combination, and referred to as "TBX20MO". TBX5MO was injected at the optimal (40 ng) or suboptimal (20 ng) doses, and TBX20MO was injected at the optimal (80 ng) or suboptimal (40 ng) doses. "Optimal dose" is defined as the dose empirically found to be efficient at blocking protein translation both in vitro and in vivo, and inducing a cardiac phenotype in nearly 100% of injected embryos, while "suboptimal dose" refers to the dose empirically found to be below the threshold of the full cardiac phenotype-

inducing dose. Sequence and details of morpholino oligonucleotides can be found at: www.unc.edu/~fconlon/SuppMat.pdf.

Whole-mount RNA *in situ* hybridization

Whole-mount *in situ* hybridizations were performed as previously described (Harland, 1991). Embryos were cleared using 2:1 benzyl benzoate/benzyl alcohol (Sigma) (Figs. 5 and 9).

Immunohistochemistry

Embryos were collected and fixed for 2 hours at 4 ºC in 4% paraformaldehyde and rinsed in PBS, incubated overnight in 30% sucrose in PBS at 4 ºC, mounted in OCT cryosectioning medium (Tissue Tek) and snap frozen. Cryostat sections (14um) sections were rinsed with wash buffer (PBS, 1% Triton, 1% serum), incubated at 4°C overnight with anti-tropomyosin (1:50; Developmental Studies Hybridoma Bank) (Kolker et al., 2000), and phalloidin conjugated to Alexa 488 flourophore (Molecular Probes). Sections were then rinsed with wash buffer and incubated with anti-mouse Cy3-conjugated secondary antibody (1:200), (Sigma). Sections were rinsed and incubated for 20 minutes at RT with DAPI, cover slipped and visualized on a Zeiss LSM410 confocal microscope.

Translation Inhibition by Morpholinos

In vitro translations were performed using TNT® Coupled Reticulocyte Lysate System (Promega) following the manufacturer's protocol. Western protocol and antibody information can be obtained at: www.unc.edu/~fconlon/SuppMat.pdf. We have recently demonstrated that *X. laevis* SHP-2 is uniformly expressed throughout early development (Y. Langdon and FLC, unpublished data) and was used as a loading control (1:2500)

(Transduction Laboratories) with peroxidase-conjugated AffiniPure donkey anti-mouse (H+L) secondary antibody (1:10,000). For in vivo translation analyses, embryos were injected with MOs and mRNA at the one-cell stage and animal caps cut at stage 8. At sibling stage 10, and 10 animal caps per treatment were collected and lysed in 100 µl of lysis buffer: 200 mM NaCl, 20 mM NaF, 50 mM Tris pH 7.5, 5 mM EDTA, 1% IGEPAL, 1% Triton X-100 (Sigma), Complete EDTA-free Protease Inhibitor (Roche). Lysates were resolved on 12% SDS-PAGE gels, and visualization was carried out using Western Lightning Chemiluminescence Reagent Plus (PerkinElmer Life Sciences, Inc.).

Glutathione-S-Transferase Pulldown Assays

GST pulldown assays were performed using the MicroSpin GST Purification Module (Amersham Biosciences) according to the manufacturer's protocol. Hemagglutinin (HA)-tagged putative interacting proteins were produced in 293T cells (www.unc.edu/~fconlon/SuppMat.pdf). Lysates were sonicated 3 times for 10 seconds prior to centrifugation at 12,000 rpm at 4°C for 10 minutes, and the supernatant was collected. GST-fusion protein lysates and putative interacting protein lysates were loaded on GST columns, incubated for 1.5 hours at 25°C, eluted, electrophoresed on a 12% SDS-PAGE gel, and transferred to PolyScreen PVDF Transfer Membranes. HA-tagged proteins were detected with mouse HA.11 primary antibody (1:1,000, Covance Research Products) and with peroxidase-conjugated AffiniPure donkey anti-mouse (H+L) secondary antibody (1:10,000). GST-fusion proteins were detected with rabbit anti-GST primary antibody (1:25,000, Sigma-Aldrich) and with Peroxidase-conjugated AffiniPure donkey anti-rabbit (H+L) secondary antibody (1:10,000, Jackson ImmunoResearch Laboratories).

RESULTS

TBX5 and TBX20 are required for heart morphogenesis

To analyze the requirement for *Tbx5* and *Tbx20* in cardiogenesis, antisense morpholinos were designed against the 5' UTRs and translational start sites of the respective cDNAs (Fig. 2.1). Due to the lack of antibodies against endogenous TBX5 or TBX20, we tested the efficiency and specificity of morpholino translation inhibition using V5 epitope-tagged versions of TBX5 and TBX20 both in vitro and in vivo. To this end, transcription/translation reactions were incubated with each cDNA construct alone and together with increasing concentrations of morpholinos (Fig. 2.1). TBX20MO was included as control for TBX5MO and vice versa, and a ControlMO used for both. Results from these assays show that TBX5MO blocks translation of TBX5-V5, while TBX20MO and ControlMO do not. Similarly, TBX20MO blocks translation of TBX20-V5 in vitro (Fig.1B, C).

To determine if TBX5MO and TBX20MO block translation in vivo, we injected *Tbx5-V5* or *Tbx20-V5* mRNA alone or in the presence of morpholinos into one-cell stage embryos. Animal caps were cut at stage 8 and allowed to develop to stage 10, at which point Western blot analyses were performed. Results from these studies demonstrate that in animal caps, TBX5MO blocks TBX5-V5 translation, while TBX20MO blocks TBX20-V5 translation (Fig. 2.1D, E). We have further shown via sequence alignments that *Tbx5* does not contain binding sites for the *Tbx20* morpholinos and vice versa (Fig. 2.S1; supplementary data). We did note that the introduction of TBX20MO results in a slight decrease in TBX5 in vivo, and vice versa (see Discussion).

To determine the requirement of TBX5 and TBX20 in heart development, we injected TBX5MO, TBX20MO, or ControlMO into one-cell stage embryos. No significant differences are seen between TBX5 morphants, TBX20 morphants, control morphants, or

uninjected siblings throughout gastrulation and neurulation stages. However, a slight delay in developmental stage is evident in TBX5 and TBX20 morphants relative to control morphants and uninjected embryos by neurulation stage, (~st. 16). By cardiac looping stages, (~st. 38) (Kolker et al., 2000; Mohun and Leong, 1999; Mohun, 2000; Newman and Krieg, 1999) a reduction in cardiac mass is evident in the morphants, and by stage 40 both morphants display grossly abnormal heart morphology (Fig. 2.2A, C, E). At this stage, 82% of TBX5 morphants and 100% of TBX20 morphants display prominent cardiac defects, as scored by the presence of an unlooped heart tube, a reduction in cardiac mass and the presence of a pericardial edema (Fig. 2.2G). After terminal cardiomyocyte differentiation has begun (~st. 45) (Kolker et al., 2000; Mohun and Leong, 1999; Mohun, 2000; Newman and Krieg, 1999) TBX5 and TBX20 morphants display dramatically smaller hearts and in many embryos cardiac tissue is barely detectable (Fig. 2.2B, C, E, F). However, the remaining cardiac tissue still retains some degree of contractility, but confined to a small patch of contractile tissue in the dorsal-most aspect of the cardiac cavity. Embryos derived from injection of *Tbx20* morpholinos directed against the antisense transcript, *Tbx5* morpholinos containing mismatches, MOs directed against zebrafish *Tbx5* and Gene Tools, LLC's MO control, gave no observable phenotype at any concentration (data not shown). These observations, and the findings that the TBX5 and TBX20 protein levels can be reduced or eliminated both in vitro and in vivo, suggest that the phenotypes we observe are specific for knocking down TBX5 and TBX20.

To further define the requirements for *Tbx5* and *Tbx20* during cardiogenesis, we carried out a detailed analysis of TBX5MO and TBX20MO derived hearts relative to those from ControlMO injections. For these analyses, staged-matched TBX5MO, TBX20MO, and ControlMO embryos were collected at stage 37, serial sectioned and stained for the terminal

differentiation markers Tropomyosin and Cardiac Actin, and counterstained with DAPI (Fig. 2.3). Results from this analysis clearly demonstrate that TBX5MO and TBX20MO derived hearts fail to undergo cardiac looping and chamber formation. In addition, quantification of cardiac cell number shows that both TBX5MO and TBX20MO hearts have a significant reduction in cell number compared to controls, and TBX20MO-derived hearts have a significantly fewer cardiomyocytes than those from TBX5MO (Fig. 2.3J).

In addition to these defects we note some unique features to both the TBX5MO and TBX20MO derived hearts, most notably TBX5MO hearts remain as an open cardiac trough (Mohun et al., 2000) throughout development and fail to form a cardiac tube (Fig. 2.3A-F). In contrast, TBX20MO derived embryos form a cardiac tube; however, the lumen often collapses and the hearts concomitantly show a dramatic decrease in the presence of cardiac actin (Fig. 2.3A-C, G-I). Together this data demonstrates a requirement for both *Tbx5* and *Tbx20* in normal heart morphogenesis, and implies that TBX5 cannot compensate for the loss of TBX20, nor can TBX20 compensate for the loss of TBX5 and suggests that *Tbx5* and *Tbx20* play non-redundant roles during normal heart development.

Analysis of hearts derived from TBX5MO and TBX20MO embryos shows a significant decrease in cardiac cell number. To determine if this is due to alterations in cardiac cell commitment, we performed whole mount in situ hybridization with the early heart marker, *Nkx2.5* (Fig. 2.4). This analysis was carried out on embryos derived from TBX5MO, TBX20MO and ControlMO embryos over the period of cardiac cell commitment and migration and differentiation (stages 16-36). We could detect no obvious difference in the number or spatial distribution of *Nkx2.5*-expressing cells prior to stage 24 (Fig. 2.4). Consistent with our initial analysis, after stage 24 the hearts from TBX5MO and TBX20MO

embryos are morphologically abnormal and smaller in size, and therefore show a reduced domain of *Nkx2.5* expression.

The above results demonstrate that *Tbx5* and *Tbx20* are required for normal heart morphogenesis, but not for specification and migration of the cardiac precursors. To extend these findings, in situ hybridizations were performed on stage 36 morphants and controls using the late heart markers *atrial natriuretic factor* (*XANF*)(Small and Krieg, 2000) and *cardiac troponin I* (*XTnIc*) (Logan and Mohun, 1993). As shown in Fig. 5, the terminally differentiated cardiomyocyte marker *XTnIc* displays properly localized expression in the cardiac tissue of morphant embryos and appears to be expressed to the same degree, although due to the reduced cardiac mass it is expressed in fewer cells (Fig. 2.5D-F). *XANF* is a putative target of *Tbx5*, and its expression is reduced in the absence of *Tbx5* (Bruneau et al., 2001). In agreement with these findings, we show that *Xenopus* TBX5 activates transcription of a rat *Nppa/ANF* reporter plasmid (Fig. 2.6) and consistent with TBX5MO blocking TBX5, *XANF* expression is either greatly reduced or absent in TBX5 morphants, however, *XANF* is still detected in TBX20 morphants (Fig. 2.5A-C). These results indicate that terminal differentiation still occurs in both TBX5 and TBX20 morphant embryos and implies that *XANF* is an evolutionarily conserved target of TBX5.

Tbx5 and *Tbx20* are not dependent on each other's expression

Since *Tbx5* and *Tbx20* are co-expressed within the heart and have similar requirements in heart development, we next asked whether *Tbx5* and *Tbx20* function linearly within the same molecular pathway. To address this question, we analyzed the expression of *Tbx20* in TBX5MO-injected embryos and *Tbx5* expression in TBX20MO-injected embryos. We could detect no differences in the expression of either gene in morpholino-injected embryos (Fig.

2.7); both genes remain expressed in the forming heart tissue, despite the reduction of cardiac tissue mass in morpholino-injected embryos. Based on these results we conclude TBX5 is not essential for *Tbx20* expression, nor is *Tbx20* dependent on TBX5.

TBX5 affects TBX20 transcriptional activity

Our results strongly suggest that *Tbx5* and *Tbx20* do not function linearly within the same pathway yet have a similar requirement in heart development. We therefore carried out a series of experiments to test if TBX5 and TBX20 have either competing or complimentary functions at the molecular level. We first tested the cellular localization of TBX5 and TBX20. For these studies V5 epitope-tagged versions of the full-length cDNAs were transfected into NIH/3T3 cells. Immunohistochemistry on the transfected cells show that similar to TBX5 (Collavoli et al., 2003; Fan et al., 2003; Zaragoza et al., 2004), TBX20 is localized exclusively to the nucleus. (Fig. 2.6C-H)

We next tested if TBX5 and TBX20 can function to regulate the levels of transcription of the TBX5 target gene *Nppa/ANF*. To test for DNA specific binding and transcriptional activities, we transfected in full-length versions of *Tbx5* and *Tbx20*, either alone or in combination, with the putative *Tbx5* target *Nppa/ANF* reporter construct into 293T cells. Consistent with studies using the mouse *Tbx5* orthologue (Hiroi et al., 2001), TBX5 can weakly activate the rat *Nppa/ANF* reporter. In contrast, *Tbx20* alone can activate the *Nppa/ANF* in a dose dependent fashion. However, in the presence of TBX5, TBX20 can have the converse effect on the *Nppa/ANF* reporter. In the presence of TBX5, at high and low doses of TBX20 there is increased activation of the reporter construct, while at moderate doses there is a repressive effect (Fig. 2.6I). Thus, the presence of TBX5 appears to alter TBX20 transcriptional activity.

TBX5 and TBX20 physically interact with one another

Given the similarity in phenotypes of TBX5 and TBX20 morphant embryos, and the observation that *Tbx5* and *Tbx20* are not dependent on one another's expression, we next assessed whether TBX5 and TBX20 can physically interact. TBX5 fused to Glutathione-S-Transferase (GST) was incubated with HA-tagged TBX20 or NKX2-5. Pulldown experiments were then performed to assess whether TBX20 can bind to TBX5. NKX2-5 has been shown to interact with TBX5 and thus serves as a positive control (Hiroi et al., 2001). As shown in Fig. 2.8A, bacterially translated GST-TBX5 is able to bind HA-TBX20 and HA-NKX2-5 produced from 293T cells, in contrast to GST alone, which does not bind either protein. These results reveal that TBX5 and TBX20 can interact in vitro. This is the first report of physical interaction between T-box proteins.

Having demonstrated that TBX5 and TBX20 interact, we next mapped the interaction domains of TBX5 and TBX20. To this end, we constructed a deletion series of both GST-tagged TBX5 and HA-tagged TBX20. As shown in Fig. 2.8B, GST-TBX5 proteins lacking the C-terminus still bind HA-TBX20, however when the small N-terminus and T-box domain are removed from GST-TBX5, HA-TBX20 fails to bind. Thus, the domain responsible for TBX20 binding lies within the N-terminus and T-domain of TBX5. Similarly, a C-terminal deletion of HA-TBX20 still binds to GST-TBX5, in contrast to deletions of the HA-TBX20 N-terminus and T-domain (Fig. 2.8C). As seen in the •N/C lane in Fig. 2.8C, the HA-TBX20 deletion containing only the T-box domain did not bind GST-TBX5. However, we were unable to obtain comparable amounts of the HA-T20-•N/C protein, as seen in the input lane. This could be due to mRNA or protein instability. In an attempt to circumvent this problem, the amount of HA-T20-•N/C protein incubated with GST-TBX5 was increased 2-fold as

compared to the rest of the experiments. These results indicate that the N-terminus and possibly the T-domain of TBX20 are required for its interaction with TBX5, although we cannot rule out the possibility that the amount of HA-T20-•N/C protein was insufficient to identify a requirement for the T-domain. In summary, our results reveal that the domains responsible for the interaction between TBX20 and TBX5 map to within the N-terminal and T-box domains in both proteins.

Tbx5 and *Tbx20* cooperate to regulate heart morphogenesis

Given that TBX5 and TBX20 physically interact with one another, we hypothesized that *Tbx5* and *Tbx20* may function cooperatively to control cardiogenesis. To test this hypothesis, we coinjected concentrations of TBX5MO and TBX20MO below the threshold at which cardiac phenotypes are efficiently induced when injected individually. At a concentration of 40 ng per embryo for *Tbx5* morpholinos and 80 ng per embryo for *Tbx20* morpholinos, injections yield consistent heart phenotypes in 82% of TBX5MO-injected embryos and in 100% of TBX20MO-injected embryos (Fig. 2.2). We refer to this dose as the "optimal" dose, because it is the dose at which we observe the efficient and penetrant cardiac phenotypes. At half doses, 20 ng per embryo for TBX5MO and 40 ng per embryo for TBX20MO, each morpholino yields significantly fewer and weaker heart phenotypes compared to the full dose (Fig. 2.9M, data not shown). We refer to this concentration as the "suboptimal" dose for inducing cardiac defects. The terms "optimal" and "suboptimal" are only used to refer to the concentrations that yield fully penetrant or partially penetrant cardiac phenotypes, respectively.

To address the question of whether *Tbx5* and *Tbx20* cooperate in cardiogenesis, we injected TBX5MO and TBX20MO individually at suboptimal doses in combination with

ControlMO to keep total morpholino concentrations equal in all injections. TBX5MO was then coinjected with TBX20MO, each at the suboptimal dose. ControlMO injected at 80 ng/embryo served as control. As shown in Fig. 2.9, only 4% of embryos injected with suboptimal TBX5MO/ControlMO displayed a pericardial edema, unlooped heart tubes, and a reduction in cardiac mass. Suboptimal TBX20MO/ControlMO yields only 13% cardiac defects. In suboptimal injections, the majority of embryos appeared normal, while the few cardiac phenotypes produced were much less severe than at optimal doses (e.g. barely detectable reduction in cardiac mass, slight perturbation of looping and little or no pericardial edema). When coinjected at suboptimal doses, 74% of TBX5MO/TBX20MO coinjected embryos display dramatic cardiac defects compared to 0% of ControlMO-injected embryos (Fig. 2.9D, H, L). The observation that the percentage of heart defects in double morphants is more than additive suggests that *Tbx5* and *Tbx20* synergistically act to control heart morphogenesis.

If *Tbx5* and *Tbx20* cooperate to regulate cardiogenesis, one might expect a more severe alteration in cardiac morphology and marker expression when the levels of both proteins are reduced. To address this question we performed in situ hybridizations on stage 36 embryos from the above double injection experiment using *Nkx2-5*, *XANF*, and *XTnIc* probes. As shown in Fig. 2.9, all three markers are expressed normally in embryos injected with suboptimal doses of TBX5MO and TBX20MO as compared to ControlMO. However, heart marker expression in the double morphant embryos is markedly reduced, particularly *XANF*. Both *Nkx2-5* and *XTnIc* are still detectable in the heart region, albeit in fewer cells. Thus, the synergistic cooperation of TBX5 and TBX20 are required for proper heart development.

DISCUSSION

Members of the T-box family of proteins play a fundamental role in patterning the developing vertebrate heart, however, the precise cellular requirements for any one family member remains largely unknown. In this study, we demonstrate that TBX5 and TBX20 are both required for early cardiac morphogenesis. Moreover, we show that TBX5 and TBX20 function in the same pathway implying a synergistic role for these two proteins during early heart development. Consistent with this proposal, we show that TBX5 and TBX20 can physically and functionally interact, therefore providing the first evidence for direct interaction between members of the T-box gene family.

Functions of *Tbx5* and *Tbx20* in Cardiac Morphogenesis

Our studies show that *Tbx5* and *Tbx20* are required for similar cellular processes in the developing heart. This data demonstrates a non-redundant function for TBX5 and TBX20 during cardiac morphogenesis; neither protein can compensate for the other in heart morphogenesis. The lack of redundancy at the molecular level is corroborated by the observation that the putative TBX5 target gene *XANF* either is not expressed or is expressed very weakly in TBX5 morphant embryos, while being expressed at the proper time, place and levels in TBX20 morphant embryos. Together this data suggests that TBX5 and TBX20 act in a non-redundant fashion to control morphogenetic movements of early heart tissue.

The cardiac defects in response to a reduction of either TBX5 or TBX20 appear to represent a block in an early morphological step in heart formation. Since the spatial distribution of *Nkx2-5* is unaltered throughout early development in TBX5MO, TBX20MO and ControlMO injected embryos, and since *Nkx2.5*, *Tbx5*, and *Tbx20* continue to be expressed until the later stages of heart development, and TBX5 and TBX20 morphants

express markers of terminal muscle differentiation, neither *Tbx5* nor *Tbx20* appear to be required for commitment, migration or terminal differentiation of cardiac tissue. Thus, both *Tbx5* and *Tbx20* appear to be required to direct the coordinated events that occur during the early steps of heart morphogenesis.

Consistent with this hypothesis, both TBX5 and TBX20 morphant derived hearts are greatly extended along the anterior-posterior axis, and the heart tube fails to correctly loop and undergo chamber formation. As a result, embryos display pericardial edemas, have impaired blood flow (Fig. 2.S2; supplementary data), an irregular heartbeat (data not shown) and ultimately die. Thus, the alteration in heart morphology appears to be the primary outcome of perturbing TBX5 or TBX20 function.

Past attempts to interfere with *Tbx5* function in *X. laevis* were carried out by the misexpression of a putative interfering form of *Tbx5* that leads to either the absence or severe malformations of the heart (Horb and Thomsen, 1999). In instances in which the heart does form, there is a reduction or block in myocardial tissue formation and a failure of the heart to undergo looping. Our results with *Tbx5*-specific morpholinos show a less severe heart phenotype than those reported with the dominant interfering *Tbx5* but bear a close resemblance to those reported for the zebrafish *Tbx5* mutant, *heartstrings* (Garrity et al., 2002). This may be due to the dominant-interfering form of *Tbx5* used in the *X. laevis* studies interfering with the function of both *Tbx5* and *Tbx20* or possibly other T-box family members expressed in the developing heart, e.g. *Tbx1* and *Tbx2* (Chapman et al., 1996), as has been shown for other *Engrailed* fusions (Horb and Thomsen, 1997). However, in the absence of a TBX5 specific antibody, we cannot formally rule out the possibility that some residual TBX5 protein is present in morphant embryos leading to a less severe phenotype in our studies.

Tbx5 and Tbx20 are not dependent on one another's function

The phenotypes of TBX5 and TBX20 morphant embryos do not appear to act in a linear pathway since the spatial and temporal expression of *Tbx5* appears unaltered in TBX20 morphants, and vice versa. These findings are in agreement with studies showing normal expression of *Tbx20* in *Tbx5* mutant mice (Stennard et al., 2003) but in apparent conflict with a second study reporting the downregulation of *Tbx5* in zebrafish embryos injected with a *Tbx20* morpholino (Szeto et al., 2002). Although the zebrafish and *X. laevis* orthologues of *Tbx20* share a very high degree of identity at the protein level (86%), the differences between the two orthologues may reflect a species difference as, for example, has been reported for the endodermal-inducing activities of the T-box-containing gene *Brachyury* (Marcellini et al., 2003). Although no alterations in *Tbx5* or *Tbx20* RNA levels were observed in morphant embryos, we did observe a downregulation of TBX5 protein in response to *Tbx20* morpholinos in vivo, and vice versa, but not in vitro (Fig. 2.1), raising the interesting possibility that cross-regulation may be occurring between TBX5 and TBX20 at the level of translation. Since similar studies have not been conducted in zebrafish, it is not possible at this time to know the mechanisms of cross-regulation or if this is a conserved response to interfering with TBX5 or TBX20.

TBX5 and TBX20 Heterodimerization

Although *Tbx5* and *Tbx20* are coexpressed and both function in early heart development, the genes appear to be regulated through separate pathways. For example, *Tbx20* but not *Tbx5* can be induced in response to *BMP2* signaling (Plageman and Yutzey, 2004). Taken together with our results demonstrating a physical interaction between TBX5 and TBX20, these data

would suggest that TBX5 and TBX20 function in parallel pathways that converge upon TBX5:TBX20 heterodimerization. This model is also supported by our results showing a functional interaction between TBX5 and TBX20: embryos derived from injections of suboptimal doses of *Tbx5* and *Tbx20* morpholinos have only minor effects on heart development in a small proportion of the embryos. However, when injected in combination 74% of all embryos examined displayed grossly abnormal heart formation.

What are the possible cellular functions of TBX5 and TBX20 in heart development? Past studies on T-box genes have shown a direct link between members of the T-box gene family and cell adhesion. For example, embryos homozygous for mutations in *Brachyury*, the founding member of the T-box gene family, show an inability of the mesoderm to properly migrate along the extracellular matrix leading to an inability of the mesodermal germ layer to complete the morphogenetic movements normally associated with gastrulation (reviewed in Showell et al., 2004). We propose an analogous model for TBX5 and TBX20 function in regulating cell polarity or adhesion events associated with heart morphogenesis. We propose that TBX5 and TBX20 function to control polarity or adhesive properties of cardiac tissue once the two heart fields merge along the anterior midline, and that target specificity is regulated through TBX5 and TBX20 protein-protein interactions. In agreement with this proposal, we have recently shown that alterations in cardiac cell numbers, survival and proliferation in TBX5MO derived embryos are a consequence of disrupting TBX5 function (S. Goetz and FLC, in preparation). This observation, taken together with our findings that cardiac gene expression patterns are not disrupted in TBX5MO or TBX20MOs derived embryos, suggests that the primary role for TBX5 and TBX20 is to control cardiac cell polarity or adhesion.

It is worth noting that neither TBX5 nor TBX20 have strong transcriptional activation or repression activity by themselves (Bruneau et al., 2001; Hiroi et al., 2001; Plageman and Yutzey, 2004; Stennard et al., 2003). Thus, transcriptional activity appears to be governed by protein-protein interactions. Past studies have identified several other interacting partners for both TBX5 and TBX20. For example, both TBX5 and TBX20 have been shown to interact with the homeobox-containing transcription factor NKX2-5 (Bruneau et al., 2001; Hiroi et al., 2001; Stennard et al., 2003), consistent with clinical studies showing that HOS patients and humans heterozygous for NKX2-5 display many of the same cardiac defects (Elliott et al., 2003; Goldmuntz et al., 2001; Prall et al., 2002).

How might TBX5:TBX20 heterodimerization affect target choice? It may be that the role of TBX5:TBX20 dimerization is to sequester TBX5 and thereby block its interaction with other proteins such as NKX2.5 thereby indirectly inhibiting the induction of cardiac specific genes such as *XANF*. However, several lines of evidence argue against such a proposal. For example, at low and high concentrations TBX20 can increase transcription of the *Nppa/ANF* reporter in the presence of TBX5, while showing a repressive activity at intermediate concentrations, suggesting that in certain contexts TBX20 can cooperate with TBX5 to activate transcription, while antagonizing TBX5 activity in others. An alternative possibility is that TBX20 target choice and ability to function as a transcriptional activator or repressor is governed by its choice of interacting partners. Consistent with this hypothesis, Stennard et al (2003) have shown that NKX2.5, GATA4, and GATA5 interact with TBX20, and the interactions occur through the same domain of TBX20 that we have shown interacts with TBX5, at least in the cases of NKX2.5 and GATA4. Furthermore, the authors demonstrated that TBX20 can repress synergistic activation of a connexin 40 reporter by NKX2.5 and GATA4, while synergistically activating the same reporter with NKX2.5 and

GATA5. Thus, TBX20 may be able to function both as a transcriptional activator or repressor, and this decision is based on its choice of protein partners. In addition, TBX5 and TBX20 have been shown to display different binding affinities for different T-box binding sites (Stennard et al., 2003). For example, TBX20 unlike TBX5 can bind to the *Brachyury* target site while TBX5 has a higher affinity than TBX20 for the T-box binding site in the *Nppa/ANF* promoter. Thus, downstream target selection may be dictated by homodimerization verses heterodimerization. This is supported by the recent findings that several genes involved in heart development are found to contain multiple T-box binding sites (R. Schwartz personnel communication, FLC unpublished findings). Our model would suggest that TBX5 and TBX20 target selection and transcriptional activity is based on partner choice in a specific tissue at a specific time. However, it still remains to be established which protein interactions take place in the developing heart and in turn, what governs the choice of partners for TBX5 or TBX20. These are presently areas under active investigation.

Acknowledgements

This work is supported by grants from the NIH, AHA and an award from the UNC Medical Alumni Association. DDB is funded by a NSF fellowship. We would like to thank Bahay Gulle for help generating constructs, Judy Chang, Amanda Marshburn, Kristian Duggan, Caroline Collins, Hui-Hua Li, and Cam Patterson for assistance. We would also like to thank Chris Showell and Larysa Pevny for critical reading of the manuscript and helpful suggestions.

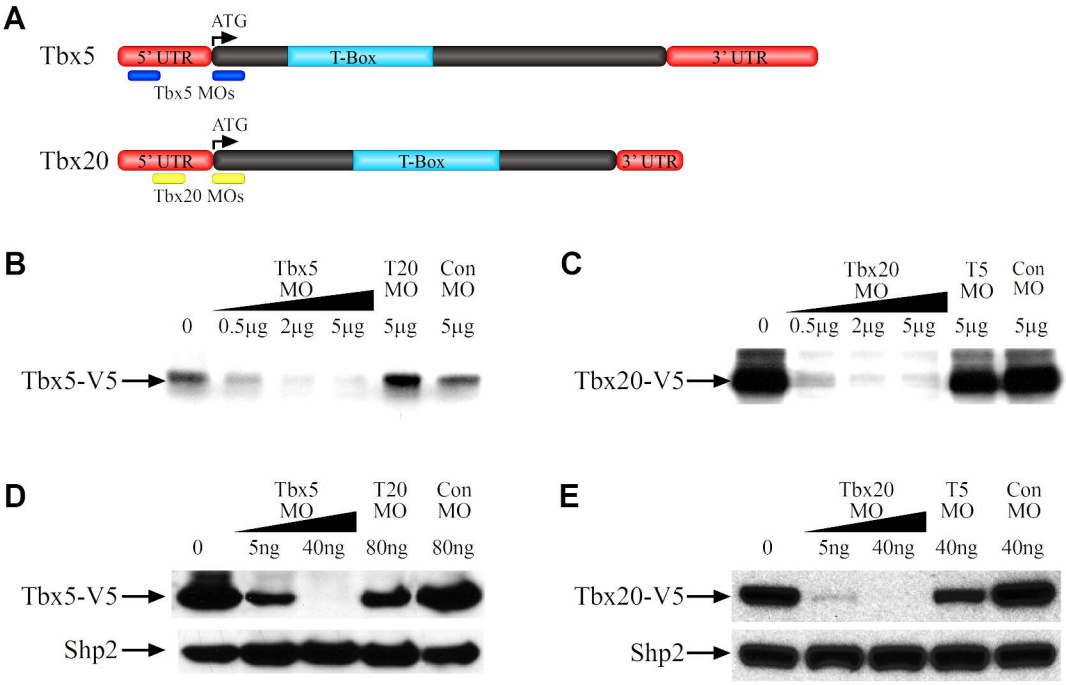

Figure 2.1. *Tbx5 and Tbx20 morpholinos block translation of their respective target proteins.*

(A) TBX5MO and TBX20MO positions relative to *Tbx5* and *Tbx20* cDNA. (B) Inhibition of TBX5-V5 translation in vitro by TBX5MO. TBX20MO and ControlMO serve as controls. Each reaction contains 1*u*g of *Tbx5*-V5 circular plasmid along with the indicated amounts of MO. (C) Inhibition of TBX20-V5 translation in vitro by TBX20MO. TBX5MO and ControlMO serve as controls. Each reaction contains 1*u*g of *Tbx20*-V5 circular plasmid along with the indicated amounts of MO. (D) Inhibition of TBX5-V5 translation by TBX5MO in animal caps. TBX20MO and ControlMO serve as controls. Probed with anti-V5 and re-probed with anti-PTP1D/SHP2 as a loading control. Embryos injected with 2 ng mRNA and the indicated amounts of MO. (E) Inhibition of TBX20-V5 translation by TBX20MO in animal caps. TBX20MO and ControlMO serve as controls. Probed with anti-V5 and re-

probed with anti-PTP1D/SHP2 as a loading control. Embryos injected with 2 ng mRNA and the indicated amounts of MO.

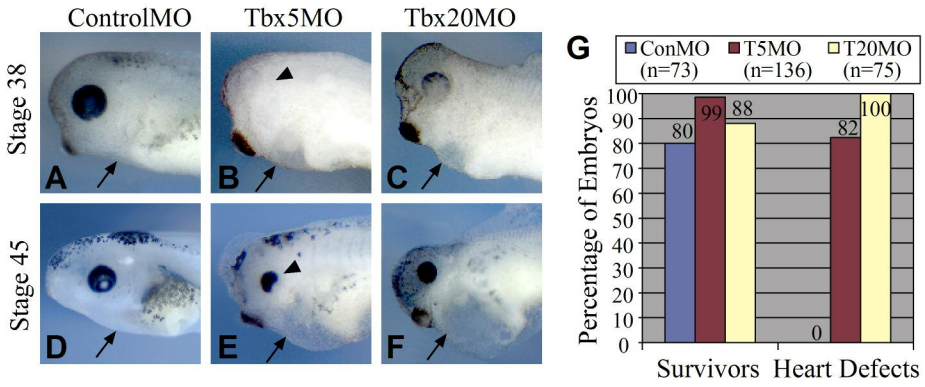

Figure 2.2*. Tbx5 and Tbx20 are required for proper cardiogenesis.*

(A-F) Morpholino-injected tadpoles at the indicated stages. Control morphant embryos (A, B), TBX5 morphant embryos (C, D), TBX20 morphant embryos (E, F). Arrows indicate the heart region, arrowheads indicate the eye. Note the reduction in eye tissue in response to TBX5MO but not TBX20MO. (G) Chart displaying the percentage of morphants surviving and displaying cardiac abnormalities as scored by the presence of an unlooped heart tube, a reduction in cardiac mass and the presence of a pericardial edema.

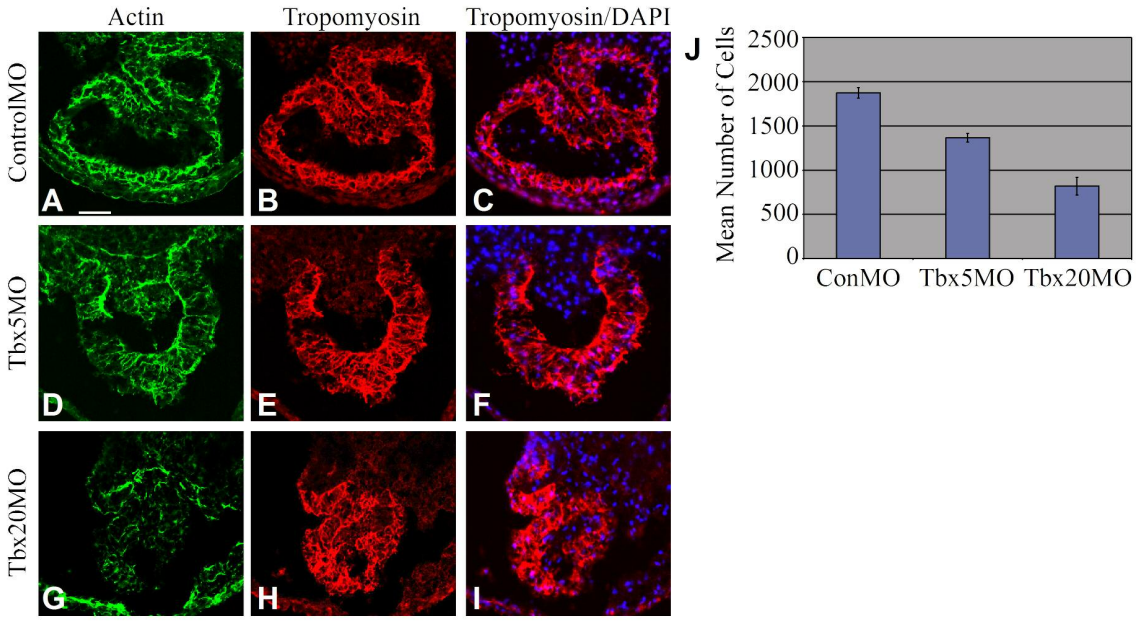

Figure 2.3. *TBX5 and TBX20 morphants fail to undergo looping and chamber formation and display reduced cardiac cell numbers.*

Cryosections of TBX5 and TBX20 morphant hearts. (A-C) ControlMO, (D-F) TBX5MO, and (G-I) TBX20MO. Sections stained for Cardiac Actin (green), Tropomyosin (red) and DAPI (blue). (J) Mean number of cells per heart counted.

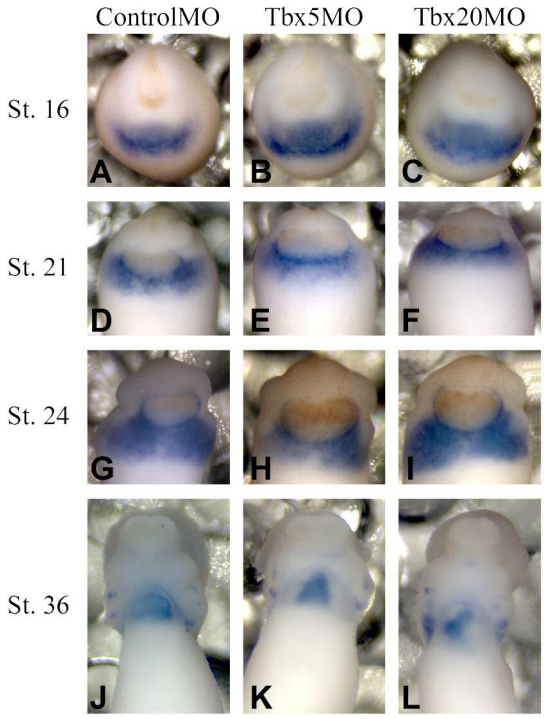

Figure 2.4. *Cardiac specification is unaltered in TBX5 and TBX20 morphants*.

Wholemount in situ with *Nkx2.5* on stage matched (A,D, G, J) ControlMO, (B,E,H,K) TBX5MO, or (C, F, I, L) TBX20MO derived embryos.

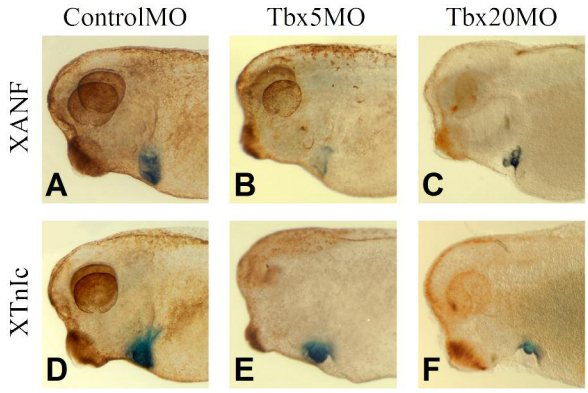

***Figure 2.5**. TBX5 and TBX20 morphants display dramatic morphological defects.*

Whole-mount in situ hybridizations of cleared stage 36 embryos. (A-C) *ANF* whole mount in situ hybridization. (D-F) *XTnIc* whole mount in situ hybridization. (A, D) ControlMO. (B, E), TBX5MO, (C, F) TBX20MO.

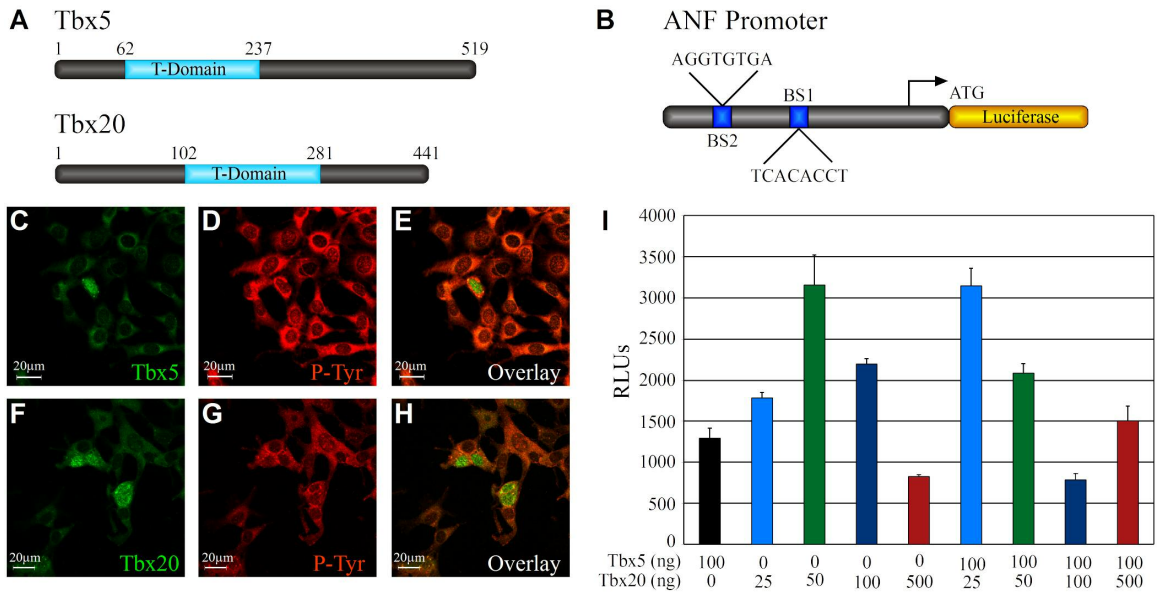

Figure 2.6. *Tbx5 and Tbx20 are localized to the nucleus and can activate transcription on the Nppa/ANF promoter.*

(A) Schematic depicting the amino acid positions of the T-box domains of *Tbx5* and *Tbx20*. (B) Schematic of Rat *Nppa/ANF-luciferase* reporter construct showing T-box binding site consensus sequences and their relative position within the promoter relative to translation start site. (C,F) Transfected cells were stained with anti-V5 (Cy2, green) for TBX5-V5 and TBX20-V5 and (D,G) anti-phosphotyrosine (Cy3, red) to visualize cytoplasmic compartment. (E,H) Overlay image of Cy2 and Cy3 staining. (I) Rat *ANF-luciferase* co-transfected with a constant amount of *Tbx5* (50 ng) and increasing amounts of *Tbx20* (25, 50, 100 and 500 ng) in 293T cells and level of transcriptional activation expressed as Relative Luciferase Units based on average of three independent experiments performed in triplicate.

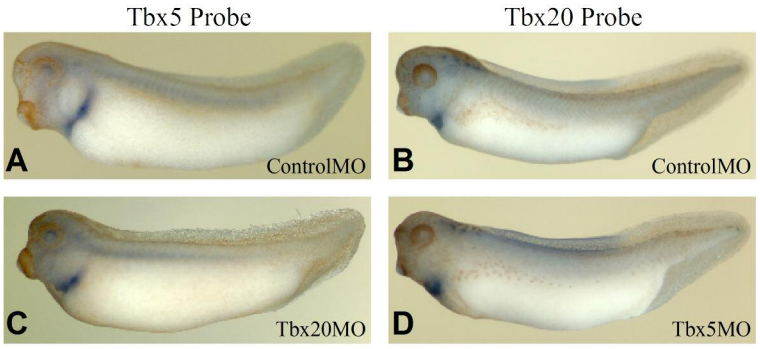

Figure 2.7. *Tbx5 and Tbx20 are not required for each other's expression.*

Embryos injected at the one-cell stage with ControlMO, TBX5MO, or TBX20MO. (A, C) Whole-mount in situ hybridization showing *Tbx5* expression. (B, D) Whole-mount in situ hybridization showing *Tbx20* expression.

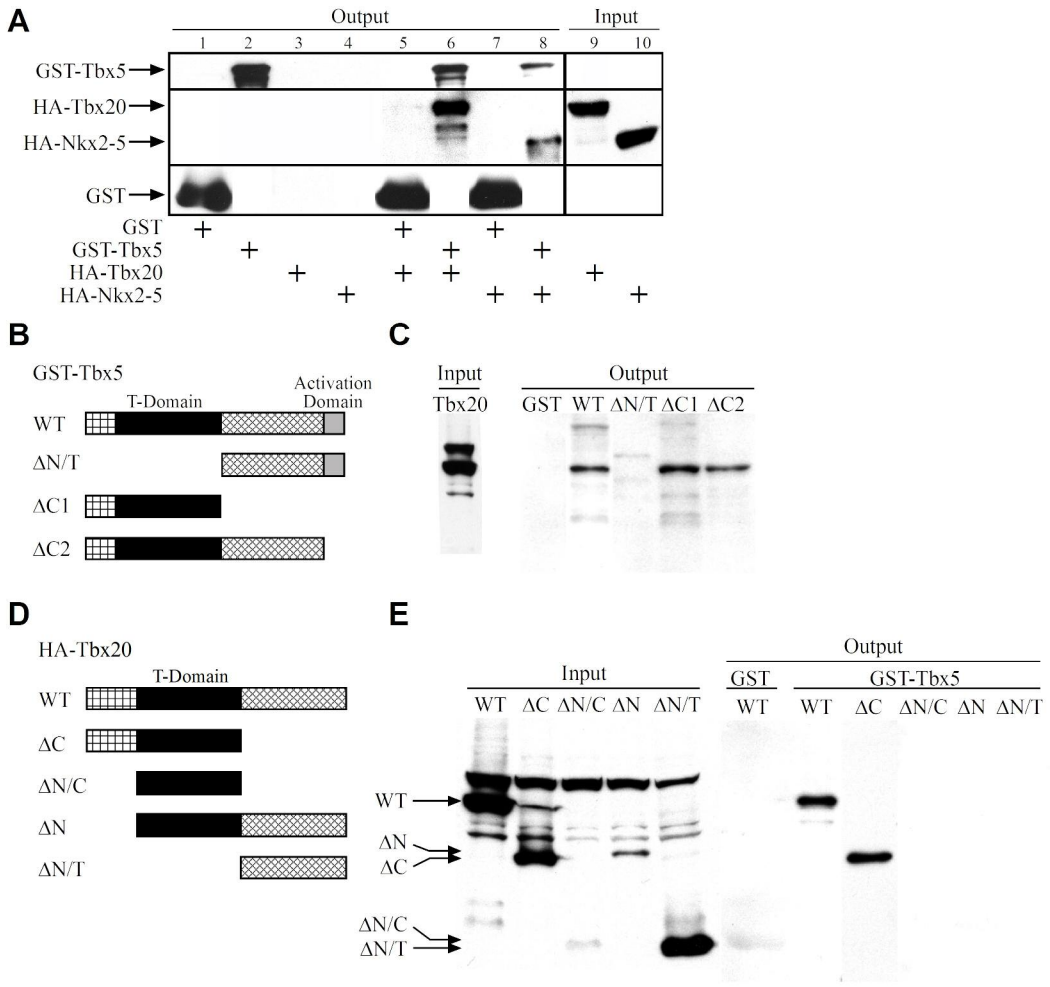

Figure 2.8. *TBX5 and TBX20 physically interact.*

Cell lysates containing GST- and/or HA-tagged proteins were incubated on GST and eluted, and separated by SDS-PAGE. GST proteins were detected using anti-GST antibodies and HA-tagged proteins were detected with anti-HA antibodies. (A) Association of TBX5 with TBX20 is shown by pulldown of HA-TBX20 with GST-TBX5. HA-NKX2-5 serves as positive control. 15% of output and 7.5% of input was probed. (B, C) Pulldown of full-length HA-TBX20 with a GST-tagged TBX5 deletion series reveals an interaction domain in the N-terminus and T-box region of TBX5. Each reaction was probed with anti-HA antibodies. 7.5% of input and 15% of output was probed. (C, D) Pulldown of HA-TBX20 deletion series

with full-length GST-TBX5 reveals an interaction domain within the N-terminus and T-box of TBX20. Each reaction was probed with anti-HA antibodies. 7.5% of input and 15% of output was probed, except in the case of •N/C in which the amount of protein probed was only 4% due to the increase in total amount of •N/C protein used in pulldown (see text).

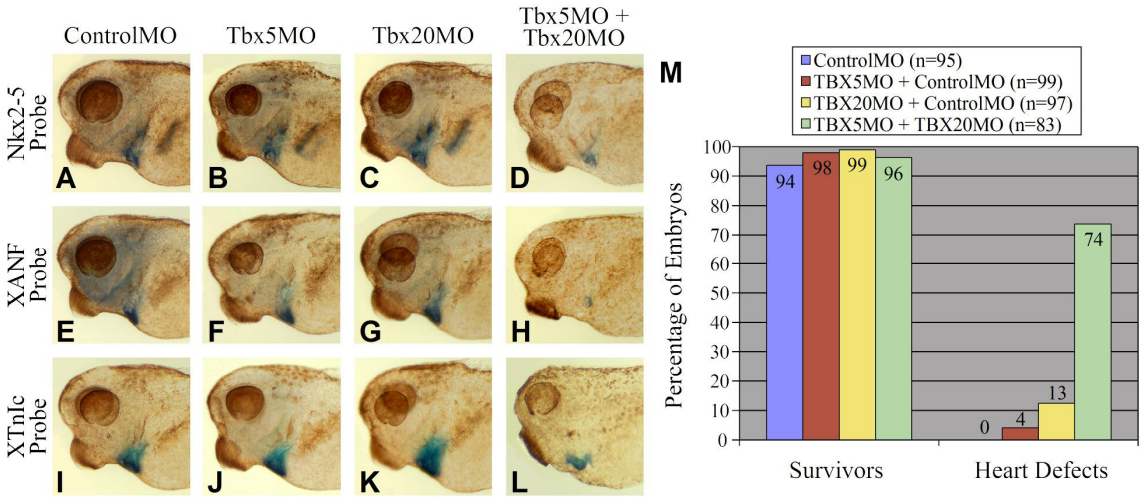

Figure 2.9. Tbx5 and Tbx20 synergistically act to regulate cardiac gene expression.

(A-L) Embryos injected with the indicated morpholinos at the one-cell stage. (A-D) *Nkx2-5* whole mount in situ hybridization. (E-H) *XANF* whole mount in situ hybridization. (I-L) *XTnIc* whole mount in situ hybridization. (A, E, I) ControlMO, (B, F, J) TBX5MO injected at suboptimal dose, (C, G, K) TBX20MO injected at suboptimal dose, (D, H, L) TBX5MO and TBX20MO injected in combination at suboptimal doses. All embryo were cleared to reveal heart expression. (M) Statistics for embryos injected with suboptimal doses of TBX5MO and TBX20MO in combination with each other or with ControlMO. Hearts were judged as having defects if they displayed a pericardial edema, an unlooped heart tube, or reduction in cardiac mass.

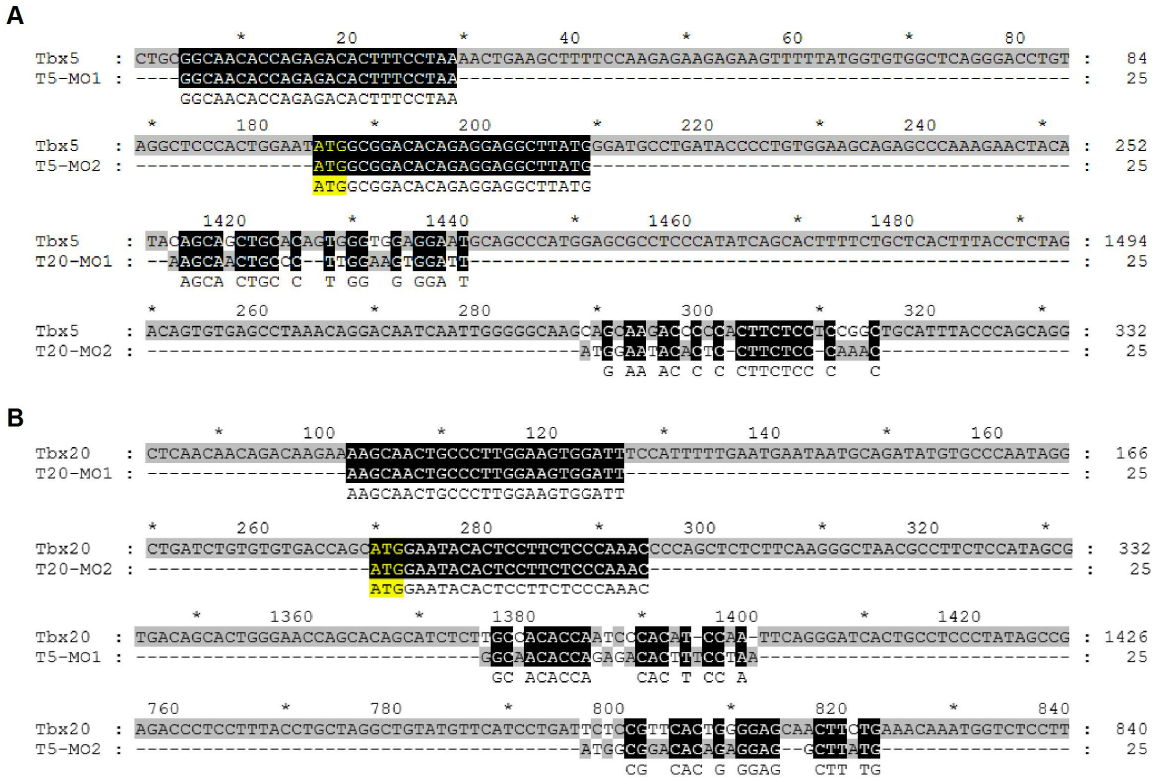

Figure 2.S1. *Sequence alignments suggest that Tbx5 and Tbx20 morpholinos cannot cross react.*

(A) Alignments of *Tbx5* morpholinos (complementary sequence) with *Tbx5* and *Tbx20* mRNA sequence. (B) Alignments of *Tbx20* morpholinos (complementary sequence) with *Tbx5* and *Tbx20* mRNA sequence.

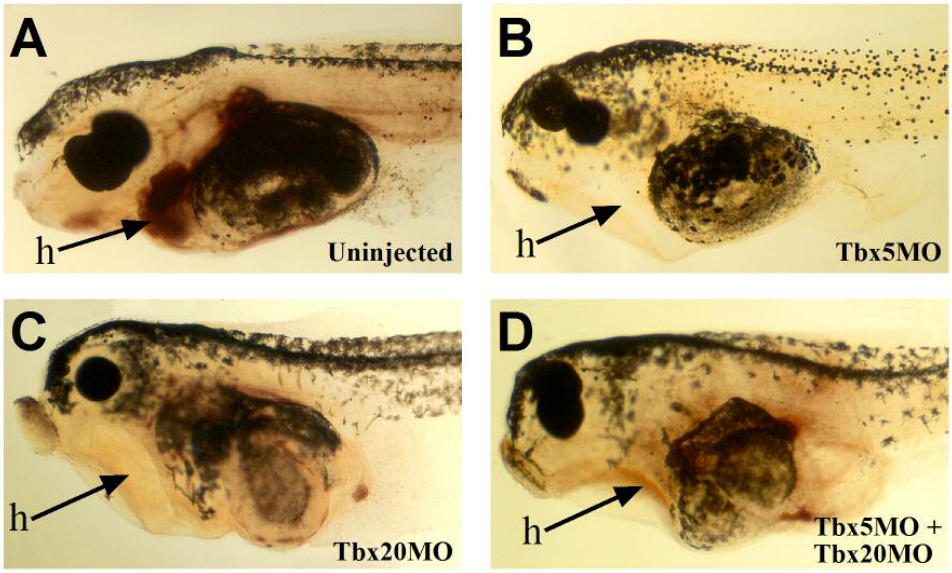

Figure 2.S2. *Tbx5 and Tbx20 morpholinos block the formation of a functional heart as assayed by benzidine staining of erythrocytes in stage 42 tadpoles.*

(A) Uninjected control, (B) TBX5MO injected at optimal dose, (C) TBX20MO injected at optimal dose, (D) TBX5MO and TBX20MO injected together at suboptimal doses. Note: Blood staining in the heart region (h) of control embryos but not morphant embryos.

REFERENCES

Baldini, A. (2004). DiGeorge syndrome: an update. *Curr Opin Cardiol* **19**, 201-4.

Basson, C. T., Bachinsky, D. R., Lin, R. C., Levi, T., Elkins, J. A., Soults, J., Grayzel, D., Kroumpouzou, E., Traill, T. A., Leblanc Straceski, J. et al. (1997). Mutations in human cause limb and cardiac malformation in Holt-Oram syndrome. *Nat. Genet.* **15**, 30-35.

Basson, C. T., Huang, T., Lin, R. C., Bachinsky, D. R., Weremowicz, S., Vaglio, A., Bruzzone, R., Quadrelli, R., Lerone, M., Romeo, G. et al. (1999). Different TBX5 interactions in heart and limb defined by Holt-Oram syndrome mutations. *Proc Natl Acad Sci U S A* **96**, 2919-2924.

Benson, D. W., Basson, C. T. and MacRae, C. A. (1996). New understandings in the genetics of congenital heart disease. *Curr. Opin. Pediatr.* **8**, 505-511.

Brown, D. D., Binder, O., Pagratis, M., Parr, B. A. and Conlon, F. L. (2003). Developmental expression of the Xenopus laevis Tbx20 orthologue. *Dev Genes Evol* **212**, 604-7.

Bruneau, B. G., Nemer, G., Schmitt, J. P., Charron, F., Robitaille, L., Caron, S., Conner, D. A., Gessler, M., Nemer, M., Seidman, C. E. et al. (2001). A Murine Model of Holt-Oram Syndrome Defines Roles of the T-Box Transcription Factor Tbx5 in Cardiogenesis and Disease. *Cell* **106**, 709-721.

Chapman, D. L., Garvey, N., Hancock, S., Alexiou, M., Agulnik, S. I., Gibson-Brown, J., Cebra-Thomas, J., Bollag, R., Silver, L. M. and Papaionnou, V. E. (1996). Expression of the T-box family genes, *Tbx1-Tbx5*, during early mouse development. *Dev. Dynam.* **206**, 379-390.

Chieffo, C., Garvey, N., Gong, W., Roe, B., Zhang, G., Silver, L., Emanuel, B. S. and Budarf, M. L. (1997). Isolation and characterization of a gene from the DiGeorge chromosomal region homologous to the mouse Tbx1 gene. *Genomics* **43**, 267-77.

Collavoli, A., Hatcher, C. J., He, J., Okin, D., Deo, R. and Basson, C. T. (2003). TBX5 nuclear localization is mediated by dual cooperative intramolecular signals. *J Mol Cell Cardiol* **35**, 1191-5.

Cripps, R. M. and Olson, E. N. (2002). Control of cardiac development by an evolutionarily conserved transcriptional network. *Dev Biol* **246**, 14-28.

Elliott, D. A., Kirk, E. P., Yeoh, T., Chandar, S., McKenzie, F., Taylor, P., Grossfeld, P.,

Fatkin, D., Jones, O., Hayes, P. et al. (2003). Cardiac homeobox gene NKX2-5 mutations and congenital heart disease: associations with atrial septal defect and hypoplastic left heart syndrome. *J Am Coll Cardiol* **41**, 2072-6.

Fan, C., Liu, M. and Wang, Q. (2003). Functional analysis of TBX5 missense mutations associated with Holt-Oram syndrome. *J Biol Chem* **278**, 8780-5.

Garrity, D. M., Childs, S. and Fishman, M. C. (2002). The heartstrings mutation in zebrafish causes heart/fin Tbx5 deficiency syndrome. *Development* **129**, 4635-45.

Goldmuntz, E., Geiger, E. and Benson, D. W. (2001). NKX2.5 mutations in patients with tetralogy of fallot. *Circulation* **104**, 2565-8.

Harland, R. M. (1991). In situ hybridization: an improved whole mount method for Xenopus embryos. *Meth. Cell Biol.* **36**, 675-685.

Harvey, R. P. (2002). Patterning the vertebrate heart. *Nat Rev Genet* **3**, 544-56.

Hiroi, Y., Kudoh, S., Monzen, K., Ikeda, Y., Yazaki, Y., Nagai, R. and Komuro, I. (2001). Tbx5 associates with Nkx2-5 and synergisticallly promotes cardiomyocyte differentiation. *Nature Genetics* **28**, 276-280.

Hoffman, J. I. (1995a). Incidence of Congenital Heart Disease: I. Postnantal Incidence. **16**, 103-113.

Hoffman, J. I. (1995b). Incidence of Congenital Heart Disease: II Prenatal Incidence. *Pediatr. Cardiol* **16**, 155-165.

Horb, M. E. and Thomsen, G. H. (1997). A vegetally localized T-box transcription factor in Xenopus eggs specifies mesoderm and endoderm and is essential for embryonic mesoderm formation. *Development* **124**, 1689-1698.

Horb, M. E. and Thomsen, G. H. (1999). Tbx5 is essential for heart development. *Development* **126**, 1739-1751.

Jerome, L. A. and Papaioannou, V. E. (2001). DiGeorge syndrome phenotype in mice mutant for the T-box gene, Tbx1. *Nat. Genet.* **27**, 286-291.

Kolker, S., Tajchman, U. and Weeks, D. L. (2000). Confocal Imaging of early heat development in Xenopus laevis. *Dev. Biol.* **218**, 64-73.

Laverriere, A. C., MacNeill, C., Mueller, C., Poelmann, R. E., Burch, J. B. and Evans, T. (1994). GATA-4/5/6, a subfamily of three transcription factors transcribed in developing heart and gut. *J Biol Chem* **269**, 23177-84.

Li, Q. Y., Newbury Ecob, R. A., Terrett, J. A., Wilson, D. I., Curtis, A. R., Yi, C. H., Gebuhr, T., Bullen, P. J., Robson, S. C., Strachan, T. et al. (1997). Holt-Oram syndrome is caused by mutations in TBX5, a member of the Brachyury (T) gene family. *Nat. Genet.* **15**, 21-29.

Lindsey, E. A., Vitelli, F., Su, H., Morishima, M., Huynh, T., Pramparo, T., Jurecic, V., Ogunrinu, G., Sutherland, H. F., Scrambler, P. J. et al. (2001). Tbx1 haploinsufficiency in the DiGeorge syndrome region causes aortic arch defects in mice. *Nature* **410**, 97-101.

Logan, M. and Mohun, T. (1993). Induction of cardiac muscle differentiation in isolated animal pole explants of Xenopus laevis embryos. *Development* **118**, 865-875.

Marcellini, S., Technau, U., Smith, J. C. and Lemaire, P. (2003). Evolution of Brachyury proteins: identification of a novel regulatory domain conserved within Bilateria. *Dev Biol* **260**, 352-61.

Merscher, S., Funke, B., Epstein, J. A., Heyer, J., Puech, A., Lu, M. M., Xavier, R. J., Demay, M. B., Russell, R. G., Factor, S. et al. (2001). TBX1 is responsible for cardiovascular defects in velo-cardio- facial/DiGeorge syndrome. *Cell* **104**, 619-29.

Mohun, T. J. and Leong, L. M. (1999). Heart Formation and the Heart Field in Amphibian Embryos.: Academic Press.

Mohun, T. J., Leong, L.M., Weninger, W. J., and Sparrow, D. B. (2000). The Morphology of Heart Development in Xenopus laevis. *Developmental Biology* **218**, 74-88.

Newbury-Ecob, R., Leanage, R., Raeburn, J. A. and Young, I. D. (1996). The Holt-Oram Syndrome: a clinical genetic study. *J. Med. Genet.* **33**, 300-307.

Newman, C. S. and Krieg, P. A. (1999). Specification and Differntiation of the Heart in Amphibia: Academic Press.

Nieuwkoop, P. D. and Faber, J. (1967). Normal Table of *Xenopus laevis* (Daudin). Amsterdam: North Holland.

Packham, E. A. and Brook, J. D. (2003). T-box genes in human disorders. *Hum Mol Genet* **12 Spec No 1**, R37-44.

Payne, R. M., Johnson, M. C., Grant, J. W. and Strauss, J. E. (1995). Toward a molecular understanding of congenital heart disease. *Circulation* **91**, 494-504.

Plageman, T. F., Jr. and Yutzey, K. E. (2004). Differential expression and function of tbx5 and tbx20 in cardiac development. *J Biol Chem* **279**, 19026-34.

Prall, O. W., Elliott, D. A. and Harvey, R. P. (2002). Developmental paradigms in heart disease: insights from tinman. *Ann Med* **34**, 148-56.

Ryan, K. and Chin, A. J. (2003). T-box genes and cardiac development. *Birth Defects Res Part C Embryo Today* **69**, 25-37.

Serbedzija, G. N., Chen, J. N. and Fishman, M. C. (1998). Regulation in the heart field of zebrafish. *Development* **125**, 1095-101.

Showell, C., Binder, O. and Conlon, F. (2003). T-box genes in early embryogenesis. *Dev. Dyn.* **In Press**.

Small, E. M. and Krieg, P. A. (2000). Expression of atrial natriuretic factor (ANF) during Xenopus cardiac development. *Dev Genes Evol* **210**, 638-640.

Stennard, F. A., Costa, M. W., Elliott, D. A., Rankin, S., Haast, S. J., Lai, D., McDonald, L. P., Niederreither, K., Dolle, P., Bruneau, B. G. et al. (2003). Cardiac T-box factor Tbx20 directly interacts with Nkx2-5, GATA4, and GATA5 in regulation of gene expression in the developing heart. *Dev Biol* **262**, 206-24.

Szeto, D. P., Griffin, K. J. and Kimelman, D. (2002). HrT is required for cardiovascular development in zebrafish. *Development* **129**, 5093-101.

Tonissen, K. F., Drysdale, T. A., Lints, T. J., Harvey, R. P. and Krieg, P. A. (1994). XNkx-2.5, a Xenopus gene related to Nkx-2.5 and tinman: evidence for a conserved role in cardiac development. *Dev. Biol.* **162**, 325-328.

Wilson, P. A. and Hemmati-Brivanlou, A. (1995). Induction of epidermis and inhibition of neural fate by Bmp-4. *Nature* **376**, 331-333.

Yagi, H., Furutani, Y., Hamada, H., Sasaki, T., Asakawa, S., Minoshima, S., Ichida, F., Joo, K., Kimura, M., Imamura, S. et al. (2003). Role of TBX1 in human del22q11.2 syndrome. *Lancet* **362**, 1366-73.

Zaffran, S. and Frasch, M. (2002). Early signals in cardiac development. *Circ Res* **91**, 457-69.

Zaragoza, M. V., Lewis, L. E., Sun, G., Wang, E., Li, L., Said-Salman, I., Feucht, L. and Huang, T. (2004). Identification of the TBX5 transactivating domain and the nuclear localization signal. *Gene* **330**, 9-18.

CHAPTER 3

A 3D Modeling Program to Rapidly Assess Cardiac Morphological Abnormalities in Vertebrate Embryos

PREFACE TO CHAPTER 3

Chapter 3 describes a 3-D modeling program developed in collaboration with the laboratory of Dr. Stephen Aylward. The purpose of this modeling program is to rapidly re-assemble serial sections through the developing heart into a 3-D reconstruction in order to assess the overall structure of the heart in greater detail than is possible through examination of wholemount tissue. We use embryos depleted of TBX-5 as a case study for the utility of this program in examining morphological abnormalities in the heart. This project was carried out in collaboration with Yvette Langdon, Tamaryn Kelley, Ashley Hayes, Jennifer Duddy, Remi Charrier, Cedric Caron, and Stephen Aylward. For this work, I performed serial sectioning, immunostaining and reconstruction of hearts from control, and TBX5 depleted embryos.

SUMMARY

Characterizing the cellular and molecular basis of heart development largely depends on the ability to describe normal heart development, as well as cardiac phenotypes arising from the disruption of specific molecular pathways. To build upon existing techniques for the examination of cardiac morphology during development, we have devised a 3-D modeling program known as HistologicalImageReconstruction. This program provides an inexpensive and rapid method for characterizing the morphology of the heart or other tissue of interest at a high level of detail. Here we provide a demonstration of the utility of HistologicalImageReconstruction to analyze both normal cardiac development, and the cardiac phenotype resulting from depletion of the transcription factor TBX5 during *Xenopus laevis* development.

INTRODUCTION

Congenital heart defects are among the most common forms of birth defects in humans, comprising approximately 1% of all live births (Hoffman, 1995a, 1995b). In recent years, numerous studies have elucidated many of the basic processes of heart development, employing both embryological and molecular approaches (Bruneau, 2002; Kolker *et al.*, 2000; Mohun, 2000; Olson and Srivastava, 1996) . However, in spite of this, our understanding of the molecular mechanisms underlying normal heart development, as well as the mechanisms of human disease states remains incomplete.

Understanding the molecular mechanisms of heart development relies upon the ability to accurately describe both normal heart development and abnormalities resulting from the disruption of certain gene products or molecular pathways. Existing tools for

visualizing cardiac phenotypes consist primarily of whole-mount immunostaining, and immunostaining of histological sections. Whole-mount immunostaining allows for the visualization of overall cardiac morphology, but is somewhat limited in ability to detect more subtle defects. In contrast, histological sections provide a greater degree of detail and more easily allow for quantitative analysis of a cardiac phenotype, such as determination of cell number. However, visualization of the overall morphology of the heart is often not possible using this technique.

To address the limitations of these methods, we have devised an inexpensive, high-throughput 3-dimensional modeling program, known as HistologicalImageReconstruction, that combines the detail of histological sections with the ability to easily observe the overall morphology of the heart. Briefly, the modeling program consists of four steps: segmentation, stitching, stacking and the three dimensional reconstruction. Utilizing sections through the *Xenopus* heart that have been stained with a cardiac muscle-specific antibody such as myosin heavy chain a 3-dimensional model of the heart can be rendered. The heart in each serial section is selected during segmentation and the images are stacked together based on reference points provided by the previous image. The stacked images are then converted to a 3D model that can be visualized using the VisualizeHistologyImage program which is a companion program to HistologicalImageReconstruction.

Xenopus is an especially valuable tool for the study of cardiovascular development because, unlike mammalian embryos, amphibian embryos can survive to late developmental stages without functional circulation. *Xenopus* embryos are highly amenable to embryological manipulations and, with the advent of antisense morpholino technology, it has been possible to generate highly specific loss-of-function phenotypes for many genes of

interest. Amphibian embryos also possess pulmonary circulation making the physiology of their circulatory system more closely related to that of the mammals than is the zebrafish.

While other modeling programs to examine heart development in *Xenopus* have been described (Mohun, 2000), the program we have developed offers several advantages and thus complements existing modeling programs. First, in HistologicalImageReconstruction, the 3D model can be reconstructed solely from corresponding points on adjacent sections through the heart without requiring the use of reference points outside the heart upon which to align the 3D model. As a result, HistologicalImageReconstruction requires the use of less tissue and allows for a rapid reconstruction of 3D images. In addition, HistologicalImageReconstruction utilizes the expression of cardiac muscle proteins to define the cardiac tissue to be imaged. In this way, we are able to distinguish cardiac tissue from surrounding mesoderm more easily at earlier developmental stages or in regions of the heart that are not morphologically well defined. Thirdly, this program can reconstruct hearts from florescent immunostaining, or from *in situ* hybridization without necessitating expensive software. Thus, this method also allows us to catalog and compare the expression patterns of various heart proteins throughout development.

RESULTS AND DISCUSSION

To demonstrate the utility of the modeling program as a tool for analyzing normal heart development, we initially reconstructed 3D models of *Xenopus* hearts at three developmental stages, determined according to Nieuwkoop and Faber (Nieuwkoop and Faber, 1967); stage 29, which corresponds to the folding of the cardiac field into the bilaminar heart tube; stage 33, which corresponds to the onset of cardiac looping; and stage 37, corresponding to early

cardiac remodeling and chamber formation. At each of these stages hearts were serial section and immunostained with an antibody against cardiac myosin heavy chain (MHC) or tropomyosin. Representative sections from the anterior, middle, and posterior regions of the heart for each stage are shown in Fig. 3.1. The series of sections were then used to reconstruct a 3D model of the heart for each stage and visualized by VisualizeHistologyImage (Fig. 3.2). These models reveal the overall morphology as detected by staining with cardiac specific antibodies of the heart at each stage as well as cataloging the expression of genes/ proteins at each of these developmental stages. Through the visualization program, the rendered surface of the heart can be made transparent and each individual section of the heart viewed providing internal details of the heart relative to overall heart morphology.

The model based on MHC expression of unmanipulated embryos at stage 29 shows that the bilateral *Xenopus* heart primordia have joined across the ventral midline to form a single heart field. The heart field has begun to round up to form a trough that is open at the dorsal-most aspect (Fig. 3.2a-c). At this stage the heart and MHC expression are in a linear configuration, with the presumptive inflow and outflow of the heart aligned along the anterior-posterior axis (Fig. 3.2b-arrows).

By stage 33, the heart tube is fully closed for much of its length (Fig. 2d-f), with the exception of the anterior-most portion of the heart, near the future outflow tract, where it remains open at the dorsal aspect (Fig. 3.2e-arrowhead). By this stage, the heart has begun the morphogenetic process of rightward looping, as seen by the visible offsetting of the inflow to the right of the outflow (Fig. 3.2e-arrows). At this stage the MHC expression domain has also increased in size due to high levels of cell proliferation within the *Xenopus*

heart (Goetz *et al.*, 2006), and has increased in length along the anterior-posterior axis (Fig. 3.2- compare f with c).

Finally, at stage 37, a greater degree of morphological complexity is evident as the heart continues to undergo cardiac looping and begins cardiac remodeling (Fig. 3.2g-i). At this stage, the heart elongates along the left-right axis (Fig. 3.2h), and the chamber primordia become more distinct (Fig. 3.2g,i-arrow heads). As was the case at stage 33, the hearts of the stage 37 embryos have fully closed with the exception of the anterior-most sections, although the dorsal opening in these anterior sections is more narrow than that of the stage 33 embryos (Fig. 3.2-compare d with g), suggesting that the anterior portion of the heart at stage 37 is continuing to complete dorsal closure to form a fully enclosed tube. By this point in development, our HistologicalImageReconstruction-generated model reveals that the outflow tract of the heart is still shifted to the right with respect to the inflow (Fig. 3.2h-arrows).

To show the utility of the HistologicalImageReconstruction modeling program in characterizing morphological abnormalities arising from loss or mis-expression of a particular gene product, we analyzed embryos in which we depleted TBX5 by morpholino antisense oligos, as a test case (Brown *et al.*, 2005; Goetz *et al.*, 2006). Mutations to the T-box transcription factor *Tbx5* are associated with the congenital heart disorder Holt-Oram syndrome in humans (Basson *et al.*, 1997; Li *et al.*, 1997) and the evolutionarily conserved requirement for TBX5 during heart development demonstrated in a number of vertebrate species (Bruneau *et al.*, 2001; Garrity *et al.*, 2002; Horb and Thomsen, 1999). Previously we have shown that depleting TBX5 in *Xenopus* leads to a reduction in heart size and a failure to undergo cardiac looping and chamber formation (Brown *et al.*, 2005; Goetz *et al.*, 2006).

Our HistologicalImageReconstruction- generated 3D models of hearts from embryos lacking TBX5, shown in Fig. 3, are consistent with these previous finding, while also revealing differences in morphology between control and TBX5-depleted embryos that were not previously described (Brown *et al.*, 2005; Goetz *et al.*, 2006). In control hearts at stage 29, the ventrally-fused heart field has begun to round up dorsally to form the linear heart tube (Fig. 3.3a,c). In TBX5-depleted hearts, tropomyosin positive cells of the cardiac field failed to migrate towards the dorsal side of the embryo to initiate heart tube formation (Fig. 3.3b,d). In addition, the number of cells expressing tropomyosin is reduced compared to controls. As previously reported, this most likely reflects a delay in the timing of expression of tropomyosin in TBX5-depleted embryos (Goetz *et al.*, 2006).

At stage 33, control and TBX5-depleted embryos contain approximately equal numbers of tropomyosin positive cells, however, several morphological abnormalities become apparent in the expression of tropomyosin in TBX5-depleted embryos (Fig. 3.3g-l). In control embryos, consistent with what we observed for the models based on MHC staining, the heart tube is fully closed for much of its length with the exception of the most anterior portions of the heart (Fig. 3g,i). Cardiac tissue has begun the process of cardiac looping (note: the inflow tract is noticeably offset to the right from the outflow tract; Fig. 3.3i- arrows). In comparison, hearts of the TBX5-depleted embryos at stage 33 still form a trough opening dorsally for all but a small, central portion of the heart tube (Fig. 3.3h-blue arrow). The hearts derived from TBX5-depleted embryos have also failed to initiated cardiac looping (note: inflow tract is aligned with the outflow along the anterior-posterior axis, rather than offset to the right; Fig. 3.3j-arrows).

By stage 37, control embryo tropomyosin staining marks the chamber primordia (Fig. 3.3m,o-arrowheads). In contrast, the hearts of TBX5- depleted embryos show fewer tropomyosin-positive cells (Fig. 3n,p,r). In addition, the inflow and outflow tracts are aligned along the anterior-posterior axis, indicating that the heart has failed to undergo cardiac looping (Fig. 3.3p-arrows) (Goetz *et al.*, 2006). We also observe that the central portion of the dorsal aspect of the heart tube remains as an open trough (denoted by the blue arrow; Fig. 3.3p). Interestingly, it appears that blood flow into the heart tube of the TBX5-depleted embryos may be offset dorsally, as the anterior most portions of the heart tube are occluded (Fig. 3.3n-blue arrow). This observation indicates that the defects seen in the TBX5-depleted embryos are not simply due to a delay in heart development, as the morphological abnormalities are more severe than those seen in earlier stage control hearts.

Our HistologicalImageReconstruction-generated 3D models both accurately recapitulate antibody expression patterns and hence morphological defects in TBX5-depleted cardiac tissue. These include the failure of the heart to properly form a linear heart tube, defects in the relative positioning of the heart, and a general decrease in cardiac mass. Although the software has allowed a rapid evaluation of molecular expression patterns and cardiac defects in *Xenopus*, the program can be easily adapted or other tissues, organs, or model organisms. A considerable advantage offered by our 3D modeling is its use of immunostaining to label the tissue of interest to be modeled. Thus, this program offers inexpensive, high-throughput 3D imaging to investigators wishing to study alterations in tissues that may not be morphologically distinct from the surrounding tissue during the developmental window of interest.

METHODS

Cryosectioning and Immunostaining of Heart Tissue

For immunostaining of histological sections, embryos were collected at the indicated stages, fixed for 2 hours in 4% paraformaldehyde, and embedded in OCT cryosectioning medium (Tissue Tek). Serial cryostat sections (14μm) corresponding to the entire heart region were collected and rinsed with wash buffer (PBS with 1% Triton and 1% heat inactivated calf serum), and incubated at 4 ºC overnight as indicated with mouse anti-tropomyosin (Developmental Studies Hybridoma Bank) at 1:50; or mouse anti-myosin heavy chain (Abcam) at 1:1000. The sections were rinsed with wash buffer and the fluorescent conjugated secondary antibody, anti-mouse-Cy3 (Sigma), was applied to the samples, diluted in wash buffer at 1:100. The slides were incubated with secondary antibody for 30 minutes at room temperature and rinsed with wash buffer. Samples were then incubated 30 minutes at room temperature with DAPI (Sigma) to stain nuclei. The samples were imaged on a Nikon E800 epiflourescent microscope and images captured using the Metamorph software package (Universal Imaging Corporation).

3-D Reconstruction

3D reconstruction of sectioned cardiac tissue was performed using the software package HistologyImageReconstruction designed by the University of North Carolina's Computer Aided Diagnosis and Display lab. Digital images of the histological sections were loaded into the histology program. To construct a 3D model positive staining cells of the heart were identified by immunostaining with a heart-specific antibody. All positive staining cells within the section were then selected based on relative staining intensity and pixels selected.

Tissue not recognized by the heart-specific antibody was thus eliminated from the model. Following the selection of heart tissue in each histological section in the series, corresponding points in each consecutive section were choosen (n= 4-8) and aligned by the HistologicalImageReconstruction software program. These corresponding points were chosen based upon a starter section containing the most morphologically distinct portion of the heart. A minimum of four corresponding points were then chosen in the remaining sections of each heart. The 2D images of the series were then transformed to allow for rotation, shifting, and deformation based on the images. The transformed sections were then examined to assess the alignment between consecutive sections. Following alignment, the newly transformed sections were then stacked and reconstructed into a 3D model of the heart. Gap size (distance between two consecutive sections) and height (height of a section) were assigned manually. Final parameters gap size= 10 and height parameter= 25. The multiplier and spacing parameters were predetermined from the pixel size of the final 3D reconstruction, with the multiplier= 1, and spacing= 1, 1 and 5 along the x-, y-, and z-axes, respectively. The data from the stacked, transformed images for each heart series were then written and compressed to a MHD file, which was visualized the VisualizeHistologyImage program. Resulting 3D models were rotated and imaged at specific angles to allow for examination and comparison of cardiac morphology in different stages or conditions.

Acknowledgements

This work is supported by grants to F.L.C from the NIH/NHLBI, and by an award from the UNC Medical Alumni Association. Y.G.L is supported by an NIH Minority Supplement. S.C.G is a trainee in the Integrative Vascular Biology program, supported by the NIH. The

antibody against tropomyosin (developed by J.-C. Lin) was obtained from the Developmental Studies Hybridoma Bank, developed under the auspices of the NICHD and maintained by the University of Iowa, Department of Biological Sciences, Iowa City, IA 52242. We thank Chris Showell for critical reading of the manuscript and helpful comments.

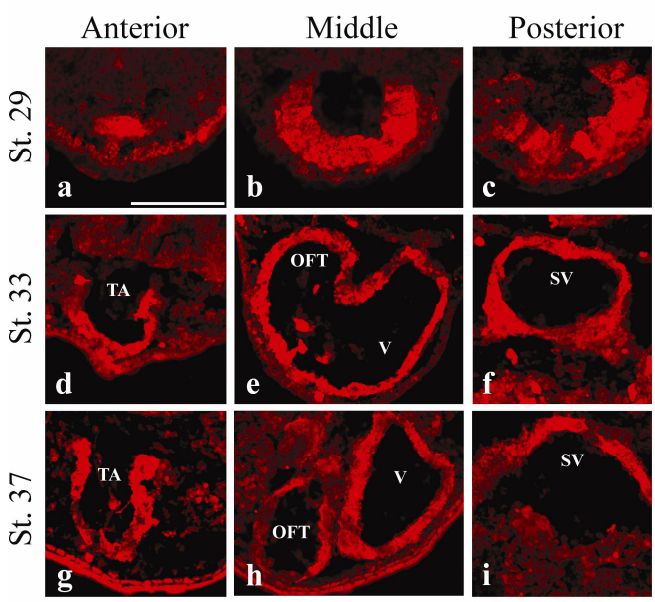

Figure 3.1. Histological sections of Xenopus hearts showing expression of myosin heavy chain.

Wild-type embryos were transversely serial sectioned at stages 29 (a-c), 33 (d-f), or 37 (g-i). Shown are representative sections from the anterior-most, middle, and posterior regions of the heart tube, as indicated, at each stage. Cardiac myosin heavy chain expression is shown in red. Scale= 100μM. TA= truncus arteriosis, OFT= outflow tract, V= Ventricle, SV= sinus venosus.

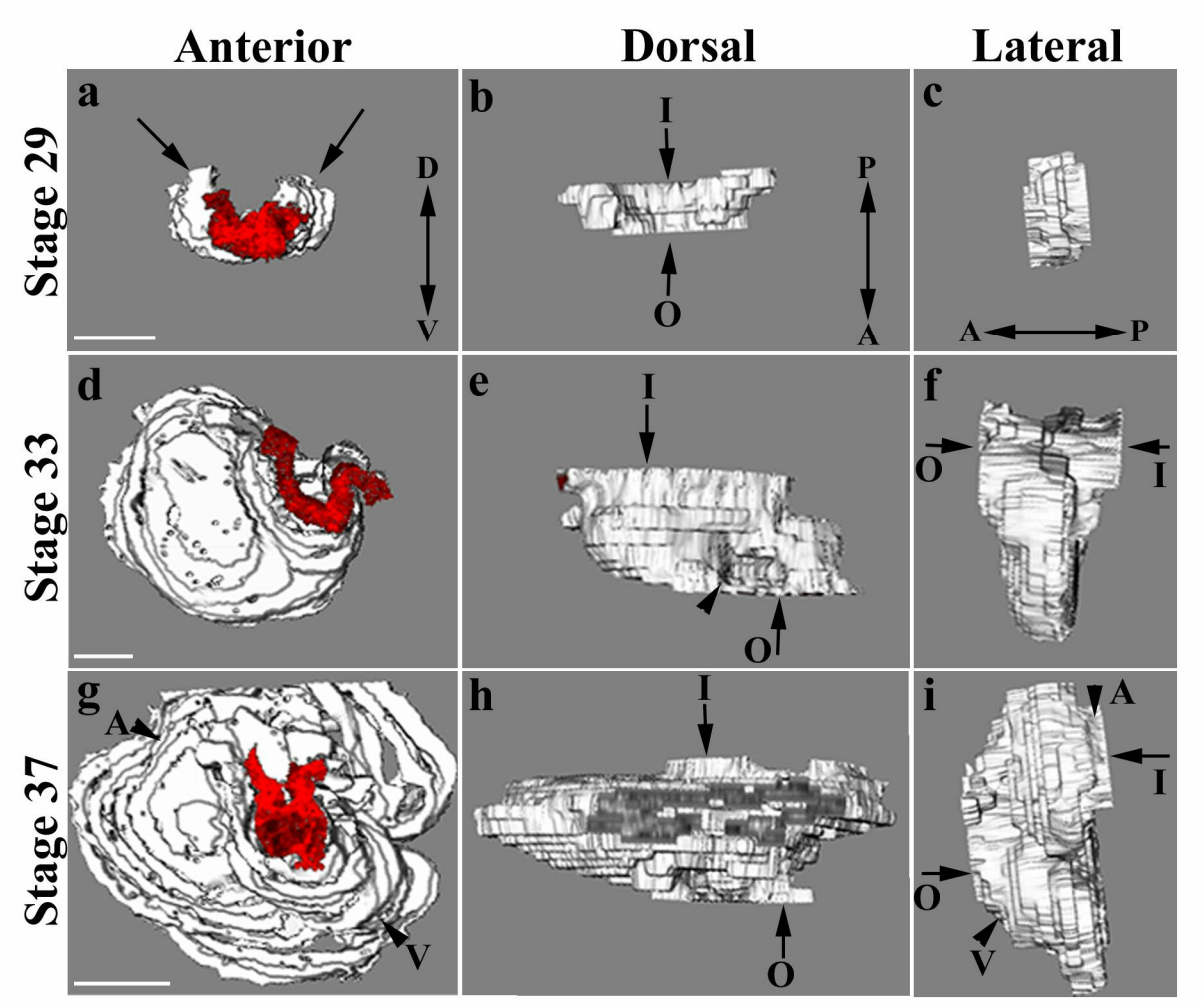

Figure 3.2. *3D models of Xenopus hearts based on myosin heavy chain expression reveal dynamic MHC expression in the developing heart.*

VisualizeHistologyImage program was used to generate 3D models of *Xenopus* hearts at stages 29 (a-c), 33 (d-f) or 37 (g-i) based on sections immunostained with myosin heavy chain. The models are shown in anterior (a,d,g), dorsal (b,e,h), and lateral (c,f,i) views, with orientation of axes is shown for each series at stage 29. A section corresponding to the most anterior region of the heart is shown in red for each stage. Arrowheads mark cardiac chambers. A= atrium, V= ventricle. Arrows in panels b-i mark the outflow (O) and inflow

(I) tracts. Orientation axis is shown for each series at stage 29 in the bottom right corner of the panel. A= anterior, P= posterior, D= dorsal, V= ventral. Scale= 50μM.

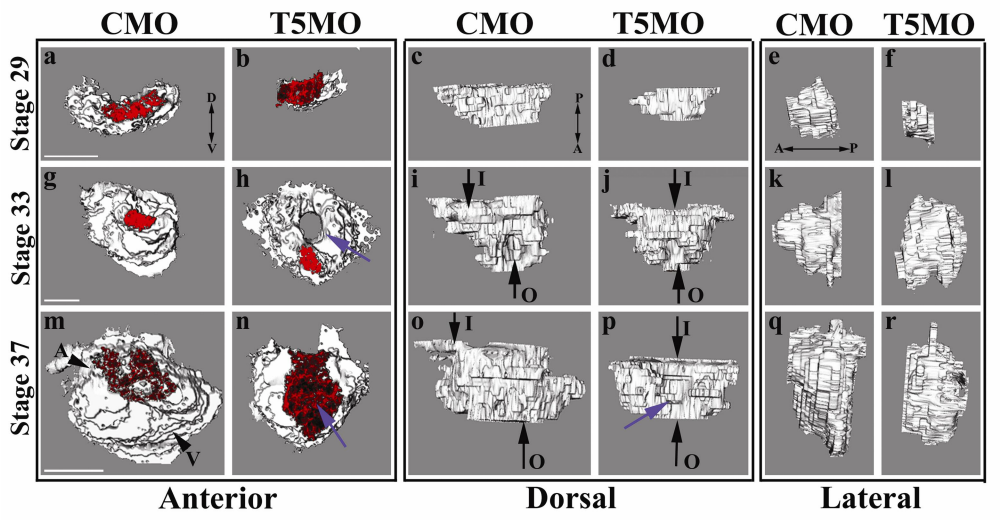

Figure3.3. *3D modeling of TBX5-depleted hearts reveals dynamic aspects of the cardiac phenotype.*

VisualizeHistologyImage program generated 3D models of *Xenopus* hearts from embryos at stages 29 (a-f), 33 (g-l), or 37 (m-r) injected with either control (CMO) or TBX5 morpholinos (T5MO) as indicated. 3D models are shown in anterior (a,b,g,h,m,n), dorsal (c,d,i,j,o,p), or lateral (e,f,k,l,q,r) views, with orientation of axes shown for each series at stage 29. Arrowheads mark cardiac chambers. A= atrium, V= ventricle. Black arrows in panels i-j,o-p mark the outflow (O) and inflow (I) tracts. Blue arrows indicate special features of the T5MO phenotype. Axes are indicated in the top left panel of each grouping. A= anterior, P= posterior, D= dorsal, V= ventral. Scale= 50

REFERENCES

Basson, C. T., Bachinsky, D. R., Lin, R. C., Levi, T., Elkins, J. A., Soults, J., Grayzel, D., Kroumpouzou, E., Traill, T. A., Leblanc Straceski, J. et al. (1997). Mutations in human cause limb and cardiac malformation in Holt-Oram syndrome. *Nat. Genet.* **15**, 30-35.

Brown, D. D., Martz, S. N., Binder, O., Goetz, S. C., Price, B. M. J., Smith, J. C. and Conlon, F. L. (2005). Tbx5 and Tbx20 act synergistically to control vertebrate heart morphogenesis. *Development* **132**, 553-563.

Bruneau, B. G. (2002). Transcriptional regulation of vertebrate cardiac morphogenesis. *Circ Res* **90**, 509-19.

Bruneau, B. G., Nemer, G., Schmitt, J. P., Charron, F., Robitaille, L., Caron, S., Conner, D. A., Gessler, M., Nemer, M., Seidman, C. E. et al. (2001). A Murine Model of Holt-Oram Syndrome Defines Roles of the T-Box Transcription Factor Tbx5 in Cardiogenesis and Disease. *Cell* **106**, 709-721.

Garrity, D. M., Childs, S. and Fishman, M. C. (2002). The heartstrings mutation in zebrafish causes heart/fin Tbx5 deficiency syndrome. *Development* **129**, 4635-45.

Goetz, S. C., Brown, D. D. and Conlon, F. L. (2006). TBX5 is required for embryonic cardiac cell cycle progression. *Development*.

Hoffman, J. I. (1995a). Incidence of Congenital Heart Disease: I. Postnantal Incidence. **16**, 103-113.

Hoffman, J. I. (1995b). Incidence of Congenital Heart Disease: II Prenatal Incidence. *Pediatr. Cardiol* **16**, 155-165.

Horb, M. E. and Thomsen, G. H. (1999). Tbx5 is essential for heart development. *Development* **126**, 1739-1751.

Kolker, S. J., Tajchman, U. and Weeks, D. L. (2000). Confocal imaging of early heart development in Xenopus laevis. *Dev Biol* **218**, 64-73.

Li, Q. Y., Newbury Ecob, R. A., Terrett, J. A., Wilson, D. I., Curtis, A. R., Yi, C. H., Gebuhr, T., Bullen, P. J., Robson, S. C., Strachan, T. et al. (1997). Holt-Oram syndrome is caused by mutations in TBX5, a member of the Brachyury (T) gene family. *Nat. Genet.* **15**, 21-29.

Mohun, T. J., Leong, L.M., Weninger, W. J., and Sparrow, D. B. (2000). The Morphology of Heart Development in Xenopus laevis. *Developmental Biology* **218**, 74-88.

Nieuwkoop, P. D. and Faber, J. (1967). Normal Table of *Xenopus laevis* (Daudin). Amsterdam: North Holland.

Olson, E. N. and Srivastava, D. (1996). Molecular pathways controlling heart development. *Science* **272**, 671-676.

CHAPTER 4

TBX5 is Required for Embryonic Cardiac Cell Cycle Progression

PREFACE TO CHAPTER 4

Chapter 4 describes the requirement for TBX5 in cell cycle progression within the heart. Previously, it has been shown that TBX5 is required for proper heart development in vertebrates (Brown et al., 2005; Brunearu et al., 2001; Horb and Thomsen, 1999), and that the hearts of embryos lacking TBX5 are hypoplastic (Brown et al., 2005; Bruneau et al., 2001). Therefore, in this chapter we test the hypothesis that TBX5 is required for cardiac cell proliferation. This work was performed in collaboration with Daniel Brown, and published in *Development* in 2006.

SUMMARY

Despite the critical importance of TBX5 in normal development and disease, relatively little is known about the mechanisms by which TBX5 functions in the embryonic heart. Our present studies demonstrate that TBX5 is necessary to control the length of the embryonic cardiac cell cycle, with depletion of TBX5 leading to cardiac cell cycle arrest in late G_1 or early S phase. Blocking cell cycle progression by TBX5 depletion leads to a

decrease in cardiac cell number, an alteration in the timing of the cardiac differentiation program, defects in cardiac sarcomere formation, and ultimately, to cardiac programmed cell death. In these studies we have also established that terminally differentiated cardiomyocytes retain the capacity to undergo cell division. We further show that TBX5 is sufficient to determine the length of the embryonic cardiac cell cycle and the timing of the cardiac differentiation program. Thus, these studies establish a role for TBX5 in regulating the progression of the cardiac cell cycle.

INTRODUCTION

Hyperplastic growth of the vertebrate heart is characterized by two distinct periods of proliferation, one that occurs during early embryogenesis and a second that takes place immediately following birth (MacLellan and Schneider, 2000; Olson and Schneider, 2003; Pasumarthi and Field, 2002). The embryonic phase of cardiac proliferation begins after cardiac cell commitment, and therefore occurs coincident with, or shortly after, gastrulation, a period when the cardiac precursor cells are positioned in two populations on both sides of the organizer or node. Once cells are committed into the cardiac lineage, the two populations of heart precursors migrate to assume their ultimate position along the anterior-ventral midline of the embryo. It is during this narrow window of time that the cardiac precursors undergo rapid cell proliferation to form two epithelial sheets that migrate and fuse, eventually forming the bilaminar heart tube (Fishman and Chien, 1997; Harvey, 2002; Kolker et al., 2000; Mohun et al., 2003; Mohun et al., 2000). During the final stages of migration, the cardiac cells decrease DNA synthesis, gradually withdraw from the cell cycle, and initiate terminal differentiation (Pasumarthi and Field, 2002).

During the embryonic stage of cell proliferation, the cardiac cells express the first molecular markers of cardiac development, including *Tbx5*, *Tbx20*, and the homologue of the Drosophila *tinman* gene, *Nkx2.5* (Harvey, 2002; Stennard and Harvey, 2005). *Tbx5* is a member of the T-box family of transcription factors, a family of proteins that are required for normal vertebrate patterning and differentiation (Papaioannou and Silver, 1998; Showell et al., 2004; Stennard and Harvey, 2005; Wilson and Conlon, 2002). Clinical studies have provided direct evidence for a role for human *Tbx5* in heart development, with *Tbx5* frequently mutated in patients with the congenital heart disease Holt-Oram Syndrome (HOS) (Basson et al., 1997; Li et al., 1997; Mandel et al., 2005). HOS is a highly penetrant autosomal dominant condition that is associated with skeletal and cardiac malformations. The HOS cardiac developmental abnormalities include atrial and ventricular septal defects, as well as conductivity defects and aberrant chamber formation (Basson et al., 1999; Benson et al., 1996; Newbury-Ecob et al., 1996). A role for *Tbx5* in HOS is supported by the observation that mice heterozygous for mutations in *Tbx5* display many of the cardiac abnormalities associated with human patients suffering from HOS (Bruneau et al., 2001). Genetic studies of a *Tbx5* mutation in zebrafish and TBX5 depletion in *Xenopus* are also consistent with a role for TBX5 in heart development (Brown et al., 2005; Garrity et al., 2002; Horb and Thomsen, 1999). The evolutionarily conserved role for *Tbx5* is further emphasized by molecular experiments carried out in tissue culture, zebrafish, *Xenopus*, chicken, and mouse, all of which show a role for TBX5 transcriptional activity in regulating the expression of heart-specific genes (Brown et al., 2005; Bruneau et al., 2001; Garrity et al., 2002; Hatcher et al., 2001; Hiroi et al., 2001; Liberatore et al., 2000; Plageman and Yutzey, 2004).

Recently, we have shown that depletion of TBX5 in *Xenopus* leads to profound morphological defects in the heart including pericardial edema, loss of circulation, and a concomitant decrease in cardiac cell number (Brown et al., 2005). In the present study, we demonstrate that the observed decrease in cell number results from defects in embryonic cardiac cell proliferation. We go on to define the expression pattern of an extensive panel of CDK and cyclin proteins in early embryonic cardiac tissue, and show that TBX5 depletion leads to a G_1/S phase arrest as demonstrated by a dramatic increase in the expression of proteins associated with the cardiac cell cycle S phase including CDC6, cyclin E2, SLBP, and PCNA. This suggests that TBX5 is involved in either G_1/S phase or the early stages of S phase progression. The G_1/S phase delay or arrest coincides with a decrease in the embryonic cardiac cell mitotic index. These events are associated with an alteration in the timing of the cardiac differentiation program, defects in cardiac sarcomere formation, and ultimately, cardiac programmed cell death. In contrast, over-expression of *Tbx5*, which we show also leads to heart-specific defects, results in an increase in the cardiac mitotic index and has a converse effect on the timing of the cardiac differentiation program. Collectively, these studies demonstrate that TBX5 is both necessary and sufficient to determine the length of cardiac G_1/S phase and the timing of the cardiac differentiation program.

MATERIALS AND METHODS

Embryo Culture and Microinjection

Xenopus embryos and *Xenopus* Cardiac Actin:GFP transgenic offspring (Latinkic et al., 2002) were prepared and injected as previously described (Wilson and Hemmati-Brivanlou, 1995), and staged according to Nieuwkoop and Faber (Nieuwkoop, 1967). For TBX5 depletion studies, embryos were injected with TBX5 and CMO morpholinos as per Brown et

al. (Brown et al., 2005). In mis-expression studies, capped mRNA for microinjections was generated using the mMessage in vitro transcription kit (Ambion) according to the manufacturer's instructions. Resulting mRNA was then purified using the RNeasy kit (Qiagen). Embryos were injected with the stated amount of *Tbx5* RNA at the one cell stage. Transgenic animals expressing GFP under the cardiac actin promoter were a gift from Dr. Tim Mohun (Latinkic et al., 2002).

Immunohistochemistry and Whole-Mount in situ Hybridization

Embryos were prepared for whole-mount immunohistochemistry according to (Kolker et al., 2000). Briefly, fixed embryos were incubated overnight at 4 ºC with an antibody against tropomyosin, (Developmental Studies Hybridoma Bank) at a dilution of 1:50. Following washes, the embryos were incubated overnight at 4ºC with a Cy3-conjugated anti-mouse secondary antibody (Sigma) at a dilution of 1:100. For imaging, embryos were cleared with 2:1 benzyl benzoate: benzyl alcohol and viewed on a Leica MZFLIII fluorescent dissecting microscope. For immunostaining of histological sections, embryos were collected at the indicated stages, fixed for 2 hours in 4% paraformaldehyde, and embedded in OCT cryosectioning medium (Tissue Tek). Cryostat sections (14um) were rinsed with wash buffer (PBS with 1% Triton and 1% heat inactivated calf serum), and incubated at 4 ºC overnight as indicated with mouse anti-tropomyosin 1:50, mouse anti-troponin 1:20, mouse anti-fibrillin 1:50, (all from Developmental Studies Hybridoma Bank); mouse anti-MHC (Abcam) rabbit anti-fibronectin 1:50 (Sigma), rabbit anti- Beta-catenin all at 1:1000 (Sigma), rabbit anti-phospho-histone H3 1:50 (Upstate), rabbit anti-cleaved Caspase 3 1:50 (Cell Signaling). The sections were rinsed with wash buffer and the appropriate fluorescent conjugated secondary

antibody diluted in wash buffer: anti-mouse-Cy3 1:100 (Sigma), anti-mouse Cy2 1:100 (Jackson), anti-rabbit-Cy3 1:100 (Sigma), anti-rabbit-FITC 1:150 (Sigma). Samples were incubated 30 minutes at room temperature with DAPI (Sigma) to stain nuclei, or phalloidin conjugated to Alexa 488 (Molecular Probes, 1:1000) to stain actin filaments. The samples were imaged on a Zeiss LSM410 confocal microscope. Whole-mount *in situ* hybridization was performed as previously described (Harland, 1991).

RT-PCR

RNA was extracted from homogenized embryos at the indicated stages (five embryos per condition) using the RNeasy (Qiagen) kit according to the manufacturer's instructions. cDNA was synthesized using Superscript II reverse transcriptase (Invitrogen). PCR reactions with Taq polymerase were performed according to established protocol using 1ul of the resulting DNA. (See Supplemental Data for primer sequences and a detailed protocol).

Western Blots

Heart tissue from a minimum of 300 embryos per condition was dissected at stage 33 and snap frozen. Tissue was homogenized, subjected to SDS-PAGE, and transferred according to established protocols. Blots were probed overnight at 4 ˚C with antibodies against Cdc6, Cdt1 (gift from M. Coué, both 1:500 (Whitmire et al., 2002)), cyclin E2 (Abcam, 1:500), PCNA (Zymed, 1:1000), MCM 4 (Abcam, 1:2000), MCM 5 (Abcam 1:400), MCM7 (LabVision, 1:200), Cdk1 (Zymed, 1:1000), Cdk2 (Upstate, 1:1000), cyclin A1, cyclin A2 (Abcam, both 1:1000), SLBP (gift from W. Marzluff, 1:1000 (Wang et al., 1999)), and cyclin B2 (gift from T. Hunt, 1:500 (Hochegger et al., 2001)). Blots were rinsed and probed with

the appropriate HRP-conjugated secondary antibody (Jackson, 1:10000), and detected with ECL. As a loading control, blots were reprobed with antibodies against Total MEK (Cell Signaling, 1:2000), alpha tubulin (Abcam, 1:1000), and/or SHP2 (BD Biosciences, 1:2500).

Transmission Electron Microscopy

Stage 37 embryos were fixed in 2% paraformaldehyde/2.5% gluteraldehyde overnight. Embryos were post-fixed in ferrocyanide-reduced osmium and embedded in Spurr's epoxy resin. Transverse ultrathin (70 nm) sections were mounted on copper grids, and post-stained with 4% aqueous uranyl acetate followed by Reynolds' lead citrate. Sections were imaged with a LEO EM-910 transmission electron microscope.

RESULTS

TBX5 depletion leads to a decrease in cardiac proliferation

To understand the role of TBX5 in heart development, we depleted TBX5 from *Xenopus* embryos using a morpholino-based approach. Results from these studies show that removal of TBX5 leads to morphologically abnormal hearts and a decrease in cardiac cell number that is not associated with a block in cardiac specification, commitment, migration, or differentiation (Brown et al., 2005); (Fig. 4.1A,B). To characterize the phenotype of TBX5-depleted embryos in more detail, and to determine the precise developmental stage at which TBX5 is required during cardiogenesis, we carried out histological analyses and cell counting studies in TBX5 morpholino-injected (T5MO) and Control morpholino-injected (CMO) embryos by double-staining for the cardiac and skeletal muscle marker tropomyosin and with DAPI, to mark cell nuclei (Fig. 4.1C-F). All cells throughout the heart for each stage were counted, and quantitative results are reported in Fig. 4.1S. There was no significant

difference between control and TBX5-depleted embryos at stage 33 (Fig. 4.1C,E,S). However, at stage 37 T5MO embryos show a significant decrease in cardiac cell number compared with their sibling controls (Fig. 4.1D,F,S). The defect in cell number precedes the expression of proposed TBX5 target genes including atrial naturitic factor (ANF/Nppa) and connexin 40 (Bruneau et al., 2001; Hiroi et al., 2001; Small and Krieg, 2000). Therefore, the reduction in cardiac cell number appears to be one of the primary cardiac defects in TBX5-depleted embryos.

To determine if the decrease in cardiac cell number is due to cell proliferation or programmed cell death, we analyzed the mitotic index (Fig. 4.1G-L,T) and apoptosis (Fig. 4.1M-R, U) at defined time points during heart development: stage 29, which corresponds to the stage when the heart field rounds up to begin forming the bilaminar heart tube; stage 33, at which time cardiac looping is initiated; and stage 37, corresponding to early chamber formation. For these studies CMO and T5MO embryos at each stage were serial-sectioned through the cardiac regions and triple immuno-stained with anti-tropomyosin (Tmy) to mark cardiomyocytes, DAPI to mark cell nuclei, and either anti-phospho histone H3 (pH3) to mark cells in M phase (Fig. 4.1 G-L), or anti-cleaved Caspase 3 to mark cells undergoing apoptosis (Fig. 4.1 M-R). In each study all cardiomyocytes and endocardial cells encompassed by the cardiomyocytes for each heart at each stage were scored for pH3 or cleaved Caspase 3.

CMO embryos show that the total cardiomyocyte cell numbers undergo a doubling every 4 stages, or 9 hours, at room temperature between stages 33 and 37 (Fig. 4.1 G-I, M-O). Since the majority of the cardiomyocytes appear to be undergoing mitosis (based on serial sections of multiple embryos at these stages), the embryonic cardiac cell cycle in *Xenopus* is approximately 9 hours in length with M phase lasting approximately 20 minutes,

with the mitotic index gradually decreasing with age (Fig. 4.1T). We note there is little to no cardiomyocyte programmed cell death during these stages (Fig. 1U).

Results from these studies clearly show a decrease in the mitotic index of T5MO-derived embryos relative to CMO embryos at stage 33 (Fig. 4.1T), however, no significant programmed cell death was observed until later stages (stage 37; Fig. 4.1U). Since we observe a dramatic decrease in the mitotic index at a time prior to the decrease in cardiac cell number or increases in cardiac programmed cell death (Fig. 4.1S-U), the primary cause of the reduction in cell number in T5MO cardiac tissue appears to be a decrease in cardiac cell proliferation. Taken together, the data suggests that the decrease in proliferation resulting from depletion of TBX5 is due to either a lengthening of the embryonic cardiac cell cycle or alternatively, a premature exit of cardiomyocytes from cell cycle.

TBX5 depletion leads to a cardiac cell cycle delay or arrest in G_1/S phase

Inference from other systems implies that the integration of growth factor signal cascades with G_1/S cell cycle passage is regulated by the cyclin/CDK complexes CDK2/cyclin E, CDK2/cyclin A, and CDK1/cylin D, many of which are expressed in *Xenopus* in a stage- and tissue-specific fashion (Vernon and Philpott, 2003). Although much is known about the cardiac cell cycle during neonatal periods, little is known about the expression of CDKs and cyclins during the early stages of embryonic heart development. To address this issue, we isolated hearts from the first stage at which we could anatomically isolate pure cardiac tissue (stage 33). The resultant tissues were analyzed relative to corresponding whole embryo lysates with an extensive panel of antibodies specific for individual cyclins and CDKs (Fig. 4.2A). Results from this analysis show that *Xenopus* cardiac tissue at stage 33 expresses cyclin E2, CDC6, PCNA, SLBP, CDK2, cyclin A2 and CDK1, as well as proteins that are

expressed uniformly throughout the cell cycle such as MCM4 and MCM7. Although we could detect high levels of CDT1, cyclin A1, cyclin B2, and MCM5 in stage 33 embryos, we were able to detect little to no expression of these proteins in the heart (Fig. 4.2A). However, due to the relative amount of cardiac tissue to that of whole embryos, we cannot formally rule out the possibility that these proteins are present at relatively lower amounts. We note that we were unable to identify any antibody that marked D cyclins in *Xenopus*. However, previous studies have suggested that neither of the *Xenopus* D cyclins, cyclin D1 or D2, are expressed in the heart at these stages (Vernon and Philpott, 2003).

We next analyzed cell cycle proteins in heart tissue derived from T5MO and CMO embryos (Fig. 4.2B). These studies show that depletion of TBX5 leads to a dramatic up-regulation of S phase proteins cyclin E2, CDC6, and CDK2 while proteins associated with other cell cycle phases, cyclin A2 and CDK1, or proteins expressed throughout the cell cycle, such as MCM4 and MCM7, show no significant differences between T5MO- and CMO-derived heart tissues (Fig. 4.2B). Together with the mitotic index data, our results strongly suggest that depletion of TBX5 leads to a prolonged/arrested G_1 or S phase and a concomitant decrease in the proportion of cardiac cells in M phase.

To confirm these findings we also analyzed CMO- and T5MO-derived hearts for the non-CDK/cyclin S phase proteins stem loop binding protein (SLBP) and proliferating cell nuclear antigen (PCNA) (Fig. 4.2C). Western blots of CMO- and T5MO-derived heart tissue show that relative to the loading controls SHP2 and total MEK, depleting TBX5 leads to an increase in both SLBP and PCNA levels. Collectively, these results strongly suggest that TBX5 depletion leads to a delay or block in the G_1 or S phase of the cardiac cell cycle.

Terminally differentiated cardiomyocytes continue to undergo cell division

Our results suggest that TBX5 is required for embryonic cardiac cell cycle progression (Fig. 4.2) but is not required for cardiac differentiation (e.g. Fig. 4.1A,B). Thus, terminally differentiated cardiomyocytes could be undergoing cell division or, alternatively, a subpopulation of *Xenopus* cardiomyocytes may undergo cell cycle arrest and terminal differentiation while a second subpopulation of cardiomyocytes continue to divide and remain in an undifferentiated state. The former is consistent with studies in chick and mouse which imply that heart tissue is capable of initiating and maintaining terminal differentiation during a period in which the cells are still dividing; i.e. not during G_1 or G_0 arrest (Anversa and Kajstura, 1998; Burton et al., 1999; Kajstura et al., 2004; McKinsey et al., 2002; Mikawa et al., 1992; Mikawa et al., 1992; Rybkin et al., 2003; Soonpaa and Field, 1998). To directly test the relationship between the cardiac cell cycle and terminal differentiation in *Xenopus* embryonic cardiac tissue, we triple-labeled cardiomyocytes at stage 37 with anti-pH3, DAPI, and a panel of antibodies that detect terminally differentiated cardiomyocytes including anti-tropomyosin (Tmy), anti-myosin heavy chain (MHC), and phalloidin, to mark cardiac actin (Fig. 4.3). Results from these studies clearly show that in CMO hearts we are able to detect cardiomyocytes that are undergoing mitosis yet also co-express all three markers of terminal differentiation (Fig. 4.3A-D). In addition, we note that cardiomyocytes expressing tropomyosin, cardiac actin, and cardiac myosin heavy chain, show the hallmarks of terminal cardiomyocyte differentiation including the assembly of cells into muscle fibers containing A- and Z-bands. Consistent with findings that fewer cardiac cells in T5MO embryos undergo mitosis (Fig. 4.1), we were able to detect very few anti-phosphorylated histone H3 positive cells in T5MO-derived hearts. However, of the few cells that expressed pH3, these cells, like

controls, also co-expressed markers of cardiomyocyte terminal differentiation, including tropomyosin, actin, and myosin heavy chain (Fig. 4.3E-H). Taken together, these data indicate that terminally differentiated cells in both control and TBX5-depleted embryos retain the capacity to undergo cell division and suggest that *Xenopus* cardiac cells during these stages do not arrest in G_1 or G_0. These data further suggest that TBX5, although required for cardiac cell cycle progression, is not required to initiate or maintain cardiac differentiation.

TBX5 is required for the proper timing of the cardiac program

Since TBX5 depletion does not block cardiac differentiation, we next addressed whether TBX5 depletion could affect the stage at which cardiac markers are initially expressed. To this end, we collected equivalently staged T5MO and CMO embryos at all early stages at which *Tbx5* has been reported to be expressed: stages 10 through 38 (early gastrula through late tadpole). In the first series of studies, we carried out RT-PCR with a panel of primers specific for markers of cardiac differentiation (cardiac myosin heavy chain, cardiac troponin, and tropomyosin) or skeletal muscle differentiation (MyoD, skeletal muscle actin) (Fig. 4.4A). Results show significant differences in the timing of cardiac gene expression in T5MO embryos relative to their stage-matched CMO siblings; T5MO embryos turn on troponin and cardiac myosin heavy chain (MHC) at earlier stages than controls (stage 28 in T5MO versus stage 32 in CMO) but initiate expression of Tmy at later stages (stage 24 in T5MO versus 22 in CMO). Since we do not observe any changes in the timing at which skeletal muscle markers are expressed, the alteration in timing of differentiation appears to be specific to cardiac tissue.

To confirm these findings, we carried out whole-mount antibody staining on T5MO and CMO embryos for tropomyosin. Consistent with the RT-PCR analysis, we observe a delay in the expression of tropomyosin in T5MO embryos in comparison to CMO embryos (Fig. 4.4 B-I). As further confirmation that the timing of differentiation is altered in response to TBX5 depletion in vivo, we injected embryos carrying the cardiac actin:GFP transgene (Latinkic et al., 2002) with T5MO or CMO and monitored skeletal muscle and heart development in living staged-matched embryos (Fig. 4.4J-Q). Although we could not detect any alteration in the timing of GFP expression in skeletal muscle (data not shown), we observed a consistent and significant delay in the time at which GFP was first expressed in the hearts of the T5MO embryos. Collectively, these results suggest that control of the cardiac cell cycle by TBX5 leads to an alteration in the timing of the cardiac program.

TBX5 depletion leads to abnormal sarcomere formation

To determine if cardiomyocyte differentiation in T5MO hearts occurs in all cardiomyocytes or only in a subset of cells, we analyzed cardiomyocyte differentiation by immunohistochemistry on cross-sections of CMO and T5MO-derived tissues (Fig. 4.5A-H). Results clearly show that by stage 37, we can detect staining of troponin T (cTnT), MHC, and Tmy throughout the myocardium of control and T5MO hearts, suggesting that all cardiomyocytes in T5MO undergo terminal differentiation.

To examine sarcomere and cytoskeletal structure in greater detail, we double- labeled hearts from CMO and T5MO embryos with the cardiomyocyte marker Tmy and antibodies that recognize either components of the cardiac extracellular matrix (ECM): fibronectin and fibrillin, or mark cardiomyocyte polarity, -catenin (Fig. 4.5I-N); (Trinh and Stainier, 2004). This analysis revealed that TBX5 depletion leads to hearts with defects in both sarcomere

and ECM development. In contrast to CMO-derived hearts, which form sarcomeres throughout the myocardium, T5MO hearts only form sarcomeres in cells adjacent to the lumen of heart (Fig. 4.5G-J,O,P). Moreover, the sarcomeres that form often lack A- and Z-bands and frequently fail to give rise to myofibrils (Fig. 4.5O, P). These alterations in cardiomyocyte differentiation coincide with elevated fibronectin deposition particularly within the dorsal portion of the T5MO in dorsal regions where the heart remains unfused (Fig. 4.5I,J) and an increase in both fibronectin and fibrillin deposition on the walls of the heart chamber (Fig. 4.5I-L). However, we could detect no alteration in -catenin expression (Fig. 4.5M,N). We also note that at this stage, it appears the majority of -catenin is associated with the myocardial membranes with little to no -catenin in the cytoplasm or nucleus. Taken together this data suggests that alteration in cardiac cell cycle progression due to the depletion of TBX5 leads to abnormal cardiomyocyte and ECM maturation.

To confirm these structural alterations in TBX5-depleted heart tissue, we carried out ultrastructure analyses on CMO and T5MO hearts by high magnification confocal microscopy (Fig. 4.5O,P) and transmission electron microscopy (TEM) (Fig. 4.5Q-V). High magnification imaging of cardiac tissue immunostained with Tmy reveals that cardiac cells in CMO embryos form myofibrils that are distributed throughout the myocardium (Fig. 4.5O). In contrast, myofibrils in T5MO cardiac cells are poorly organized and form only adjacent to the cardiac lumen (Fig. 4.5P).

Consistent with immunostaining for cardiac muscle, we find in transverse TEM sections of CMO embryos that cardiac muscle bundles are located throughout the myocardium, positioned in both longitudinal as well as concentric arrays (Fig. 4.5Q). In contrast, T5MO hearts show far fewer sarcomeres than controls, and the cells bordering the pericardial space of T5MO hearts, in contrast with those bordering the heart lumen,

completely lack bundles of cardiac muscle fibers (Fig. 4.5R,S,V). Moreover, the sarcomeres that form frequently lack distinct A- and Z-bands, and the A- and Z-bands that are present are poorly defined (Fig. 4.5T,U). This does not appear to represent simply a delay in myofibril formation since during normal development myofibrils form throughout the myocardium and do not show any temporal differences in differentiation between distal and proximal cardiomyocytes (Kolker et al., 2000; Langdon, et al., submitted).

Taken together, our immunohistochemistry and ultrastructure analysis suggest that the G_1/S phase delay or arrest in TBX5-depleted embryos results in an alteration in the timing of the cardiac program leading to asymmetric and aberrant sarcomere formation. Moreover these results imply that TBX5 is not required for the onset of cardiac differentiation but is required to either establish or maintain cardiomyocyte and cytoskeletal architecture.

TBX5 is both necessary and sufficient for the progression of the embryonic cardiac cell cycle

Our analysis of T5MO embryos shows a requirement for TBX5 in embryonic cell cycle progression and a role in controlling the correct timing of cardiac differentiation. To determine if TBX5 is sufficient to regulate these two processes, we mis-expressed *Tbx5* in early *Xenopus* embryos (Fig. 4.6). Although injection of *Tbx5* RNA at the single cell stage causes *Tbx5* mis-expression throughout the embryo, phenotypic abnormalities are restricted to the anterior and cardiac regions of the early tadpole (Fig. 4.6A-C, data not shown). To further analyze these defects, we carried out whole-mount *in situ* hybridization analyses on uninjected control and *Tbx5*-injected embryos (Fig. 4.6D-G; data not shown). Similar to results from TBX5 depletion, this analysis shows *Tbx5* mis-expression does not block cardiac

commitment, migration, or terminal differentiation as judged by *Nkx2.5* and Myosin Light Chain (MLC) expression (Fig. 4.6D-G).

To test if *Tbx5* cardiac defects are associated with alteration in the cardiac cell cycle, we serial sectioned embryos at stage 37 and stained with the mitotic marker anti-pH3. We found that *Tbx5* mis-expression has the opposite effect of depleting TBX5, leading to a two-fold increase in the cardiac cell mitotic index (Fig. 4.6H).

To ensure that the increase in mitotic index is tissue specific, we calculated the mitotic index in the ventricular zone of the neural tube in the same sections as those containing the heart tissue; i.e. sections that correspond exactly to the same point along the anterior-posterior axis. We could not detect a difference between control or *Tbx5* mis-expressing derived neural tissue. Therefore, the increase in mitotic index within appears to be cardiac specific.

To test whether TBX5 is also sufficient for the correct timing of cardiac differentiation, we again collected stage-matched embryos from stage 10 to stage 38 and carried out RT-PCR with primers specific for the early cardiac marker *Nkx2.5*, and for markers of cardiac and skeletal muscle differentiation (Fig. 4.6J). Consistent with our results for the in situ hybridization experiment, we found no alteration in *Nkx2.5* expression in *Tbx5* injected embryos. Results for the cardiac differentiation markers show the exact opposite of those for TBX5 depletion; *Tbx5* injected embryos initially express Troponin and MHC at later stages than controls (stage 38 in *Tbx* injected versus stage 28 in control embryos) but turn on Tmy at earlier stages (stage 16 in *Tbx5* injected versus 22 in control embryos). Since we do not observe any changes in the timing at which skeletal muscle markers are expressed, the alteration in timing of expression again appears to be specific to cardiac tissue. Collectively, these studies strongly suggest that TBX5 is both necessary and sufficient to

regulate progression of the embryonic cardiac cell cycle and the timing of the cardiac program.

DISCUSSION

Despite the critical importance of understanding cell cycle control for both normal development and disease, relatively little is known about the proteins that regulate these processes in the embryonic heart. We demonstrate that that TBX5 is both necessary and sufficient to control embryonic cardiac cell proliferation and cell number by regulating the length of the embryonic cardiac cell cycle. Our results show that depletion of TBX5 leads to a delay or arrest in G_1 or S phase as judged by the up-regulation of the G_1/S phase-associated proteins and the concomitant decrease in the cardiac mitotic index. If the arrest was occurring at the S/G2 transition, Cdc6 and Cyclin E2 levels should be equivalent between T5MO and control heart tissue. Moreover, cyclin A2 and Cdk1 should be significantly elevated in the T5MO hearts. Since our results clearly show that the level of neither protein is altered in the T5MO tissue relative to the control our data strongly suggest that the arrest does not occur at S/G2 but at the G_1/S phase transition. Since cyclins E and A are thought to be expressed sequentially during S phase, and since we observe an increase in cyclin E2 but not in cyclin A2, our results would predict that S phase arrest in TBX5-depleted embryos occurs at the G_1/S transition or in early S phase. Based on these findings, we propose that depleting TBX5 results in a prolonged or blocked early S phase resulting in fewer rounds of proliferation, in turn leading to the reduced cardiac cell number we observe in T5MO embryos (Fig. 4.7).

Past studies have implied that the myocardium undergoes a fixed number of intrinsically determined cell divisions before entering a post-mitotic state and undergoing cardiac differentiation (Burton et al., 1999). It appears that TBX5 interferes with this

autonomous program by forcing cells into a prolonged or arrested S phase and thus, differentiating without undergoing a predetermined number of cell divisions. Since in the TBX5-depleted embryos and embryos mis-expressing *Tbx5* the timing of the cardiac differentiation program is altered compared to controls, our results imply that proper S phase progression and possibly a determined number of divisions, are required for the proper timing, but not the initiation, of heart differentiation. Our results further imply that a reduced number of cardiac divisions leads to a delay in the expression of some markers of terminal differentiation including cardiac actin, and tropomyosin. In contrast, we note that troponin and MHC are expressed earlier in T5MO cardiac tissue and later in hearts from embryos mis-expressing *Tbx5* suggesting that these markers are controlled in a different fashion relative to other cardiac terminal markers.

TBX5 and embryonic cardiac cell cycle control

Like other members of the T-box gene family, TBX5 has been shown to function as a transcription factor; TBX5 is localized to the nucleus, it binds to DNA in a sequence specific fashion, and regulates the transcriptional level of its target genes. Our present studies suggest that at least one of the targets of TBX5 either directly or indirectly functions to control the progression of the embryonic cardiac cell cycle. What are the mechanisms by which this may occur? One possibility is that TBX5 could function to induce the expression of a growth factor, for example EGF or FGF, which in turn is required for cell cycle progression. In the absence of this growth factor the cell cycle may not proceed through to the completion of G_1 (Fig. 7). Alternatively, TBX5 may function to regulate the expression of a key component of the pre-replication complex. In the absence of this key component the pre-replication

complex may not assemble or may not load onto the origins of replication (ORCs) thus, blocking DNA synthesis and hence cell cycle progression (Fig. 4.7).

Cell cycle progression through G_1/S is regulated by members of the E2F family of transcription factors, whose function is governed through their interaction with the retinoblastoma protein (Rb). In its hypophosphorylated state Rb interacts with E2F inhibiting its transcriptional activation activity. Upon Rb phosphorylation, the Rb-E2F interaction is disrupted and E2F is released and able to activate its downstream genes required for S phase entry (Cobrinik, 2005). Thus, one function of TBX5 may be to indirectly regulate the state of pRB phosphorylation. Finally, TBX5 may function to negatively regulate general cell cycle inhibitors such as $p27^{Xic}$ (Fig. 4.7). Our data cannot distinguish between these possibilities and the exact molecular pathway by TBX5 functions awaits the identification of TBX5 cell cycle target genes.

Tbx5 mis-expression leads to cardiac-specific defects

We show that mis-expression of *Tbx5* leads to cardiac defects in vivo. This effect appears to be specific since mis-expression of other T-box containing genes does not give a similar phenotype (Showell et al., 2004). These results demonstrate that the absolute levels of TBX5 are critical for normal heart development in vivo; increased levels of TBX5 result in abnormal heart formation and reduction of TBX5 levels by just half leads to HOS. Interestingly, the defects we observe with *Tbx5* mis-expression are specific to the anterior and cardiac regions of the embryo, with the cardiac defects resembling those seen with *Nkx2.5* mis-expression (Cleaver, 1996; Tonissen et al., 1994). The similarity between the *Tbx5* and *Nkx2.5* over-expression phenotypes raises the possibility that mis-expression phenotype we observe in TBX5 is due to an up-regulation of *Nkx2.5*. However, a number of

our findings would suggest this is not the case. Most critically, we have conducted in situ hybridization as well as RT-PCR to examine *Nkx2.5* expression in embryos mis-expressing *Tbx5* during early stages of early heart development. We show that mis-expression of TBX5 does not lead to altered spatial or temporal patterns or levels of *Nkx2.5* expression at any stage. These results are consistent with our previously published results showing that the loss of TBX5 has no effect on the temporal or spatial expression of *Nkx2.5* (Brown et al., 2004). Therefore, mis-expression of *Tbx5* appears to alter the cardiac mitotic index in an *Nkx2.5* independent fashion.

Our finding that *Tbx5* mis-expression results in an increased mitotic index differs from two previous studies implying that *Tbx5* expression inhibits cell growth or survival (Hatcher et al., 2001; Liberatore et al., 2000). However, in these reports *Tbx5* was mis-expressed after expression of endogenous *Tbx5* is initiated and consequently, after the commitment and differentiation of the heart have taken place. Thus, it may be possible that TBX5 has two opposing functions during development: an early function in regulating cardiac cell cycle progression and a late function instructing cardiac cells to undergo cell cycle arrest. Alternatively, over-expression of TBX5 may lead to it binding and activating non-endogenous targets, in particular those of other T-box gene genes, such as TBX2, TBX3, TBX18, or TBX20 (Harvey, 2002; Stennard and Harvey, 2005), which may function during the later stages of cardiogenesis to regulate cell cycle exit.

Holt Oram syndrome

HOS is an autosomal dominant disease arising from haploinsufficiency of TBX5 and is associated with conduction-system abnormalities, secundum atrial defect (ASD), and ventricular septal defects (VSD) (Basson et al., 1997; Li et al., 1997; Newbury-Ecob et al.,

1996). Consistent with these phenotypic abnormalities, *Tbx5* has been shown to be expressed in the atrial wall, the atrial septa and the atrial aspects of the atrioventricular valves (Hatcher et al., 2000). The role of TBX5 in heart development is further emphasized by the observation that mice heterozygous for mutations in *Tbx5* display many of the abnormalities described in HOS patients (Bruneau et al., 2001). However, the cellular basis for defects in HOS remains unclear. Our results would suggest that TBX5 functions to regulate the length of the G_1/S cycle within the subset of heart tissues in which it is expressed. In HOS, G_1/S phase would be significantly lengthened or blocked, leading to a decrease in cell cycle progression and defects in cell proliferation due to a successive decrease in the number of cell divisions, and ultimately programmed cell death in the affected regions.

Acknowledgements

This work is supported by grants to FLC from the NIH/NHLBI, RO1 HL075256 and R21HL083965, and an award from the UNC Medical Alumni Association. SCG is a trainee in the Integrative Vascular Biology program supported by T32HL69768 from the National Institutes of Health. The antibodies against tropomyosin and cardiac troponin (developed by J.-C. Lin) and fibrillin (developed by C.D. Little) were obtained from the Developmental Studies Hybridoma Bank developed under the auspices of the NICHD and maintained by the University of Iowa, Department of Biological Sciences, Iowa City, IA 52242. We are grateful to Drs. Martine Coué for the Cdt1 and Cdc6 antibodies, William Marzluff for the SLBP antibody and Timothy Hunt for the cyclin B2 antibody. We wish to thank Victoria Madden and Elena Davis of the UNC Microscopy Services Laboratory for assistance with TEM. We thank Dr. Olav Binder for in situ hybridization images used in Figure 6. We

would like to acknowledge Robert Duronio for his time, patience and help with this work. We would also like to thank Larysa Pevny, Elizabeth Mandel, and Mark Majesky for critical reading of the manuscript and helpful suggestions.

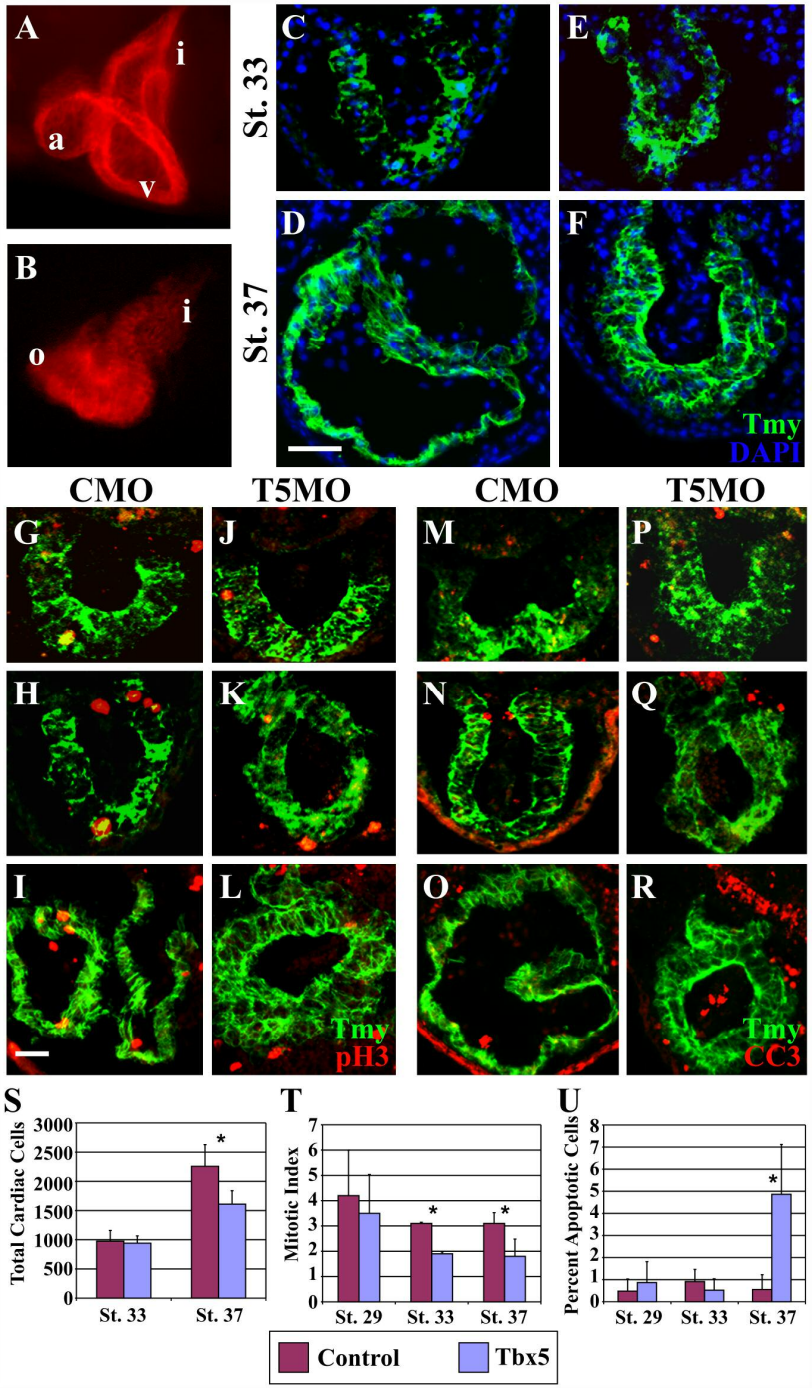

Figure 4.1. TBX5 is required for cardiac proliferation.

Whole-mount antibody staining with trypomyosin (Tmy) of stage 37 (A) control morpholino (CMO) or (B) TBX5 morpholino (T5MO) embryos (a, atrium; v, ventricle; i, inflow tract; o, outflow tract). Transverse heart sections through (C, E) stage 33 and (D, F) stage 37

embryos stained with Tmy, to mark cardiac tissue, and DAPI, to mark cell nuclei, (C, D) CMO-derived tissue, (E, F) T5MO-derived tissue. (G-L) Examples of proliferating cardiac cells in transverse heart sections from (G-I) CMO and (J-L) T5MO embryos sectioned through the cardiac region at stage 29, 33, and 37, as indicated. Proliferating cardiomyocytes are identified as those positive for Tmy (myofibrilis shown as green) and anti-phopho-histone H3 (pH3; localized to the nucleus and shown in red). (M-R) Examples of cardiac cells undergoing apoptosis in transverse heart sections from (M-O) CMO and (P-R) T5MO embryos at stage 29, 33, and 37, as indicated. Apoptotic cardiomyocytes are identified as those positive for Tmy (myofibrilis shown as green) and anti-cleaved caspase 3 (CC3; localized to the nucleus and shown in red). Quantification of results from (S) total cardiomyocyte cell numbers, (T) mitotic index, and (U) programmed cell death. In all cases, bars represent the average of at least 3 embryos. CMO, red bar and T5MO, blue bar. Error bars denote the standard deviation and * denotes a statistically significant difference (at $p < 0.05$) between CMO and T5MO embryos at a given stage. (Scale bars = 50 μm). Results are derived from a single set of experiments, all experiments being repeated at least once with an independent batch of embryos.

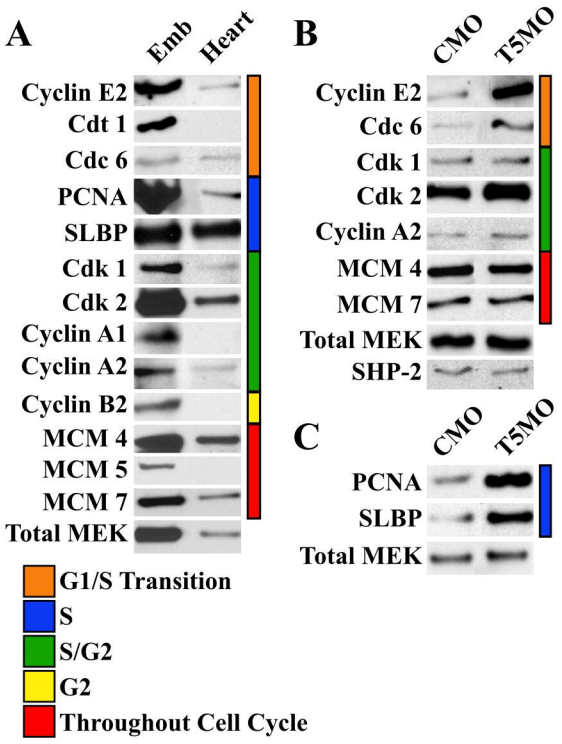

Figure 4.2. *TBX5 depletion results in dramatic up-regulation of proteins associated with G_1/S phase within the heart.*

(A) Expression profile of cell-cycle associated proteins as determined by Western blot analysis performed using lysate from either whole stage 33 embryos (emb), or corresponding heart tissue (heart). (B) Relative differences in embryonic cardiac CDK and cyclin proteins between CMO and T5MO-derived heart tissue (stage 33). Note increased levels of Cyclin E2, CDC6, CDK2. (C) Relative differences in embryonic cardiac S-phase associated proteins SLBP and PCNA between CMO and T5MO-derived heart tissue (stage 33). Colored bars denote the stage of the cell cycle at which the proteins are expressed, as indicated in the key.

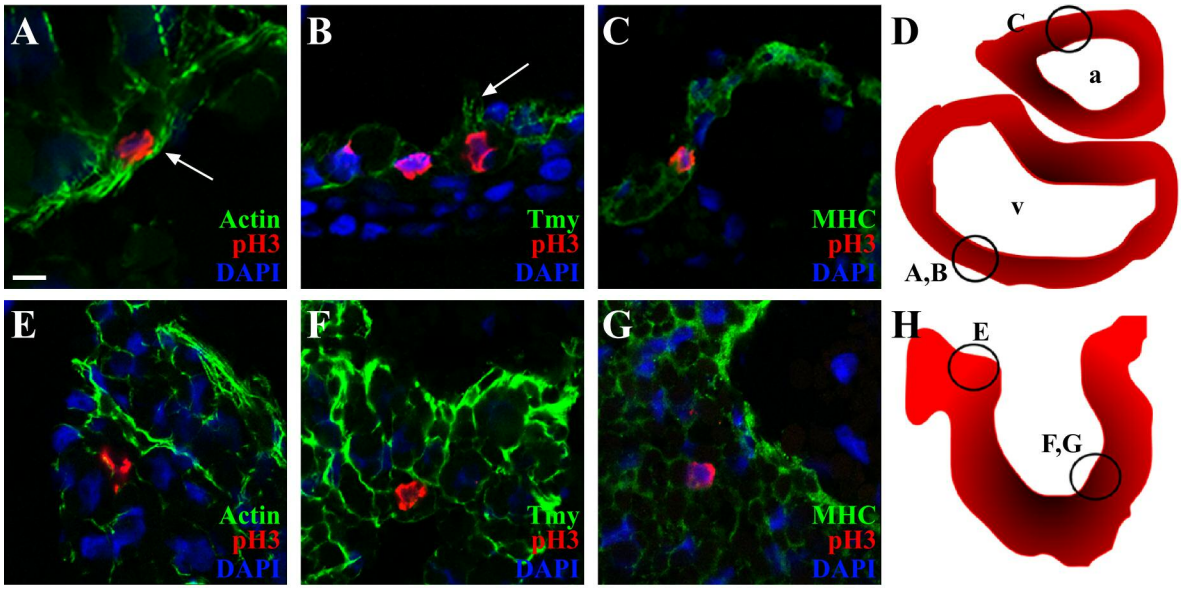

Figure 4.3. *Terminally differentiated cardiomyocytes retain the capacity to undergo cell division.*

Transverse sections of (A-C) CMO or (E-G) T5MO heart tissues at stage 37, showing cells co-expressing pH3 (red), DAPI (blue), and either (A, E) actin, (B, F) Tmy, or (C, G) MHC (all shown in green). (D) Schematic of a CMO heart displaying the relative positions of each panel. (A) and (B) were imaged from an area corresponding with 'A,B'; (C) was imaged from a region corresponding with 'C' (a, atrium; v, ventricle). (H) Schematic of a T5MO heart displaying the relative positions of each panel. (E) corresponds with 'E'; (F) and (G) correspond with 'F,G'. White arrows denote sarcomeric bundles (Scale bar = 10 μm).

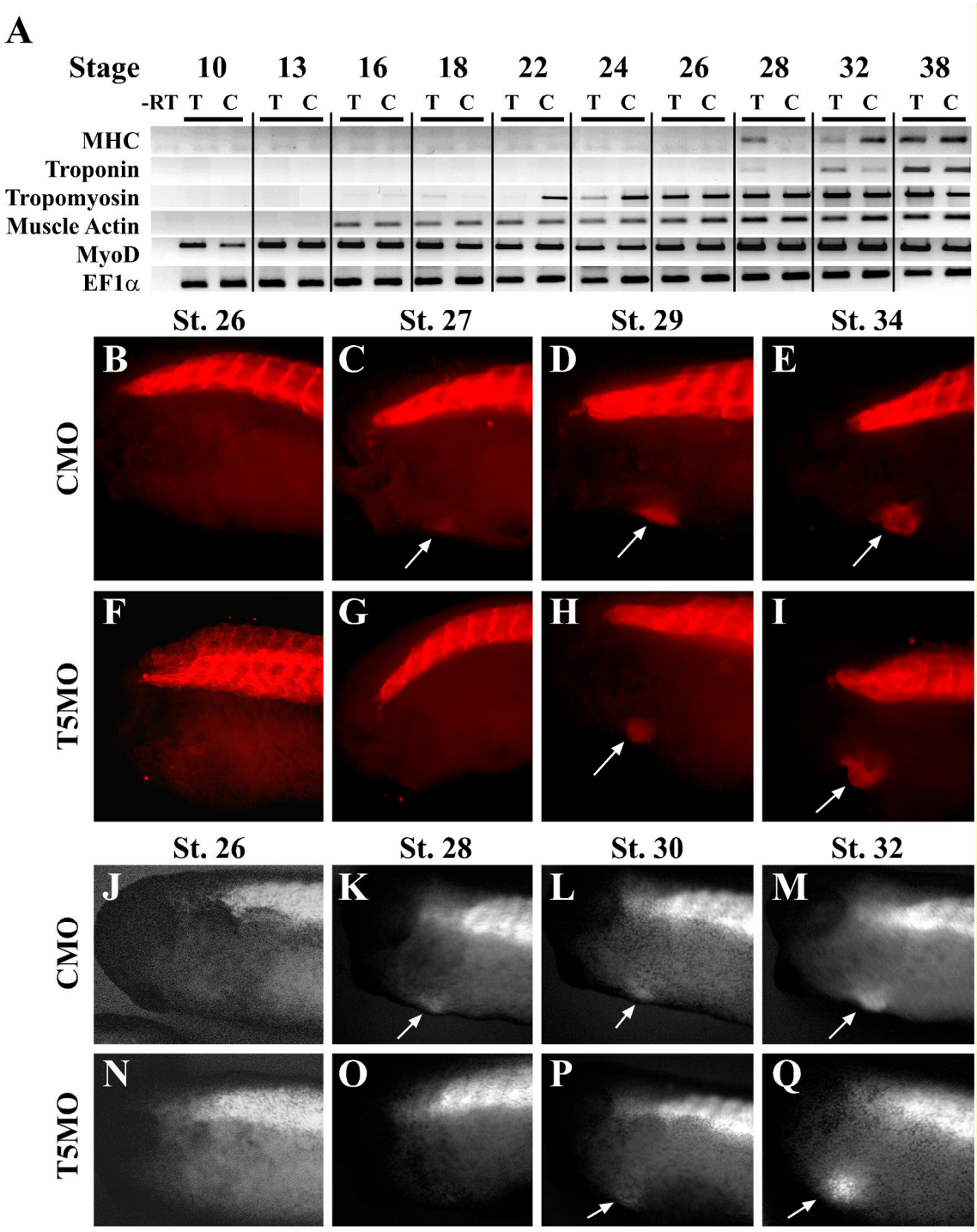
A
Stage 10 13 16 18 22 24 26 28 32 38
-RT T C T C T C T C T C T C T C T C T C T C
MHC
Troponin
Tropomyosin
Muscle Actin
MyoD
EF1α
St. 26
St. 27
St. 29
St. 34
CMO
T5MO
B
C
D
E
F
G
H
I
St. 26
St. 28
St. 30
St. 32
CMO
T5MO
J
K
L
M
N
O
P
Q

Figure 4.4. *The timing of the cardiac differentiation program is altered in TBX5 depleted embryos.*

(A) RT-PCR analysis of the expression of heart-specific isoforms of MHC, troponin, and tropomyosin; and skeletal muscle-specific genes MyoD and muscle actin, throughout early and mid-gestation stages of development in CMO ("C") and T5MO ("T") staged matched embryos. All samples are derived from a single batch of eggs and identical results were achieved in at least two independent sets of experiments for each marker. EF1-Alpha was used as a loading control for all RT-PCR reactions. (B-I) Images depicting embryos injected with (B-E) CMO, or (F-I) T5MO and immunostained for Tmy showing delayed expression of Tmy in the hearts of T5MO embryos. Shown are representative sibling embryos imaged at the indicated stages. White arrows denote expression of Tmy within the heart. (J-Q) Images of living cardiac actin:GFP transgenic embryos showing a delay in the onset of cardiac actin expression in the heart. Representative sibling embryos obtained from a single batch of embryos were injected with (J-M) CMO or (N-Q) T5MO and imaged at the indicated stages. Shown is a representative pair of embryos, while identical results were observed in over 50 embryos. White arrows denote expression of GFP within the heart field.

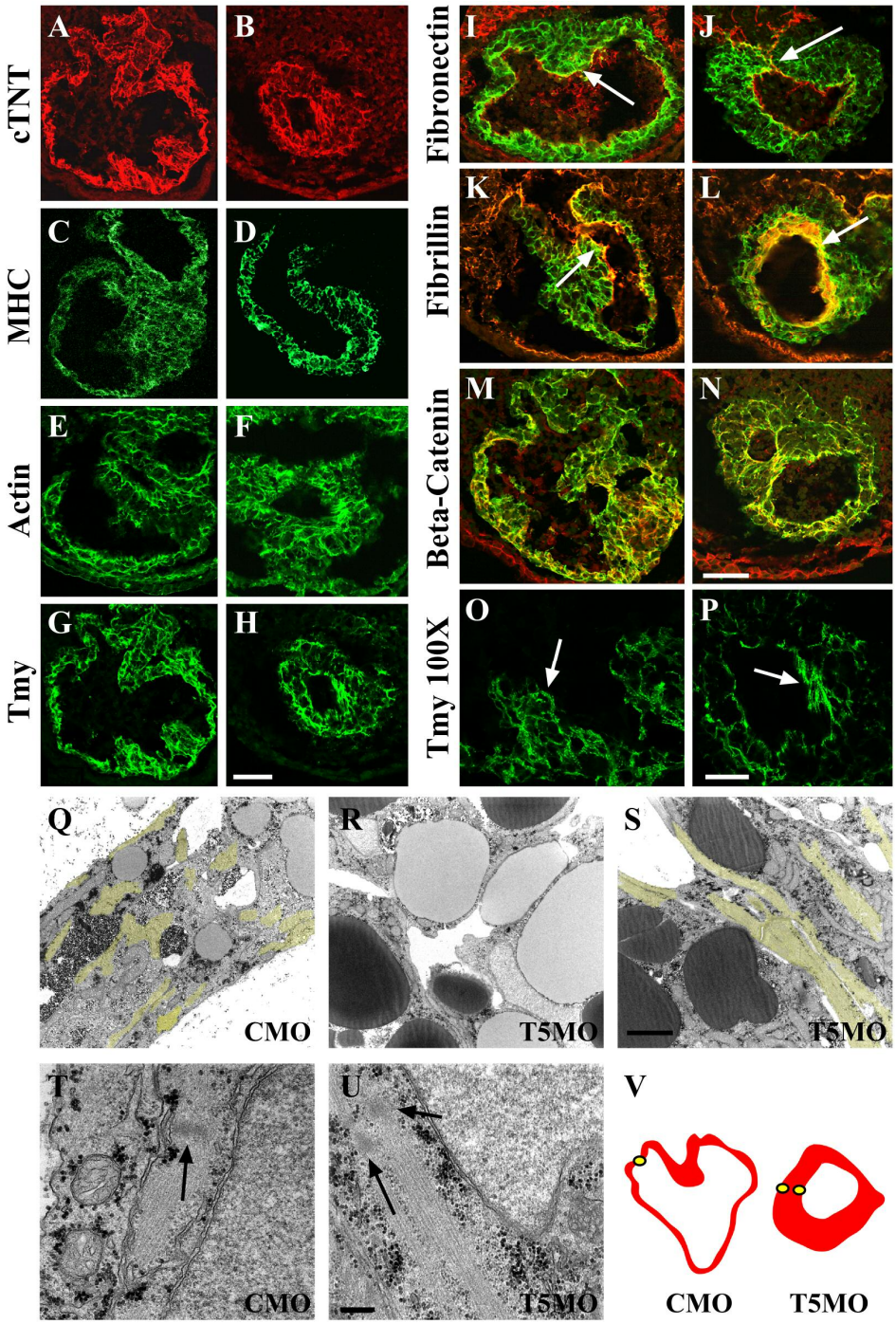

Figure 4.5. *TBX5 depletion leads to a disruption in cardiac myofibril structure.*

Cardiomyocyte structure in transverse sections through the hearts of (A, C, E, G) CMO or (B, D, F, H) T5MO stage 37 embryos as detected by immunostaining for (A, B) cardiac

troponin T (cTNT), (C, D) MHC, (E, F) actin, or (G, H) Tmy (scale bar = 50 μm). (I, K, M) Stage 37 CMO or (J, L, N) T5MO embryos double-immunostained for tropomyosin (green) and (I, J) fibronectin, (K, L) fibrillin, or (M, N) β-catenin, all shown in red (scale bar = 50 μm). Note increase in fibrillin staining on the walls of the chamber of T5MO hearts relative to CMO (compare panel K to L, white arrows) and ectoptic expression of fibronectin, shown by white arrow, in the dorsal portion of the heart in panel J relative to panel I. (O, P) High magnification confocal images of hearts from (O) CMO or (P) T5MO stage 37embryos. Note that formation of organized cardiac muscle bundles in T5MO hearts is limited to a single cluster adjacent to the cardiac lumen. (Q-S) Representative transmission electron micrographs of transverse images of stage 37 embryos taken from (Q) CMO cardiac tissue or (R) T5MO cardiac tissue adjacent to the pericardial cavity and (S) T5MO cardiac tissue adjacent to the cardiac lumen. Cardiac muscle fibrils are shown pseudo-colored in yellow. (Scale bars = 2 μm). Note that sarcomeres in T5MO hearts can only be identified adjacent to the cardiac lumen (compare R to S) and only found in concentric arrays. In contrast, CMO-derived hearts show both longitudinal as well as concentric arrays (compare Q to S). High magnification TEM images reveal the ultrastructures of (T) CMO and (U) T5MO cardiac sarcomeres. Arrows denote A-bands. Note the smaller, non-continuous A-bands in the T5MO-derived sarcomeres (U) (scale bar = 0.2 μm). (V) Traces of the heart sections from CMO and T5MO embryos imaged by TEM are depicted schematically. Yellow circles represent the location of TEM imaging.

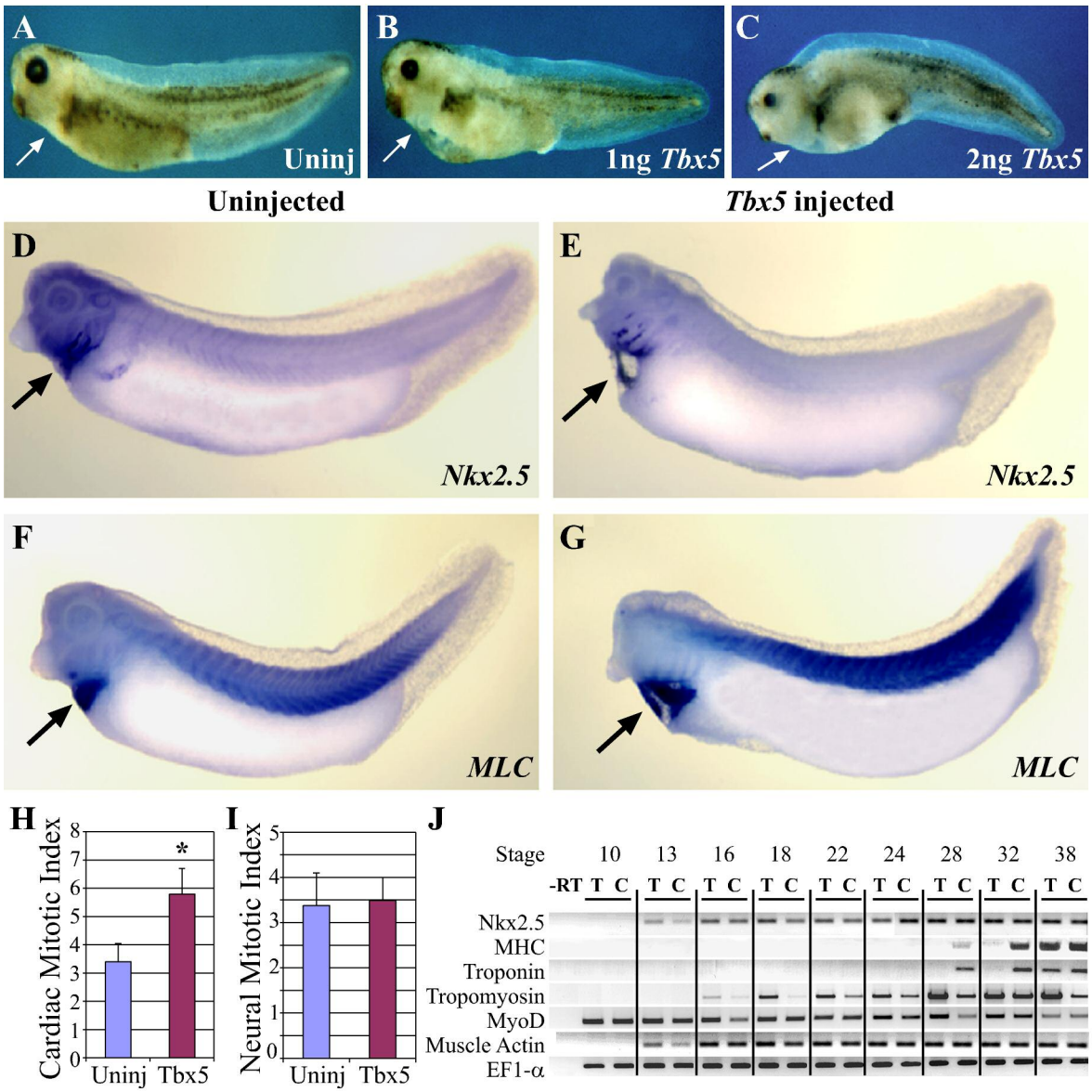

Figure 4.6. *Tbx5* ***mis-expression leads to changes in cardiac proliferation and morphology.***

The overall morphology of stage 40 (A) uninjected embryos or (B, C) embryos injected with increasing amounts of *Tbx5* RNA as indicated. Arrows denote the location of the heart. (D-G) Whole-mount *in situ* hybridization showing expression of (D, E) *Nkx2.5* and (F, G) myosin light chain (MLC) in (D, F) uninjected stage 37 embryos and (E, G) stage-matched

embryos injected with 1 ng of *Tbx5* RNA. (H) *Tbx5* mis-expression leads to an increase in the cardiac mitotic index in control and *Tbx5*-injected embryos at stage 37. Mitotic index was calculated as the percentage of cardiac cells labeled with pH3. The data represents the mean of at least 3 different embryos. Error bars denote the standard deviation and * denotes a statistically significant difference between *Tbx5* injected and control embryos (at $p < 0.05$). (I) Mitotic index for sections of the neural tube corresponding to the same position as the heart along the anterior-posterior axis. The data represents the mean mitotic index of 4 different embryos per condition, with 4 sections analyzed per embryo. Error bars denote the standard deviation. (J) *Tbx5* mis-expression leads to an alteration in the timing and order of the cardiac differentiation program. RT-PCR analysis of the expression of *Nkx2.5* as well as heart-specific isoforms of MHC, troponin, and tropomyosin, and skeletal muscle specific genes, MyoD and muscle actin, throughout early and mid-gestation stages of development in control ('C') or *Tbx5* injected ('T') stage-matched embryos. All samples are derived from a single batch of eggs and identical results were achieved in at least two independent sets of experiments for each marker. EF1-alpha was used as a control for all RT-PCR reactions.

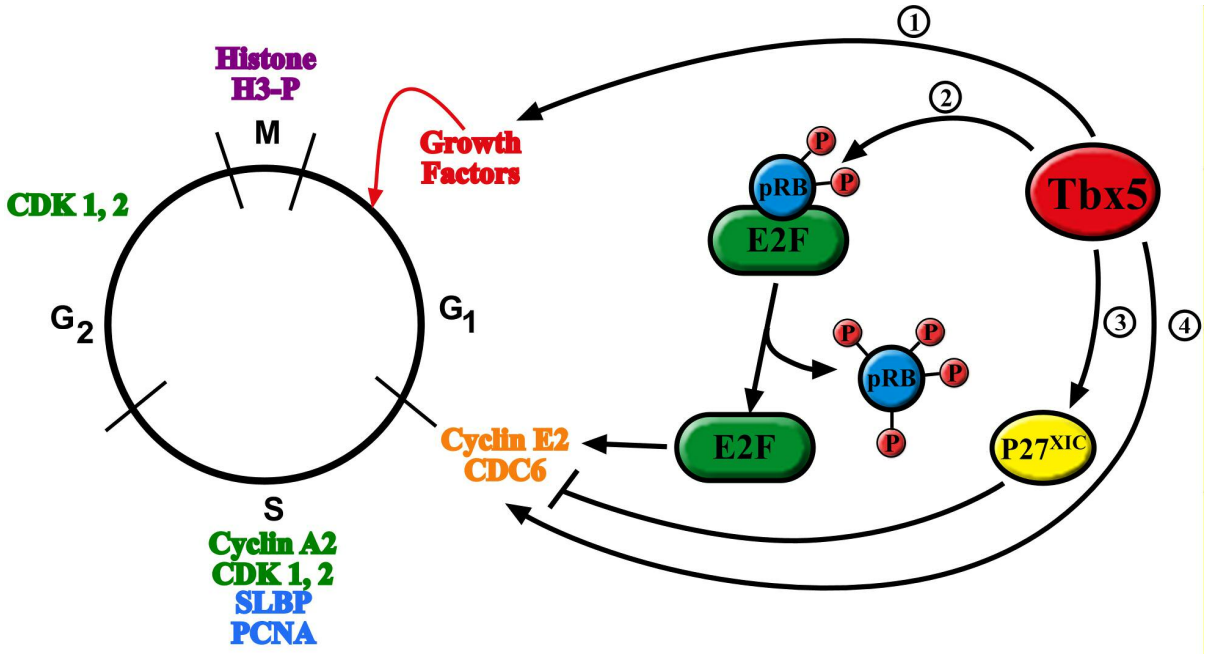

Figure 4.7. *Model for potential mechanisms by which TBX5 functions to control embryonic cardiac cell cycle progression.*

Schematic of embryonic cardiac cell cycle shown in left hand panel and potential roles for TBX5 in regulating G_1/S progression. (1) TBX5 may function to induce the expression of a growth factor, for example EGF or FGF required for cell cycle G_1 progression. (2) TBX5 may function to regulate E2F activity by controlling the phosphorylation state of pRB. (3) TBX5 could also negatively regulate general cell cycle inhibitors such as $p27^{Xic}$. (4) Alternatively TBX5 may function to regulate the expression of a key component of the CDK-cyclin complexes required for G_1/S progression.

REFERENCES

Anversa, P. and Kajstura, J. (1998). Ventricular myocytes are not terminally differentiated in the adult mammalian heart. *Circ Res* **83**, 1-14.

Basson, C. T., Bachinsky, D. R., Lin, R. C., Levi, T., Elkins, J. A., Soults, J., Grayzel, D., Kroumpouzou, E., Traill, T. A., Leblanc-Straceski, J. et al. (1997). Mutations in human TBX5 [corrected] cause limb and cardiac malformation in Holt-Oram syndrome. *Nat Genet* **15**, 30-5.

Basson, C. T., Huang, T., Lin, R. C., Bachinsky, D. R., Weremowicz, S., Vaglio, A., Bruzzone, R., Quadrelli, R., Lerone, M., Romeo, G. et al. (1999). Different TBX5 interactions in heart and limb defined by Holt-Oram syndrome mutations. *Proc Natl Acad Sci U S A* **96**, 2919-24.

Benson, D. W., Basson, C. T. and MacRae, C. A. (1996). New understandings in the genetics of congenital heart disease. *Curr Opin Pediatr* **8**, 505-11.

Brown, D. D., Martz, S. N., Binder, O., Goetz, S. C., Price, B. M., Smith, J. C. and Conlon, F. L. (2005). Tbx5 and Tbx20 act synergistically to control vertebrate heart morphogenesis. *Development* **132**, 553-63.

Bruneau, B. G., Nemer, G., Schmitt, J. P., Charron, F., Robitaille, L., Caron, S., Conner, D. A., Gessler, M., Nemer, M., Seidman, C. E. et al. (2001). A murine model of Holt-Oram syndrome defines roles of the T-box transcription factor Tbx5 in cardiogenesis and disease. *Cell* **106**, 709-21.

Burton, P. B., Raff, M. C., Kerr, P., Yacoub, M. H. and Barton, P. J. (1999). An intrinsic timer that controls cell-cycle withdrawal in cultured cardiac myocytes. *Dev Biol* **216**, 659-70.

Cleaver, O. B., PAtterson, K. D. and Krieg, P. A. (1996). Overexpressoin of the *tinman*-related genes XNkx-2.5 and XNkx-2.3 in *Xenopus* embryos results in myocardial hyperplasia. *Development* **122**, 3549-3556.

Cobrinik, D. (2005). Pocket proteins and cell cycle control. *Oncogene* **24**, 2796-809.
Fishman, M. C. and Chien, K. R. (1997). Fashioning the vertebrate heart: earliest embryonic decisions. *Development* **124**, 2099-117.

Garrity, D. M., Childs, S. and Fishman, M. C. (2002). The heartstrings mutation in zebrafish causes heart/fin Tbx5 deficiency syndrome. *Development* **129**, 4635-45.

Harland, R. M. (1991). In situ hybridization: an improved whole-mount method for Xenopus embryos. *Methods Cell Biol* **36**, 685-95.

Harvey, R. P. (2002). Patterning the vertebrate heart. *Nat Rev Genet* **3**, 544-56.

Hatcher, C. J., Goldstein, M. M., Mah, C. S., Delia, C. S. and Basson, C. T. (2000). Identification and localization of TBX5 transcription factor during human cardiac morphogenesis. *Dev Dyn* **219**, 90-5.

Hatcher, C. J., Kim, M. S., Mah, C. S., Goldstein, M. M., Wong, B., Mikawa, T. and Basson, C. T. (2001). TBX5 transcription factor regulates cell proliferation during cardiogenesis. *Dev Biol* **230**, 177-88.

Hiroi, Y., Kudoh, S., Monzen, K., Ikeda, Y., Yazaki, Y., Nagai, R. and Komuro, I. (2001). Tbx5 associates with Nkx2-5 and synergistically promotes cardiomyocyte differentiation. *Nat Genet* **28**, 276-80.

Hochegger, H., Klotzbucher, A., Kirk, J., Howell, M., le Guellec, K., Fletcher, K., Duncan, T., Sohail, M. and Hunt, T. (2001). New B-type cyclin synthesis is required between meiosis I and II during Xenopus oocyte maturation. *Development* **128**, 3795-807.

Horb, M. E. and Thomsen, G. H. (1999). Tbx5 is essential for heart development. *Development* **126**, 1739-51.

Kajstura, J., Leri, A., Castaldo, C., Nadal-Ginard, B. and Anversa, P. (2004). Myocyte growth in the failing heart. *Surg Clin North Am* **84**, 161-77.

Kolker, S. J., Tajchman, U. and Weeks, D. L. (2000). Confocal imaging of early heart development in Xenopus laevis. *Dev Biol* **218**, 64-73.

Latinkic, B. V., Cooper, B., Towers, N., Sparrow, D., Kotecha, S. and Mohun, T. J. (2002). Distinct enhancers regulate skeletal and cardiac muscle-specific expression programs of the cardiac alpha-actin gene in Xenopus embryos. *Dev Biol* **245**, 57-70.

Li, Q. Y., Newbury-Ecob, R. A., Terrett, J. A., Wilson, D. I., Curtis, A. R., Yi, C. H., Gebuhr, T., Bullen, P. J., Robson, S. C., Strachan, T. et al. (1997). Holt-Oram syndrome is caused by mutations in TBX5, a member of the Brachyury (T) gene family. *Nat Genet* **15**, 21-9.

Liberatore, C. M., Searcy-Schrick, R. D. and Yutzey, K. E. (2000). Ventricular expression of tbx5 inhibits normal heart chamber development. *Dev Biol* **223**, 169-80.

MacLellan, W. R. and Schneider, M. D. (2000). Genetic dissection of cardiac growth control pathways. *Annu Rev Physiol* **62**, 289-319.

Mandel, E. M., Callis, T., Wang, D.-Z. and Conlon, F. L. (2005). Transcriptional mechanisms of heart disease. *Drug Discovery Today: Disease Mechanisms* **2**, 33-38.

McKinsey, T. A., Zhang, C. L. and Olson, E. N. (2002). MEF2: a calcium-dependent regulator of cell division, differentiation and death. *Trends Biochem Sci* **27**, 40-7.

Mikawa, T., Borisov, A., Brown, A. M. and Fischman, D. A. (1992). Clonal analysis of cardiac morphogenesis in the chicken embryo using a replication-defective retrovirus: I. Formation of the ventricular myocardium. *Dev Dyn* **193**, 11-23.

Mikawa, T., Cohen-Gould, L. and Fischman, D. A. (1992). Clonal analysis of cardiac morphogenesis in the chicken embryo using a replication-defective retrovirus. III: Polyclonal origin of adjacent ventricular myocytes. *Dev Dyn* **195**, 133-41.

Mohun, T., Orford, R. and Shang, C. (2003). The origins of cardiac tissue in the amphibian, Xenopus laevis. *Trends Cardiovasc Med* **13**, 244-8.

Mohun, T. J., Leong, L. M., Weninger, W. J. and Sparrow, D. B. (2000). The morphology of heart development in Xenopus laevis. *Dev Biol* **218**, 74-88.

Newbury-Ecob, R. A., Leanage, R., Raeburn, J. A. and Young, I. D. (1996). Holt-Oram syndrome: a clinical genetic study. *J Med Genet* **33**, 300-7.

Nieuwkoop, P. D. (1967). The "organization centre". 3. Segregation and pattern formation in morphogenetic fields. *Acta Biotheor* **17**, 178-94.

Olson, E. N. and Schneider, M. D. (2003). Sizing up the heart: development redux in disease. *Genes Dev* **17**, 1937-56.

Papaioannou, V. E. and Silver, L. M. (1998). The T-box gene family. *Bioessays* **20**, 9-19.

Pasumarthi, K. B. and Field, L. J. (2002). Cardiomyocyte cell cycle regulation. *Circ Res* **90**, 1044-54.

Plageman, T. F., Jr. and Yutzey, K. E. (2004). Differential expression and function of Tbx5 and Tbx20 in cardiac development. *J Biol Chem* **279**, 19026-34.

Rybkin, II, Markham, D. W., Yan, Z., Bassel-Duby, R., Williams, R. S. and Olson, E. N. (2003). Conditional expression of SV40 T-antigen in mouse cardiomyocytes facilitates an inducible switch from proliferation to differentiation. *J Biol Chem* **278**, 15927-34.

Showell, C., Binder, O. and Conlon, F. L. (2004). T-box genes in early embryogenesis. *Dev Dyn* **229**, 201-18.

Small, E. M. and Krieg, P. A. (2000). Expression of atrial natriuretic factor (ANF) during Xenopus cardiac development. *Dev Genes Evol* **210**, 638-40.

Soonpaa, M. H. and Field, L. J. (1998). Survey of studies examining mammalian cardiomyocyte DNA synthesis. *Circ Res* **83**, 15-26.

Stennard, F. A. and Harvey, R. P. (2005). T-box transcription factors and their roles in regulatory hierarchies in the developing heart. *Development* **132**, 4897-910.
Tonissen, K. F., Drysdale, T. A., Lints, T. J., Harvey, R. P. and Krieg, P. A. (1994). XNkx-2.5, a Xenopus gene related to Nkx-2.5 and tinman: evidence for a conserved role in cardiac development. *Dev Biol* **162**, 325-8.

Trinh, L. A. and Stainier, D. Y. (2004). Fibronectin regulates epithelial organization during myocardial migration in zebrafish. *Dev Cell* **6**, 371-82.

Vernon, A. E. and Philpott, A. (2003). The developmental expression of cell cycle regulators in Xenopus laevis. *Gene Expr Patterns* **3**, 179-92.

Wang, Z. F., Ingledue, T. C., Dominski, Z., Sanchez, R. and Marzluff, W. F. (1999). Two Xenopus proteins that bind the 3' end of histone mRNA: implications for translational control of histone synthesis during oogenesis. *Mol Cell Biol* **19**, 835-45.

Whitmire, E., Khan, B. and Coue, M. (2002). Cdc6 synthesis regulates replication competence in Xenopus oocytes. *Nature* **419**, 722-5.

Wilson, P. A. and Hemmati-Brivanlou, A. (1995). Induction of epidermis and inhibition of neural fate by Bmp-4. *Nature* **376**, 331-3.

Wilson, V. and Conlon, F. L. (2002). The T-box family. *Genome Biol* **3**, REVIEWS3008.

CHAPTER 5

SHP-2 is Required for the Maintenance of Proliferating Cardiac Progenitor Cells

PREFACE TO CHAPTER 5

Chapter 5 deals with the requirement for the protein tyrosine phosphatase SHP-2 during heart development. SHP-2 functions to potentiate signaling downstream of receptor tyrosine kinases such as FGF (Qu, 2000). Previous studies have suggested that SHP-2 functions during heart development, as several mutations to SHP-2 that cause it to become constitutively active have been associated with the congenital heart disorder Noonan Syndrome (Tartaglia et al., 2001). However, the requirements for SHP-2 during heart development have not been addressed, as mouse embryos null for SHP-2 and *Xenopus* embryos in which a dominant negative form of SHP-2 is expressed arrest at gastrula stages (Tang et al., 1995; Yang et al., 2006). Here, we make use of a specific inhibitor of SHP-2, NSC-87877. By treating heart field explants excised from embryos prior to the onset of cardiac differentiation with this inhibitor, we bypass earlier requirements for SHP-2 in mesoderm formation, and study the requirement for SHP-2 in heart development.

These experiments were performed in collaboration with Yvette Langdon, Anna Berg, and Jackie Swanik. For this work, I developed and tested the heart field explant assay

(based on Raffin et al., 2000), performed the FGF inhibitor experiments and mitotic index studies, and assisted with the SHP-2 inhibitor and cell cycle inhibitor studies.

SUMMARY

The isolation and culturing of cardiac progenitor cells has demonstrated that growth factor signaling is required to maintain cardiac cell survival and proliferation. In this study, we demonstrate that SHP-2 activity is required for the maintenance of cardiac precursors *in vivo*. In the absence of SHP-2 signaling, cardiac progenitor cells down-regulate genes associated with early heart development and fail to initiate cardiac differentiation. We further show that this requirement for SHP-2 is restricted to cardiac precursor cells undergoing active proliferation. By demonstrating that SHP-2 is phosphorylated on Y542/Y580 and that it binds to FRS-2, we place SHP-2 in the FGF pathway during early embryonic heart development. Furthermore, we demonstrate that inhibition of FGF signaling mimics the cellular and biochemical effects of SHP-2 inhibition and that these effects can be rescued by constitutive active/Noonan syndrome associated forms of SHP-2. Collectively, these results show that SHP-2 functions within the FGF/MAPK pathway to maintain survival of proliferating populations of cardiac progenitor cells and further suggest that the FGF/SHP-2/MAPK pathway may represent a general pathway required to maintain proliferating progenitor populations.

INTRODUCTION

Cells of the cardiac lineage are amongst the first mesodermal cells to be allocated to a specific tissue type in vertebrates. By the onset of gastrulation, the cells which will give rise to cardiac tissue are located in two regions at the anterior edge of the mesoderm. Extirpation,

explantation, and tissue isolation studies in amphibian and avian embryos are all consistent with the cells of the cardiac lineage being specified and committed to the heart lineage during these early stages of development (Dehaan, 1963; Sater and Jacobson, 1989; Warkman and Krieg, 2006). Once cells are committed to the cardiac lineage, the cells migrate laterally and anteriorly, and subsequently fuse at the ventral anterior midline to form the bilaminar heart tube comprised of an outer myocardial and an inner endocardial layer (van den Hoff et al., 2004). It is during this period that the vertebrate heart expresses the first molecular markers of cardiac development *Tbx5*, *Gata4*, *Tbx20* and *Nkx2.5*, the homologue of the *Drosophila* gene *tinman* (Fishman and Chien, 1997; Harvey et al., 2002). It is also during this time that the cardiac precursors begin a period of rapid proliferation (Pasumarthi and Field, 2002).

The isolation and culturing of cardiac progenitor cells has strongly implied the requirement for growth factor function to maintain cardiac cell survival. Collectively these studies have shown that survival and proliferation of cardiac progenitor populations requires either the aggregation of clonal colonies, that the cells be co-cultured with heart tissue, or that the cultures be supplemented with a mixture of growth factors and cytokines (Kattman et al., 2006; Kouskoff et al., 2005; Moretti et al., 2006; Parmacek and Epstein, 2005; Srivastava, 2006; Wu et al., 2006). However the precise nature of the endogenous growth factors and the downstream signaling pathways required for survival or proliferation remain unidentified.

SHP-2, also known as SH-PTP2, Ptpn11, PTP1D, or PTP2C, is the vertebrate homologue of the Drosophila gene *corkscrew* (*Csw*), a widely expressed non-receptor protein tyrosine phosphatase (PTP) known to function genetically and biochemically downstream of a number of growth factors including epidermal growth factors (EGFs), platelet derived growth factor (PDGF) and fibroblast growth factors (FGFs) (Feng, 1999; Pawson, 1994; Qu,

2000; Van Vactor et al., 1998; Zhang et al., 2000). The sequence, expression pattern and function of SHP-2 are highly conserved throughout evolution with genetic studies in a number of animal models all suggestive of a critical role for SHP-2 in early development. For example, mice homozygous for a null mutation in *Shp-2* die at implantation, due to a failure in the development of the extra-embryonic trophectodermal lineage, while introduction of a dominant negative form of SHP-2 in *Xenopus* can completely block mesoderm formation in response to the FGF/MAPK pathway and leads to gastrulation arrest (Tang et al., 1995; Yang et al., 2006). Studies have also suggested a role for SHP-2 in heart development. Noonan syndrome, a relatively common autosomal dominant disorder that leads to a number of cardiac abnormalities including atrial septal defects, ventricular septal defects, pulmonary stenosus and hypertrophic cardiomyopathy, is associated with mutations in *Shp-2* in approximately half of affected individuals (Noonan and O'Connor, 1996; Tartaglia et al., 2001). All SHP-2 associated Noonan syndrome mutations are mis-sense mutations and occur within one of the two SRC-homology 2 (SH2) domains, a region required for protein-protein interactions, or within the phosphatase domain. These mutations are thought to be involved in switching SHP-2 between its inactive and active states, and to act in a constitutive active fashion (Allanson, 2002; Digilio et al., 2002; Ion et al., 2002; Legius et al., 2002; Maheshwari et al., 2002; Schollen et al., 2003; Tartaglia et al., 2002; Tartaglia et al., 2001). However, the precise requirement for Shp-2 in heart development remains to be established.

In this study, we have bypassed the early embryonic requirements for SHP-2 by means of a cardiac explant assay. Using this assay, we define, a requirement for SHP-2 in maintaining cardiac precursor populations in vivo. In the absence of SHP-2 signaling all early cardiac makers are down regulated and cardiac cells fail to initiate cardiac

differentiation. We further show that SHP-2 is required for cardiac progenitor populations that are actively proliferating but not those that have exited the cell cycle. We show that SHP-2 functions directly downstream of FGF in this process; we show that inhibiting FGF gives the same phenotype as SHP-2 inhibition, that SHP-2 is directly phosphorylated on specific residues in vivo in response to FGF signaling, that SHP-2 co-immunoprecipitates with FRS, a component of the FGF pathway, and most critically that we can rescue the cardiac lineage and the downstream signaling pathways in FGF inhibited tissues by the expression of a constitutive active/Noonan syndrome version of SHP-2, implying that the FGF/SHP-2 pathway is a general pathway in development that functions to maintain progenitor cell populations.

RESULTS

SHP-2 is required for MHC expression in cardiac tissue

To begin to elucidate the molecular pathways involved in cardiac cell survival, we have focused on the role of SHP-2 during the early stages of heart development. Clinical studies in humans and genetic studies in mice are all consistent with a role for SHP-2 in early heart development. However it remains unclear if SHP-2 acts directly or indirectly in the cardiac lineage. Western blot analysis with an antibody specific for total SHP-2 shows SHP-2 to be present throughout stages of early *Xenopus* embryogenesis, and in embryonic heart tissue (Figure S1A-B).

Having established that SHP-2 is expressed in early embryos, we next tested the requirement for SHP-2 in early heart development. To bypass the early embryonic requirement for SHP-2, we have used a cardiac explant assay. Based on anatomical and gene

expression studies in *Xenopus,* at late neurulation (stage 22) the cardiac precursors exist in two cell populations which lie directly posterior to the cement gland along the anterior-ventral aspects of the embryo (Dale and Slack, 1987; Moody, 1987; Raffin et al., 2000; Sater and Jacobson, 1989). When dissected and cultured in isolation this tissue forms a beating heart while the donor embryo completely lacks any cardiac tissue (*Xenopus* can develop to late tadpole stage in the absence of a functioning heart or circulation). We have carried out an extensive analysis of these explants using early, mid and late molecular markers of heart tissue and show that the explants display a temporal and spatial expression of cardiac genes that faithfully recapitulates that of control (unmanipulated) embryos (Figure 1A-B). However, if explants are treated with a specific SHP-2 inhibitor NSC-87877 (Chen et al., 2006), the cardiac marker myosin heavy chain (MHC) is dramatically down-regulated (Figure 1C). Previous studies have shown that NSC-87877 can also inhibit SHP-1, however since SHP-1 is not expressed during the earlier stages of embryogenesis the defects we observe are most likely due to the inhibition of SHP-2. To confirm the specificity of NSC-87877, we show that its effect on MHC can be rescued by injection of the Noonan syndrome-associated constitutively active form of human SHP-2, N308D (Shp-2 N308D) but not a phosphatase dead version of N308D (Figure 1C; data not shown). Together, these data indicate that SHP-2 signaling is required to induce or maintain expression of MHC.

SHP-2 signaling is required for the maintenance of cardiac progenitors

Since we observed that the SHP-2 is required for MHC expression in cardiac tissue, we addressed whether this effect is specific for MHC or reflects a general requirement for SHP-2 signaling in heart development. To establish the role of SHP-2 in heart development and to

determine how rapidly SHP-2 inhibition effects cardiac gene expression, we assayed cardiac explants for expression of *Nkx2.5*, *Tbx5*, *Tbx20* and the cardiac differentiation marker *MLC1v'* at time points corresponding to stage 22, the stage when the cardiac precursors are two distinct lateral populations of cells; stage 26, the period when the two cardiac precursors populations are positioned at the anterior, ventral region of embryo flanking the midline; stage 29 when the cardiac fields fuse across the ventral midline and stage 33 when the bilaminar heart tube initiates cardiac looping. These studies show that there is a progressive loss of all three early markers with increasing length of SHP-2 inhibition. We observe that controls and treated tissue are indistinguishable at stage 22 (Figure 2A-C) however by early tailbud stage (St. 26) cardiac precursors in treated explants remain in two bilateral populations while the cardiac precursors in controls have migrated toward the midline (Figure 2A-C). At stage 29, when the hearts in control explants have formed a linear heart tube, the cardiac fields in SHP-2 inhibited explants remain unfused and display reduced expression of *Nkx2.5*, *Tbx5*, and *Tbx20*. Similarly, at stage 33, *Nkx2.5*, *Tbx5*, and *Tbx20* expression appears to continue to be restricted to a subset of tissue at the leading edge of the cardiac field or is absent entirely. The expression of the cardiac differentiation marker MLC1v' is never initiated in SHP-2 inhibited explants (Figure 2D). Overall there appears to be a progressive and rapid loss of early cardiac marker expression in SHP-2 inhibited explants and markers of cardiac differentiation fail to be expressed (Figure 2A-D). We do note however, that cardiac cells at the leading edge continue to express *Tbx5* until at least stage 33 (Figure 2B, arrows).

To confirm and extend these findings we tested explants for expression of the early cardiac/endoderm markers *Gata4*, *Gata5*, and *Gata6*. Similar to *Nkx2.5*, *Tbx5*, and *Tbx20*, we detect a dramatic down-regulation of *Gata4, Gata5* and *Gata6* (Figure S2). Moreover, we

have found that expression of the early cardiac markers *Nkx2.5* and *Tbx5* can be restored in SHP-2 inhibited explants by constitutively active SHP-2 N308D (Figure 1C, 2E, data not shown). Thus the effects of SHP-2 inhibition on the expression of both early and late heart markers can be rescued by restoring SHP-2 activity. Collectively, these results suggest that SHP-2 is required to maintain the expression of early cardiac markers in most of the cardiac field and for the onset of cardiac differentiation.

SHP-2 signaling is required for pharyngeal mesoderm but is not required for the induction and/or maintenance of endodermal or endothelial tissue types

To determine whether the requirements for SHP-2 are cardiac-specific, we assayed the effects of SHP-2 inhibition on the additional cell types present in tissue explants; endoderm, endothelial cells, and overlying pharyngeal mesoderm (Figure 3A). Similar to our findings with cardiac-specific markers, SHP-2 signaling is required for the maintenance of the pharyngeal mesoderm-associated genes *Fgf8*, *Tbx1,* and *Isl1* as inhibition of SHP-2 signaling results in loss of expression of these genes in explanted tissue (Figure3B and data not shown). In contrast, results show that SHP-2 signaling is not required for the expression of genes associated with the deep endoderm (*Edd* and *Endocut* positive tissue), or pharyngeal endoderm (*Sox2* positive) (Figure 3C). Similarly, we observe that SHP-2 signaling is not required for the expression of the endothelial cell markers *Xmsr* and *Ami* (Figure 3C). We do note however, that *Xmsr* and *Ami* are expressed in SHP-2 inhibited tissue in coherent un-branched patterns verses control explants. Collectively, these results show SHP-2 is required for the maintenance of early markers of cardiac and pharyngeal mesoderm but is not required for endodermal or endothelial cell types.

Inhibition of SHP-2 Results in a Progressive Increase in Cell Death

To determine if the loss of cardiac tissue in response to SHP-2 inhibition is due to defects in cardiac cell survival or proliferation, we examined programmed cell death in control explants and explants in which SHP-2 signaling was inhibited. Explants were treated with the SHP-2 inhibitor beginning at stage 22, and analyzed at stages 22, 26, 29, and 33. TUNEL staining of cardiac explants reveals that at stage 22 there is no apparent difference in cardiac cell death in the ridge of mesodermal tissue which contains the cardiac tissue in either control or SHP-2 inhibited explants (Fig. 4A) however, by stage 26 we begin to detect an increase in TUNEL positive cells in SHP-2 inhibited explants along the cardiac ridge (Fig. 4A). By stages 29 and 33, the number of apoptotic cells in the SHP-2 inhibited explants has further expanded in the cardiac ridge (Fig. 4A). Therefore, in the absence of SHP-2 signaling, cardiac cells cease development and undergo programmed cell death initiated by stage 26.

Since studies have implied a role for SHP-2 in cell cycle progression (Guillemot et al., 2000; Yuan et al., 2003; Yuan et al., 2005), we tested if withdrawal from the cell cycle could account for the observed loss of cardiac marker expression and programmed cell death in SHP-2 inhibited explants. Therefore, we treated explants with cell cycle inhibitors and determined the effects on the expression of early and late heart markers. As expected, the culture of explants in media containing aphidicolin (Aph) leads to a dramatic reduction in the number of mitotic cells (Figure 4B). Results show that arrest of tissue at the G1/S phase by the addition of Aph leads to a loss of the early cardiac markers *Nkx2.5*, *Tbx5*, *Tbx20,* and *Gata6* (Figure 4D,E). *Gata4* and *Gata5* are still expressed in Aph-treated explants, though reduced in expression (Figure 4E). In contrast to SHP-2 inhibition, G1/S interphase arrest by

Aph has no effect on the expression of the expression of markers of cardiac differentiation including *Hsp27*, *MLC1v'*, MHC, and tropomyosin (Figure 4E,F). However, as predicted, we observed a reduction in the size of the hearts in the Aph-treated explants. These results are not due to treatment with Aph per se since identical results were obtained with M phase arrest by treatment with colchicine (Figure 4G). Thus, these results suggest that the lack of cardiac differentiation in SHP-2 inhibited tissue is not the result of cell cycle arrest and further implies that cell cycle arrest and cardiac differentiation are independently regulated *in vivo*.

SHP-2 is preferentially required in proliferating cardiomyocytes

At the early stages of heart development, when cardiac explants are removed, the majority of cardiac cells are proliferating. However as cardiac differentiation is initiated, cells progressively begin to exit the cell cycle, and a smaller proportion of cardiac cells continue to cycle (Goetz et al., 2006). To determine if SHP-2 is required for the maintenance of proliferating cardiomyocytes, SHP-2 signaling was blocked in cardiac explants at a series of developmental stages: late neurula (St. 22 and 24), early tailbud (St. 26), and late tailbud (St. 29); and cultured to tadpole stage (St. 37) (Fig. 5A). Results from these studies show that SHP-2 signaling is required during a specific developmental period for MHC expression; treatment at stage 22 shows no MHC expression, stages 24 and 26 show a marked reduction in MHC expression, while treatment from stage 29 results in hearts with high levels of MHC expression, but that are reduced in size (Fig. 5A). Our results demonstrate that SHP-2 signaling is required during late neurula stages for the expression of MHC in cardiac tissue

with SHP-2 signaling becoming less critical at a time point when increasing numbers of cardiac cells begin to exit the cell cycle (Fig. 5B).

To determine if SHP-2 signaling is required for the maintenance of proliferating cardiac cells, we inhibited SHP-2 signaling beginning at stage 29, a period when the heart consists of both dividing cardiomyocytes as well as cardiomyocytes that have exited the cell cycle (Goetz et al., 2006). By stage 37, SHP-2 inhibited explants have a mitotic index that is approximately half that of control explants (Fig. 5C,D), suggesting a requirement for SHP-2 in the maintenance of proliferating cardiac cells. Collectively this data suggests that SHP-2 signaling is preferentially required for the maintenance and survival of proliferating cardiac cells.

SHP-2 functions downstream of FGF pathway to regulate cardiac survival

The phosphorylation state of SHP-2 has been demonstrated to be reflective of its function within a specific RTK pathway (e.g. (Bjorbaek et al., 2001)). For example, SHP-2 has been shown to be phosphorylated on tyrosine residues 542 and 580 in response to FGF or PDGF stimulation but not EGF stimulation (Araki et al., 2004). To determine the phosphorylation state of SHP-2 in heart tissue we immunpoprecipitated SHP-2 from embryonic and adult hearts and conducted western blots with a SHP2-phospho-Y542 antibody. Results show that SHP-2 is phosphorylated at residue Y542 in cardiac tissue during the period when SHP-2 functions to maintain cardiac cell survival (Figure 6B). Consistent with these results, immunohistochemistry shows that both phospho-Y542 SHP-2 and phospho-Y580 SHP-2 are expressed in the developing myocardium (Figure 6A). Collectively these results demonstrate that phosphorylation of SHP-2 is tissue specific and SHP-2 is present in its phosphorylated

state in developing myocardial tissue, and therefore most likely acting within the FGF and/ or PDGF pathways.

In tissue culture SHP-2 directly interacts with the docking protein FRS upon FGF but not PDGF stimulation. To test if SHP-2 is functioning downstream of FGF in embryonic heart tissue *in vivo*, we carried out co-immunoprecipitation experiments from isolated embryonic heart tissue. Results show that in isolated embryonic heart tissue SHP-2 directly interacts with FRS (Figure 6B). This is the first demonstration that SHP-2 interacts with FRS *in vivo*.

Since the decrease in *Nkx2.5* expression in SHP-2-inhibited explants is similar to that reported in embryos which genetically lack *Fgf8* (Reiter et al., 1999) or those in which the endoderm adjacent to the cardiac mesoderm has been surgically removed (Alsan and Schultheiss, 2002), and since we observe phophorylation of SHP-2 on tyrosine residues 542 and 580 and direct association of SHP-2 with FRS, we reasoned that FGF acts through SHP-2 to maintain the cardiac lineage. To investigate this possibility, we tested the effects of inhibiting FGF signaling in cardiac explants. Results from these assays show that similar to SHP-2 inhibition, treatment of cardiac explants with the FGFR inhibitor SU5402 leads to a decrease in expression of early and late cardiac markers (Figure 7A). However, we note that in contrast to SHP-2 inhibition, FGF inhibition leads to a decrease of *Tbx5* both in lateral tissue and at the leading edge of the cardiac ridge (Fig. 7A,B). To determine if the loss of cardiac gene expression temporally mimics that seen with SHP-2 inhibition, explants were treated with SU5402 at defined time points of cardiac development. As observed with SHP-2 inhibition, the cardiac explants strongly respond to FGF inhibition between stages 22 and 26 (data not shown) and western blots of cardiac explants lacking SHP-2 activity or FGF

signaling show a dramatic decrease in phospho-ERK (3 fold or more in response to inhibition as assayed by densitometry) (Figure 7C-D). Consistent with SHP-2 acting downstream of FGF, injection of a constitutive active SHP-2 (N308D) in FGFR inhibited explants rescues expression of the early heart markers *Nkx2.5* and *Tbx5*. (Figure 7B and data not shown). Taken together these studies demonstrate that SHP-2 functions in the FGF pathway to regulate cardiac progenitor survival.

Discussion

There has been great clinical interest in identifying cardiac progenitor cells from various sources however, little effort has been expended to understand the precise nature of the endogenous growth factor signaling pathways required for survival or proliferation of cardiac cells (Kattman et al., 2006; Kouskoff et al., 2005; Moretti et al., 2006; Parmacek and Epstein, 2005; Srivastava, 2006; Wu et al., 2006). To date, studies of early cardiac tissue have implied a requirement for growth factors to maintain cardiac cell survival, with survival and proliferation of cardiac progenitor populations requiring either the aggregation of clonal colonies, that cardiac progenitors be co-cultured with heart tissue, or that the cultures be supplemented with a mixture of growth factors and cytokines. However, neither the endogenous growth factor nor the signaling cascade required for cardiac progenitor survival has been identified (Parmacek and Epstein, 2005; Srivastava, 2006). To address these issues, we have characterized the endogenous role for SHP-2, a non-receptor protein phosphatase disrupted in the congenital heart disease Noonan syndrome, and have demonstrated that SHP-2 functions in the FGF pathway to maintain the survival of proliferating cardiomyocytes *in vivo*.

SHP-2 and cardiac cell cycle

The time at which SHP-2 is required for the maintenance of cardiac progenitor cells corresponds with a period of rapid cardiac proliferation (Fishman and Chien, 1997; Goetz et al., 2006; Pasumarthi and Field, 2002). In many tissues, such as muscle and the nervous system, the withdrawal of cells from the cell cycle is tightly associated with the onset of terminal differentiation (Alexiades and Cepko, 1996; Dyer and Cepko, 2001; Lathrop et al., 1985; Li and Vaessin, 2000; Walsh and Perlman, 1997). In contrast, relatively little is known about the relationship between the cell cycle progression and terminal differentiation in the heart.

Our previous work has demonstrated cardiac cells that initiate terminal differentiation retain the ability to divide (Goetz et al., 2006). In the current study, we have extended these findings to demonstrate that while cardiomyocytes of the adult frog ultimately exit the cell cycle, cells expressing markers of terminal differentiation are still undergoing cell division (as shown by pH3) at stage 42. By this stage, cardiac morphogenesis is largely complete and all cardiac cells, including those still dividing, possess the anatomical and molecular hallmarks of differentiation suggesting that, at least in the heart, the onset of terminal differentiation does not require cell cycle exit. Our findings are broadly consistent with recent work showing that cell cycle exit and terminal differentiation are mechanistically separable processes (Grossel and Hinds, 2006; Nguyen et al., 2006; Vernon and Philpott, 2003) . As a corollary to these experiments, we have also examined here the consequences of induced cell cycle arrest on cardiac differentiation and found that blocking the cell cycle in S phase with aphidicolin, or in M phase with colchicine does not result in a block in cardiac

differentiation. Interestingly, however, we have found that cell cycle arrest results in reduced expression of the early cardiac markers *Tbx5*, *Tbx20*, and *Nkx2.5*. Thus, these findings are consistent with the observation that none of these early cardiac proteins are required for cardiac differentiation, and further imply that the expression of these early cardiac transcription factors may be cell cycle-dependent.

Coinciding with program cell death, we also observe that blocking SHP-2 signaling leads to a failure of early cardiac cells to fuse at the ventral midline. At present we can not distinguish between a role for SHP-2 as a trophic factor and/or a role for SHP-2 in cell adhesion. However, genetic studies in zebrafish and mouse strongly imply that the inability of the cardiac fields to fuse is not the primary cause of the donwregulation of early cardiac markers or the failure of SHP-2 inhibited explants to initiate cardiac differentiation. For example, genetic mutations resulting in cardiac bifidia, such as *Gata5*, *hand2*, *Casanova*, and *Bonnie and clyde* and *miles apart* in zebrafish (Alexander et al., 1999; Kupperman et al., 2000; Reiter et al., 1999) or *Gata4* and *MesP1* (Molkentin et al., 1997; Saga et al., 1999) in mouse, as well as genetic mutations in cardiac cell adhesion proteins (Trinh and Stainier, 2004), show no alteration in the expression of early cardiac markers such as *Nkx2.5* or of markers associated with terminal differentiation. Therefore, it is most likely that the failure of cardiac cells to migrate is a secondary consequence of cell survival or it maybe that SHP-2 has two temporally distinct roles in heart development one, regulating cell adhesion and a second in cell survival.

SHP-2 and the FGF pathway

In this study we show SHP-2 to be phosphorylated on tyrosines 542 and 580 in the embryonic heart and that it co-immunoprecipitates with FRS-2, demonstrating an *in vivo* interaction between SHP-2 and FRS-2 for the first time. Moreover, given that we have shown inhibitors of both SHP-2 and FGFR to cause comparable cardiac phenotypes, and that a constitutive active form of SHP-2 can rescue formation of cardiac tissue in FGF inhibited explants, we conclude that SHP-2 participates in the FGF signal transduction pathway in *Xenopus* embryonic hearts.

Recent work examining the role of FGFs in response to cardiac damage or injury lends further support for the direct role of SHP-2 in cardiac cell survival. The over-expression of both FGF-1 and FGF-2 have been shown to promote the survival of adult cardiomyocytes in response to ischemic injury *in vivo* (House et al., 2005; Jiang et al., 2002; Jiang et al., 2004; Palmen et al., 2004) and the cardioprotective effects of FGF-2 in the adult myocardium are mediated through the MAPK pathway (House et al., 2005); the same branch of the FGFR signaling cascade which we have shown in cardiac tissue functions through SHP-2. Interestingly, the specific function of FGF-2 in preventing programmed cell death in response to ischemic insult was shown to be independent of its mitogenic or angiogenic functions, suggesting that FGF-2 is functioning specifically to promote cardiomyocyte cell survival (Jiang et al., 2004). Together with our data showing that SHP-2 activity downstream of FGFR is required for the maintenance of proliferating cardiac progenitor cells, these data suggest that the FGF/MAPK pathway functions in promoting cardiac progenitor cell survival during development and further suggests that the FGF/SHP-2/MAPK pathway must be maintained to promote survival of cardiac progenitor cells in vitro. Intriguingly, the FGF/SHP-2 has also recently been shown to be required for the survival of trophectoderm

stem cells and for the ability of hematopoitetic stem cells to self-renew (Chan et al., 2006; Yang et al., 2006) thus, raising the possibility that the FGF/SHP-2 pathway is a common pathway for cell progenitor survival.

Experimental Procedures

DNA Constructs

SHP-2 N308D and N308D-PTP were generated by site-directed mutagenesis (Stratagene) according to the manufacturer's protocol. Primer sequences available upon request. For epitope labeling, each construct was subcloned into a HA modified pcDNA3.1(+) vector kindly provided by Da-Zhi Wang.

Embryo Injections

Xenopus embryos were obtained by *in vitro* fertilization (Smith and Slack, 1983), cultured in 0.1X Modified Barth's Saline (MBS) and staged according to the Normal Table of *Xenopus laevis* (Nieuwkoop and Faber, 1975). RNA for injection was synthesized using the mMessage *in vitro* transcription kit (Ambion) according to the manufacturer's instructions. Embryos were injected at the one-cell stage with 2ng RNA dissolved in 10nl water.

Cardiac Explants

Tissue posterior to the cement gland and including the heart field was excised at stage 22 in a manner similar to that described by Raffin et al. (Raffin et al., 2000). The explants include overlying pharyngeal endoderm and some foregut endoderm. Explants were cultured at 23°C in either 2.5mM DMSO, 500μM NSC-87877 (Sigma), 50μM SU5402 (Pfizer), 150μM

aphidicolin (Sigma), 20mM hydroxyurea (Sigma), or 50μM colchicine (Sigma) in 1X MBS (Chemicon) (Chen et al., 2006; Dasso and Newport, 1990; Harris and Hartenstein, 1991; Mason et al., 2002). Explants were cultured until specified stages and fixed for 2 hours in MEMFA at room temperature.

Immunoblotting

To detect endogenous SHP-2, five embryos per condition were homogenized in lysis buffer (100 mM NaCl, 20 mM NaF, 50 mM Tris pH 7.5, 10 mM Sodium Pyrophosphate, 5 mM EDTA, 1% NP40 and 1% Sodium Deoxycholate) with the addition of complete protease inhibitor cocktail (Roche) and PMSF (Sigma) and processed according to standard protocols. *In vitro* translation of SHP-2 was performed using wheatgerm TNT coupled transcription/translation (Promega) according to manufacturer's instructions.

Western blots were probed with anti-mouse total SHP-2 antibody PTP1D/SHP-2 (BD Transductions Laboratories) at 1:2500. Heart explant western blots were probed with antibodies against phospho-ERK1/2 and total ERK1/2, with each antibody used at 1:1000 (Cell Signaling). Whole heart immunoblots were prepared from seventy dissected hearts as described above and probed with antibodies against total SHP-2. Calf intestinal phosphatase (CIP) treatment was carried out by incubating whole embryo lysate or heart lysate with 5U of CIP, CIP buffer, EDTA-free Complete protease inhibitors at 37°C for 1.5 hr prior to western blot analysis. Loading levels of tissue were standardized in pilot runs of western blots assayed by densitometry.

Whole Mount Antibody Staining and *in situ* hybridization:

Whole-mount antibody staining of whole embryos and explants were performed as described (Kolker et al., 2000) with anti-tropomyosin (1:50; Developmental Studies Hybridoma Bank), anti-Myosin Heavy Chain (MHC) (1:500 Abcam), and phospho-histone H3 (1:200 Upstate) to mark cells in M phase (Goetz et al., 2006) and visualized on a Leica MZFLIII microscope. Immunostaining of histological sections was performed according to protocols and procedures described previously (Goetz et al., 2006). For these studies, phospho-SHP-2 (Tyr542) (Cell Signaling) and phospho-SHP-2 (Tyr580) (Cell Signaling) were both used at 1:1000 to mark phosphorylated SHP-2 in the heart. Whole-mount *in situ* hybridizations were performed with *Nkx2.5* (Tonissen et al., 1994), *Tbx5* (Brown et al., 2003; Horb and Thomsen, 1999), *Tbx20* (Brown et al., 2003), *Gata4* (Jiang and Evans, 1996), *Gata5* (Jiang and Evans, 1996), *Gata6* (Gove et al., 1997), *MLC1v'* (IMAGE clone 4408657, GenBank Accession No.: **BG884964**)), *Sox2* (Lu et al., 2004), *Endocut* (Costa et al., 2003), *Ami* (Inui and Asashima, 2006), *Xmsr* (*Xenopus* EST clone XL327k24ex (Mills et al., 1999)), using protocols as previously described (Harland, 1991). Embryos were cleared using 2:1 benzyl benzoate/benzyl alcohol.

Whole Mount TUNEL Staining

Apoptotic cells were detected by TUNEL staining as previously described (Hensey and Gautier, 1998). The chromogenic detection of DIG-dUTP incorporation was carried out with BCIP (175ug/mL, Roche), and nitro blue tetrazolium (337 ug/mL, Roche) substrates.

Immunoprecipitation

Embryos were injected, as described above, with 2ng of HA-tagged full length SHP-2 RNA. 1300 hearts were dissected at stage 35 and homogenized in lysis buffer (50 mM Tris 7.6, 150

mM NaCl, 10 mM EDTA, 1 % Surfact-Amps Triton-100, 25 mM PMSF supplemented with 1 Complete protease inhibitor mini tablet (Roche). Supernants were precleared with protein A/G beads for two hours at 4°C. 20 µl of HA beads (Covance) or 30 µl of Shp-2 agarose beads (Santa Cruz Biotechnology) was added to the supernant and rotated overnight at 4°C. Immunoblotting was performed using anti-HA (Covance) at 1:1000, anti-FRS-2 (Santa Cruz) at 1:200, anti-Shp-2 (BD Transduction Labs at 1:2500, and anti-phospho Y-580 Shp-2 (Cell Signaling) at 1:1000.

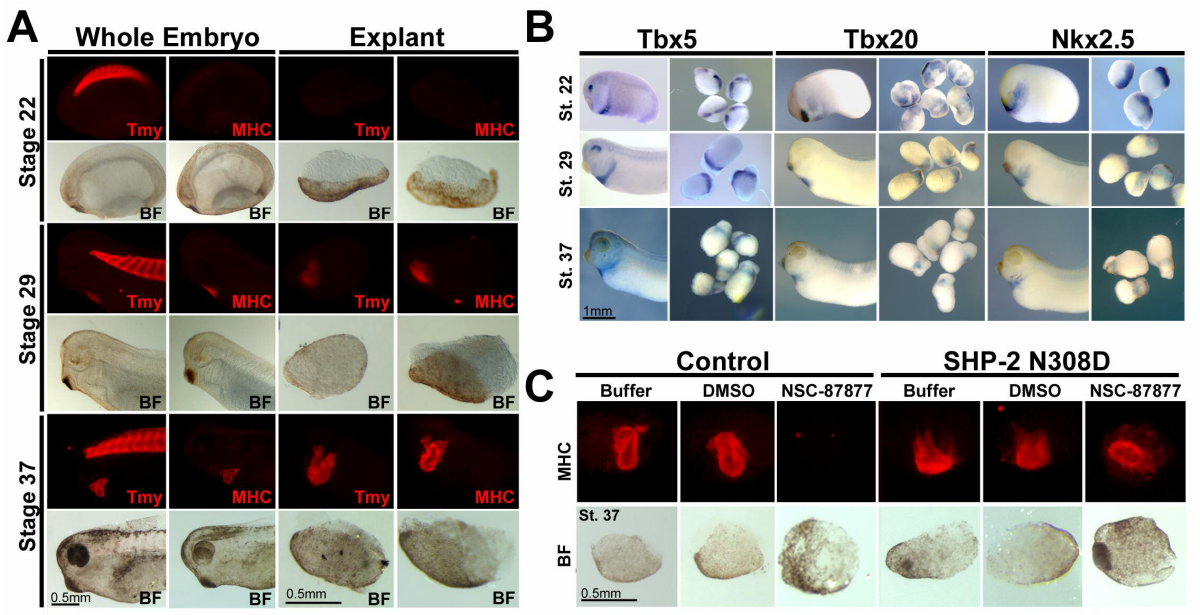

Figure 5.1. *Inhibition of SHP-2 activity results in loss of MHC expression.*

Tissue explants show identical cardiac expression profiles as intact embryos. (A) Whole mount antibody staining of cardiac differentiation with tropomyosin (Tmy; red) or myosin heavy chain (MHC; red) antibodies as indicated, in whole embryos and cardiac explants at stages 22 (neurula), 29 (tailbud), and 37 (tadpole). (Scale bar = 0.5 mm).(B) Whole mount *in situ* hybridization for early heart markers *Tbx5*, *Tbx20*, *Nkx2.5* in whole embryos and cardiac explants at stage 22, 29 and 37, as indicated (Scale bars = 1 mm).

(C) MHC expression is dependent on SHP-2 activity. Whole mount antibody staining for MHC (red) in cardiac explants taken from uninjected (Control) embryos or embryos injected with Shp-2 N308D and treated with either buffer or DMSO carrier as controls or with NSC-87877 as indicated. BF= bright field. (Scale bars = 0.5 mm).

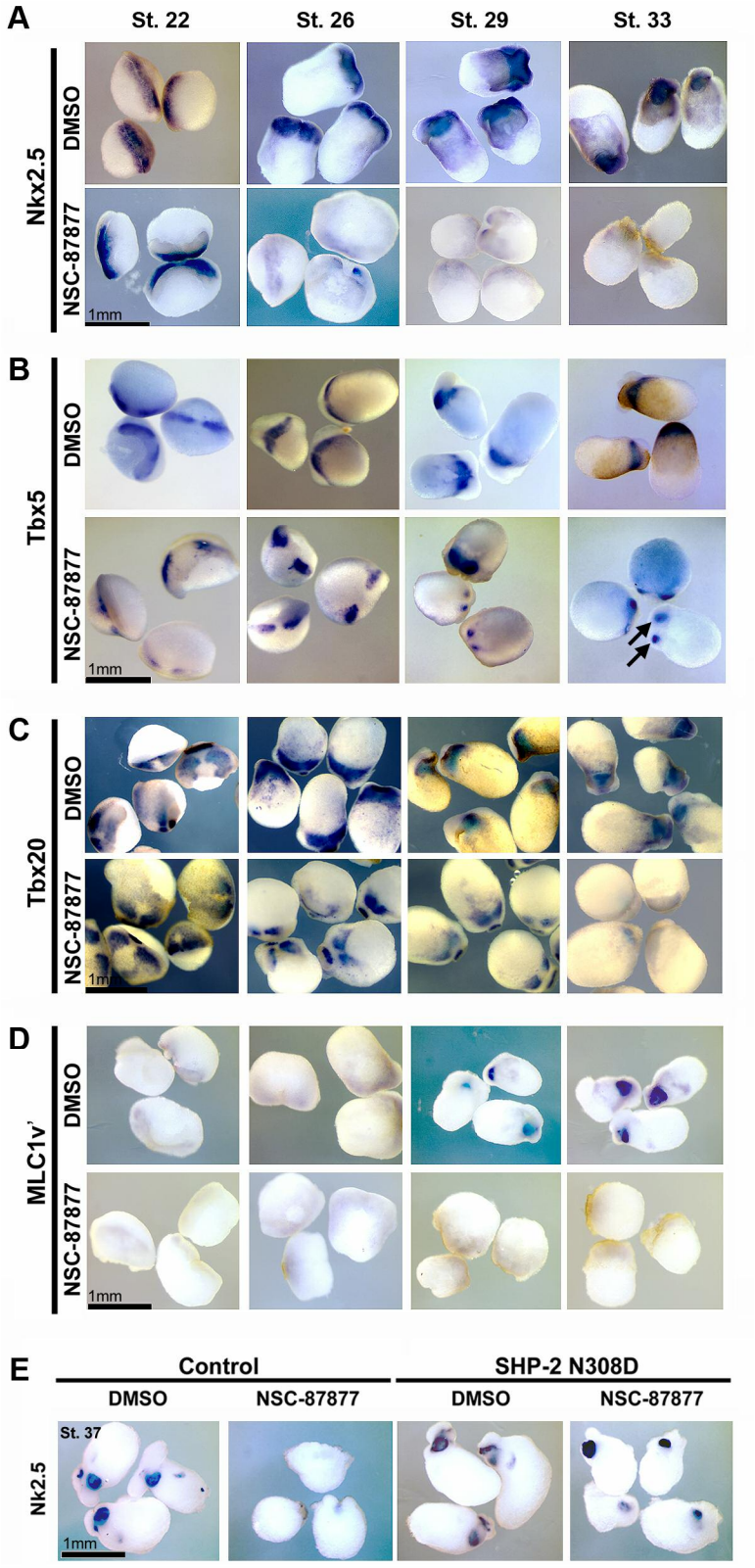
A
St. 22
St. 26
St. 29
St. 33
Nkx2.5
DMSO
NSC-87877
1mm
B
Tbx5
DMSO
NSC-87877
1mm
C
Tbx20
DMSO
NSC-87877
1mm
D
MLC1v'
DMSO
NSC-87877
1mm
E
Control
SHP-2 N308D
DMSO
NSC-87877
DMSO
NSC-87877
Nk2.5
St. 37
1mm

Figure 5.2. *SHP-2 activity is required for the maintenance of cardiac markers*

(A-D) Cardiac explants were isolated and cultured in DMSO or NSC-87877 beginning at stage 22. *In situ* hybridization was performed on explants with *Nkx2.5* (A), *Tbx5* (B), *Tbx20* (C), and *MLC1v′*(D) at stages 22, 26, 29, and 33, as indicated. (Scale bars = 1 mm).

(E) *In situ* hybridization of *Nkx2.5* in uninjected (control) or *Shp-2* N308D injected explants treated with DMSO or NSC-87877. (Scale bar = 1mm).

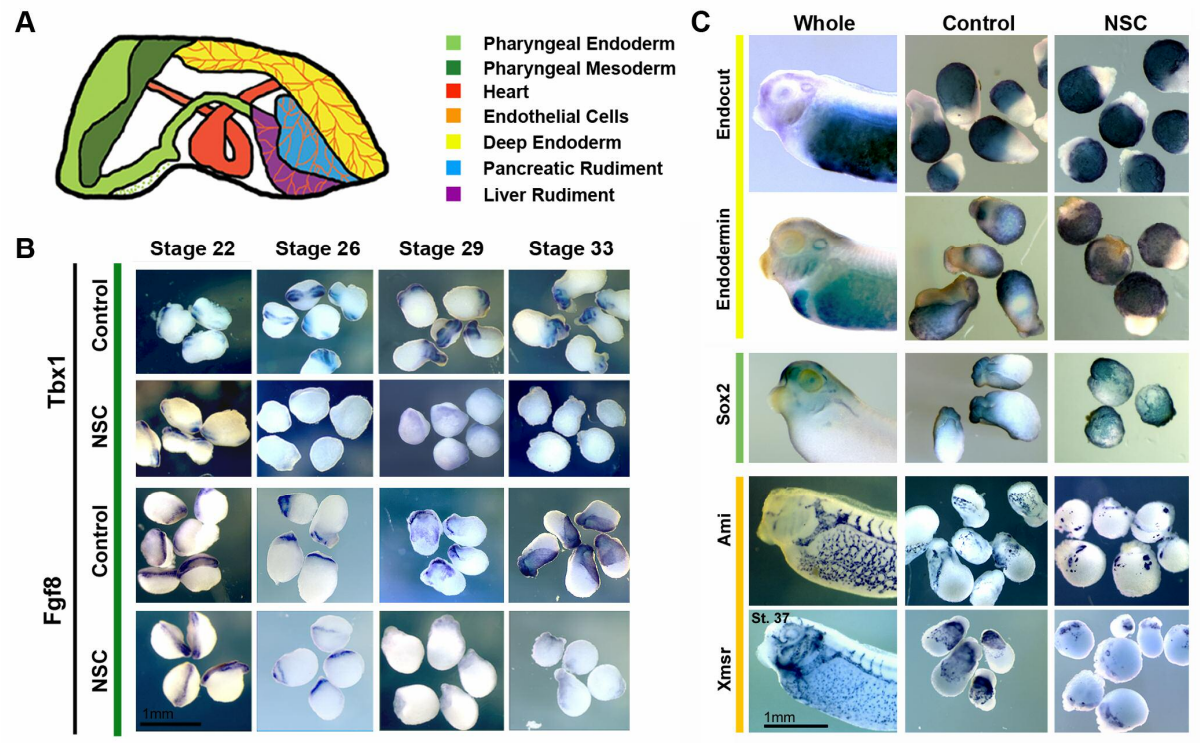

Figure 5.3. *SHP-2 signaling is required for pharyngeal mesoderm*

(A) Schematic of tissues and rudimentary organ structures contained in the explants. (B) Cardiac explants were isolated and cultured in DMSO or NSC-87877 beginning at stage 22. *In situ* hybridization was performed on explants with *Tbx1* or *Fgf8*, at stages 22, 26, 29, and 33. (Scale bar = 1 mm). (C) Whole mount *in situ* hybridization of *endocut*, *endodermin*, *Sox2*, *Ami*, and *Xmsr* in stage 37 whole embryos and cardiac explants treated with DMSO or NSC-87877, as indicated (Scale bar = 1 mm).

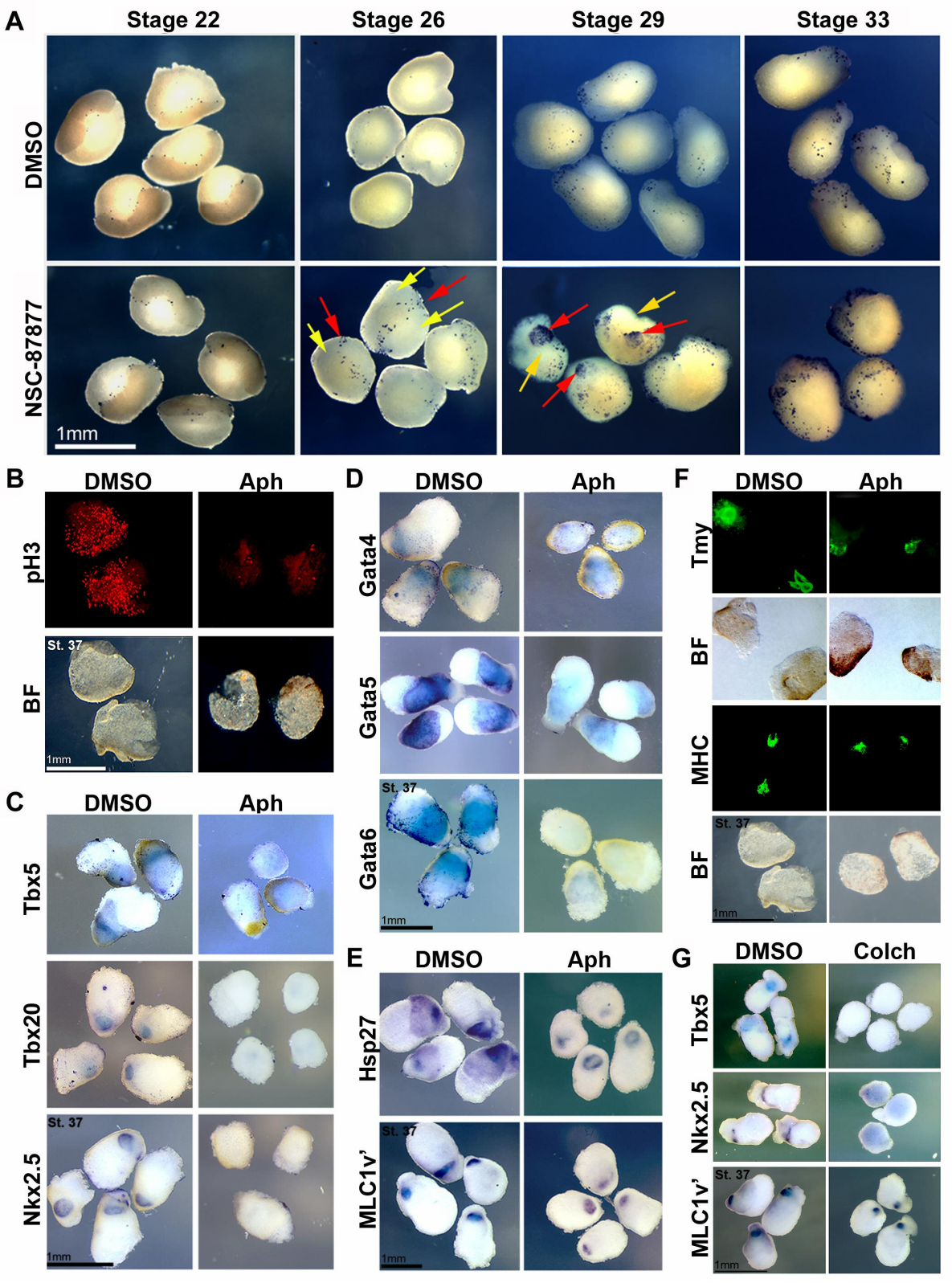
A
Stage 22
Stage 26
Stage 29
Stage 33
DMSO
NSC-87877
1mm
B
DMSO
Aph
pH3
BF
St. 37
1mm
C
DMSO
Aph
Tbx5
Tbx20
Nkx2.5
St. 37
1mm
D
DMSO
Aph
Gata4
Gata5
Gata6
St. 37
1mm
E
DMSO
Aph
Hsp27
MLC1v'
St. 37
1mm
F
DMSO
Aph
Tmy
BF
MHC
BF
St. 37
1mm
G
DMSO
Colch
Tbx5
Nkx2.5
MLC1v'
St. 37
1mm

Figure 5.4. *Blocking the cardiac cell cycle results in loss of early, but not late, cardiac markers.*

(A) TUNEL staining of control cardiac explants (DMSO) and explants treated with NSC-87877. Cell death examined in explants at stages 22, 26, 29, and 33, as indicated. Red arrows denote cardiac cells, yellow arrows denote endodermal cells (Scale bar = 1 mm). (B) Cardiac explants isolated and cultured in DMSO or Aphidicolin (Aph) beginning at stage 22 and fixed at stage 37. Whole mount immunostaining of explants with phospho-histone H3 specific antibody (pH3; red). (Scale bars = 1mm). *In situ* hybridization on explants with early the cardiac markers (C) *Tbx5*, *Tbx20, Nkx2.5*, (D) *Gata4*, *Gata5*, and *Gata6*. (Scale bar = 1 mm); (E) with the cardiac differentiation markers *Hsp27* and *MLC1v'* and (F) by whole mount immunostaining with the cardiac differentiation markers Tmy and MHC. (BF- bright field, scale bar = 1 mm).(G) Explants were treated with DMSO or colchicine (Colch) to block cells in M phase of the cell cycle. *In situ* hybridization was performed to examine expression of *Tbx5*, *Nkx2.5*, and *MLC1V'*, as indicated. (Scale bar = 1mm)

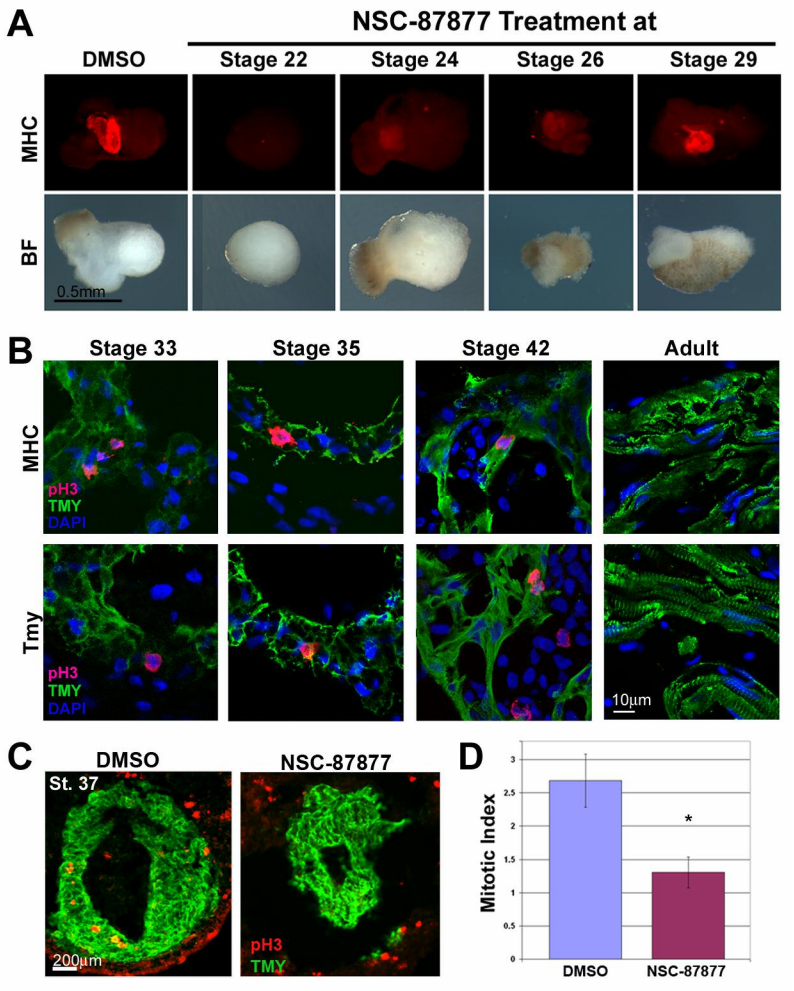

Figure 5.5. *SHP-2 is required for the survival of proliferating cardiac cells.*

(A) Cardiac explants were treated with the SHP-2 inhibitor NSC-87877 beginning at stage 22, 24, 26, or 29 as indicated, cultured to stage 37 and stained with an MHC antibody (red); BF= bright field. (Scale bars = 0.5 mm). (B) Representative transverse sections through stage 33, 35, 42 and adult *Xenopus* hearts with antibodies against MHC (green) or Tmy (green), phospho histone H3 (pH3; red) and DAPI (blue) (Scale bar = 10 µm). (C) Representative transverse sections through the cardiac tissue of a DMSO-treated and an explant treated with NSC-87877 beginning at stage 29, and stained with antibodies against phospho-histone H3

(pH3, red), and Tmy (green), as assessed at stage 37 (Scale bar = 200 μm). (D) Cardiac mitotic index of explants treated beginning at stage 29 with DMSO (blue bar) or NSC-87877 (magenta bar) and assessed at stage 37. Bars represent the mean mitotic index of 4 explants per condition. Error bars denote the standard deviation. * denotes a statistically significant reduction in mitotic index of NSC-87877 treated explants (P = 0.0021).

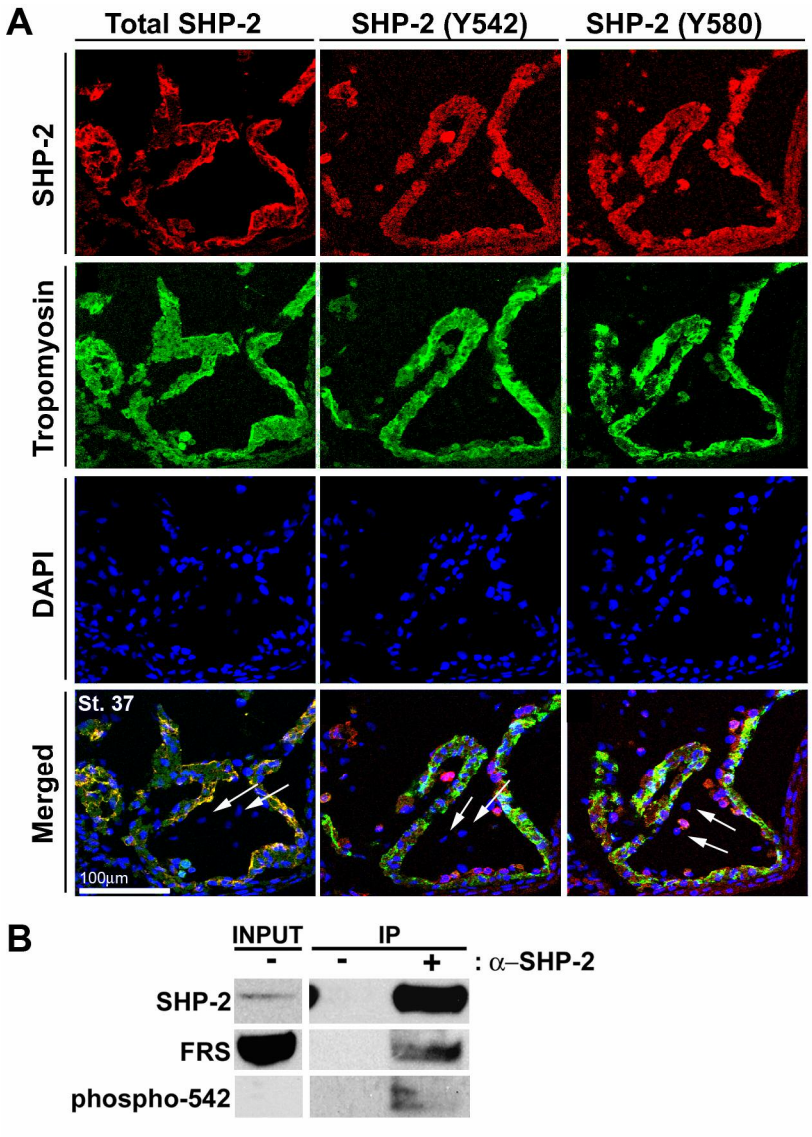

Figure 5.6. *Phosphorylated SHP-2 is expressed in early cardiac tissue.*

(A) Transverse cryosections through the heart of control embryos stained with tropomyosin to mark cardiac tissue (Tmy; green), DAPI, to mark cell nuclei (blue), and anti-total SHP-2, anti-phospho-542 SHP-2 or anti-phospho-580 SHP-2 (all shown in red). Arrows denote endocardial cells that are negative for SHP-2. (All samples from stage 37, scale bars = 100 μm).(B) SHP-2 interacts with FRS *in vivo*. Hearts from FL-HA-SHP-2 derived embryos

were dissected at stage 35 embryos and immunoprecipitated with an anti-SHP-2 antibody (+) or beads with no antibody (-).Western analysis was then performed using antibodies specific for SHP-2 total, phospho-542 SHP-2 and FRS-2. Note the level of SHP-2 phopho-542 in input was below levels of detection.

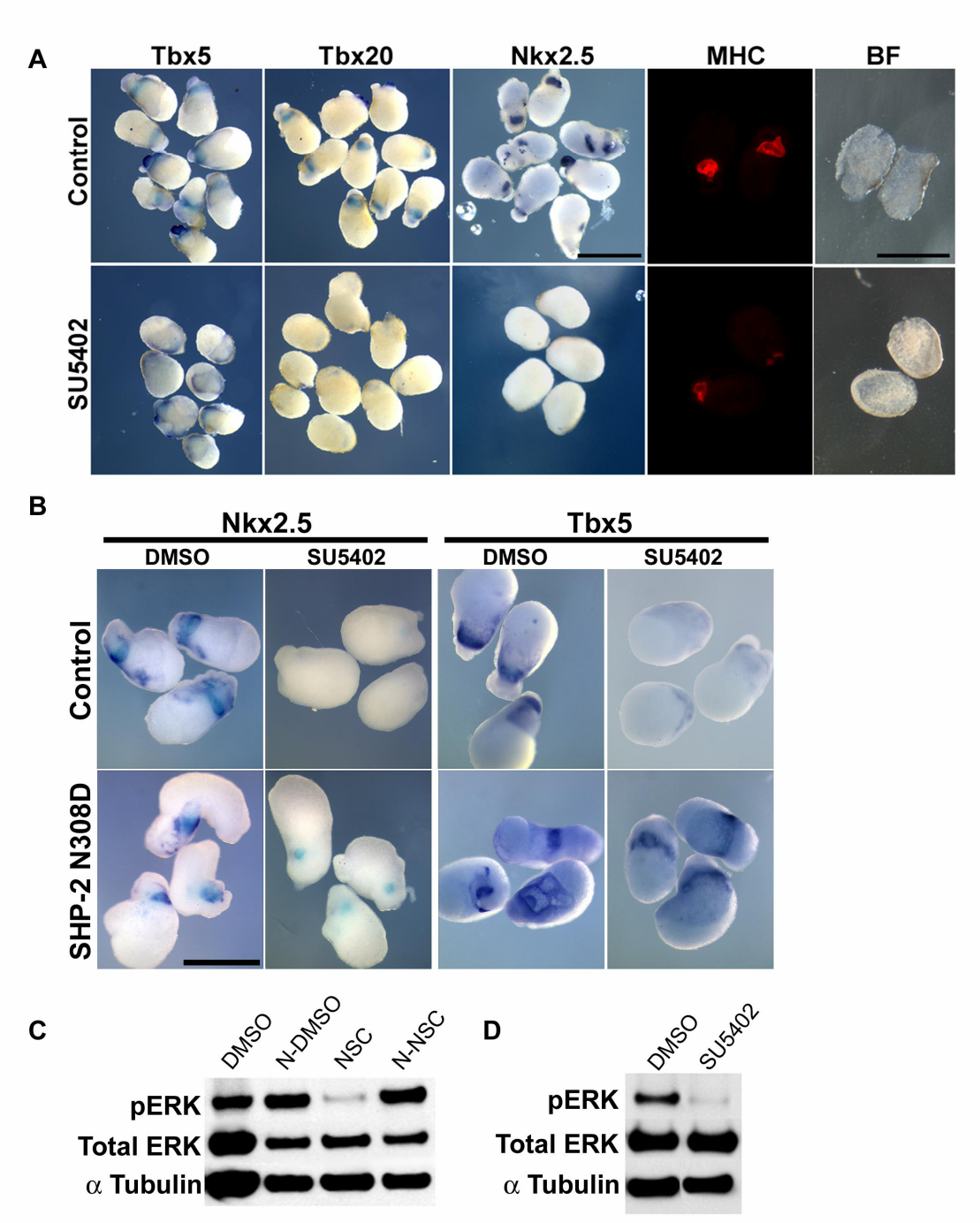

Figure 5.7. *MAPK signaling through the FGF pathway in the heart requires SHP-2.* (A) Whole mount *in situ* hybridization for *Tbx5*, *Tbx20*, and *Nkx2.5* and whole mount immunostaining for MHC (red) a marker of cardiac differentiation were performed on

explants treated with DMSO as a control, or the FGFR1 inhibitor SU5402 (Scale bars = 1 mm). (B) Explants isolated from uninjected (Control) or SHP-2 N308D injected embryos were cultured in DMSO or inhibitor (NSC-87877 or SU5402) and *in situ* hubridizations were performed for the early cardiac markers *Nkx2.5* and *Tbx5* (Scale bars = 1 mm). (C-D) Western blot analysis of NSC-87877 (C) or SU5402 (D) treated explants for phosphorylated and total ERK expression, α-tubulin is used as a loading control.

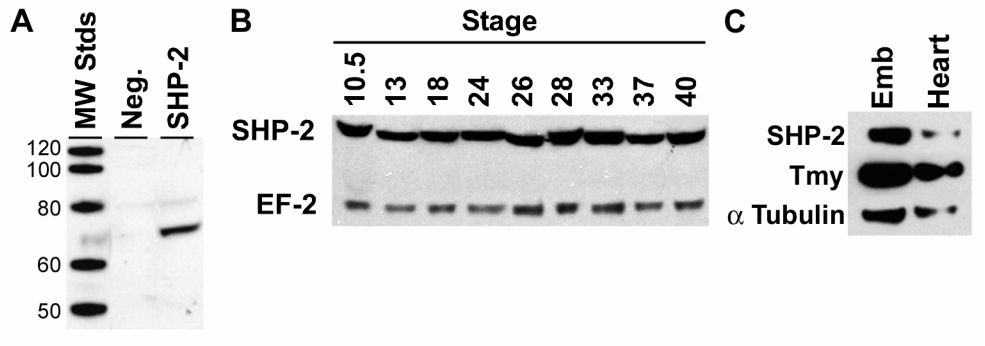

Figure 5.S1. *SHP-2 is expressed in during early Xenopus development*

(A) *In vitro* translation of *Xenopus* SHP-2 in the sense orientation or anti-sense orientation (Neg.) probed with an anti-SHP-2 antibody. (B) Western blot analysis of SHP-2 expression during early embryogenesis using lysate from whole embryos at stages 10.5 (gastrula) through stage 40 (late tadpole). Anti-EF-2 was used as a loading control. (C) Western blot analysis of SHP-2 and Tmy in whole embryos and isolated heart tissue from stage 37 embryos. α-Tubulin is the loading control.

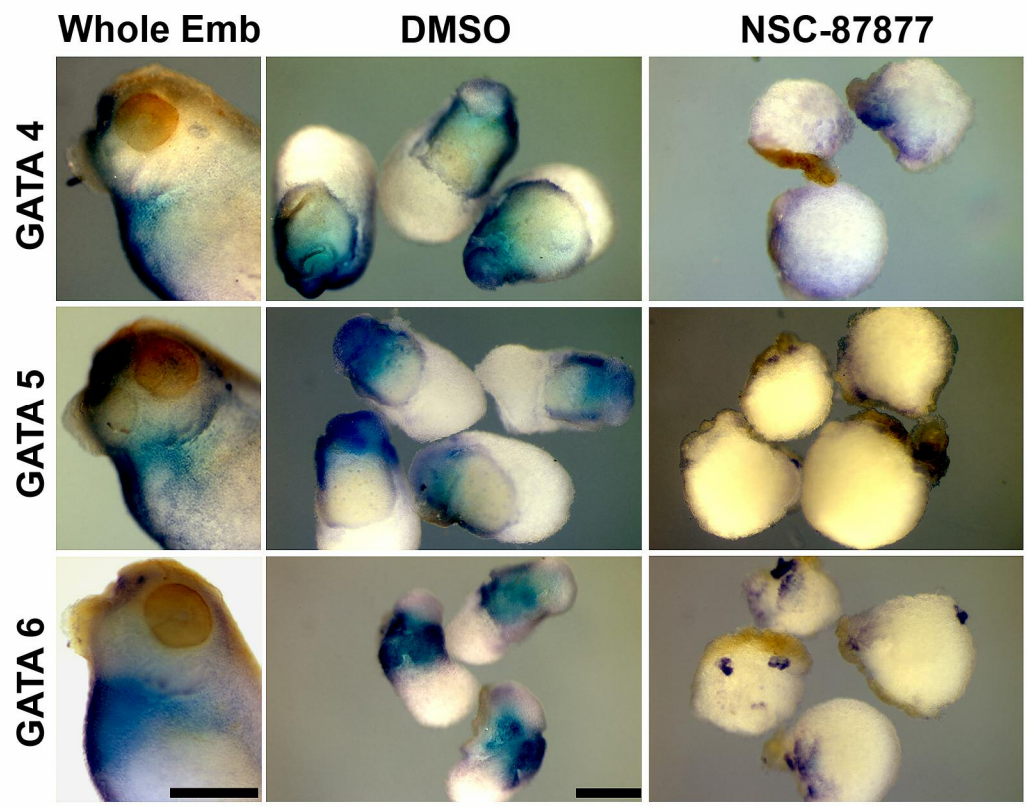

Figure 5.S2. *Gata 4, 5, and -6 expression is reduced in SHP-2 inhibited explants.*

Cardiac explants were isolated and cultured in DMSO or NSC-87877 beginning at stage 22. *In situ* hybridization was performed on explants with G*ata4, Gata5* and G*ata6*. (Scale bars = 0.5mm).

REFERENCES

Alexander, J., Rothenberg, M., Henry, G. L. and Stainier, D. Y. (1999). casanova plays an early and essential role in endoderm formation in zebrafish. *Dev Biol* **215**, 343-57.

Alexiades, M. R. and Cepko, C. (1996). Quantitative analysis of proliferation and cell cycle length during development of the rat retina. *Dev Dyn* **205**, 293-307.

Allanson, J. (2002). The first Noonan syndrome gene: PTPN11, which encodes the protein tyrosine phosphatase SHP-2. *Pediatr Res* **52**, 471.

Alsan, B. H. and Schultheiss, T. M. (2002). Regulation of avian cardiogenesis by Fgf8 signaling. *Development* **129**, 1935-43.

Araki, T., Mohi, M. G., Ismat, F. A., Bronson, R. T., Williams, I. R., Kutok, J. L., Yang, W., Pao, L. I., Gilliland, D. G., Epstein, J. A. et al. (2004). Mouse model of Noonan syndrome reveals cell type- and gene dosage-dependent effects of Ptpn11 mutation. *Nat Med* **10**, 849-57.

Bjorbaek, C., Buchholz, R. M., Davis, S. M., Bates, S. H., Pierroz, D. D., Gu, H., Neel, B. G., Myers, M. G., Jr. and Flier, J. S. (2001). Divergent roles of SHP-2 in ERK activation by leptin receptors. *J Biol Chem* **276**, 4747-55.

Brown, D. D., Binder, O., Pagratis, M., Parr, B. A. and Conlon, F. L. (2003). Developmental expression of the Xenopus laevis Tbx20 orthologue. *Dev Genes Evol* **212**, 604-7.

Chan, R. J., Li, Y., Hass, M. N., Walter, A., Voorhorst, C. S., Shelley, W. C., Yang, Z., Orschell, C. M. and Yoder, M. C. (2006). Shp-2 heterozygous hematopoietic stem cells have deficient repopulating ability due to diminished self-renewal. *Exp Hematol* **34**, 1230-9.

Chen, L., Sung, S. S., Yip, M. L., Lawrence, H. R., Ren, Y., Guida, W. C., Sebti, S. M., Lawrence, N. J. and Wu, J. (2006). Discovery of a novel shp2 protein tyrosine phosphatase inhibitor. *Mol Pharmacol* **70**, 562-70.

Costa, R. M., Mason, J., Lee, M., Amaya, E. and Zorn, A. M. (2003). Novel gene expression domains reveal early patterning of the Xenopus endoderm. *Gene Expr Patterns* **3**, 509-19.

Dale, L. and Slack, J. M. (1987). Fate map for the 32-cell stage of Xenopus laevis. *Development* **99**, 527-51.

Dasso, M. and Newport, J. W. (1990). Completion of DNA replication is monitored by a feedback system that controls the initiation of mitosis in vitro: studies in Xenopus. *Cell* **61**, 811-23.

Dehaan, R. L. (1963). Migration patterns of the precardiac mesoderm in the early chick embrvo. *Exp Cell Res* **29**, 544-60.

Digilio, M. C., Conti, E., Sarkozy, A., Mingarelli, R., Dottorini, T., Marino, B., Pizzuti, A. and Dallapiccola, B. (2002). Grouping of multiple-lentigines/LEOPARD and Noonan syndromes on the PTPN11 gene. *Am J Hum Genet* **71**, 389-94.

Dyer, M. A. and Cepko, C. L. (2001). Regulating proliferation during retinal development. *Nat Rev Neurosci* **2**, 333-42.

Feng, G. S. (1999). Shp-2 tyrosine phosphatase: signaling one cell or many. *Exp Cell Res* **253**, 47-54.

Fishman, M. C. and Chien, K. R. (1997). Fashioning the vertebrate heart: earliest embryonic decisions. *Development* **124**, 2099-2117.

Goetz, S. C., Brown, D. D. and Conlon, F. L. (2006). TBX5 is required for embryonic cardiac cell cycle progression. *Development* **133**, 2575-84.

Gove, C., Walmsley, M., Nijjar, S., Bertwistle, D., Guille, M., Partington, G., Bomford, A. and Patient, R. (1997). Over-expression of GATA-6 in Xenopus embryos blocks differentiation of heart precursors. *Embo J* **16**, 355-68.

Grossel, M. J. and Hinds, P. W. (2006). From cell cycle to differentiation: an expanding role for cdk6. *Cell Cycle* **5**, 266-70.

Guillemot, L., Levy, A., Zhao, Z. J., Bereziat, G. and Rothhut, B. (2000). The protein-tyrosine phosphatase SHP-2 is required during angiotensin II-mediated activation of cyclin D1 promoter in CHO-AT1A cells. *J Biol Chem* **275**, 26349-58.

Harland, R. M. (1991). In situ hybridization: an improved whole mount method for Xenopus embryos. *Meth. Cell Biol.* **36**, 675-685.

Harris, W. A. and Hartenstein, V. (1991). Neuronal determination without cell division in Xenopus embryos. *Neuron* **6**, 499-515.

Harvey, R. P., Lai, D., Elliott, D., Biben, C., Solloway, M., Prall, O., Stennard, F., Schindeler, A., Groves, N., Lavulo, L. et al. (2002). Homeodomain factor Nkx2-5 in heart development and disease. *Cold Spring Harb Symp Quant Biol* **67**, 107-14.

Hensey, C. and Gautier, J. (1998). Programmed cell death during Xenopus development: a spatio-temporal analysis. *Dev Biol* **203**, 36-48.

Horb, M. E. and Thomsen, G. H. (1999). Tbx5 is essential for heart development. *Development* **126**, 1739-1751.

House, S. L., Branch, K., Newman, G., Doetschman, T. and Schultz Jel, J. (2005). Cardioprotection induced by cardiac-specific overexpression of fibroblast growth factor-2 is mediated by the MAPK cascade. *Am J Physiol Heart Circ Physiol* **289**, H2167-75.

Inui, M. and Asashima, M. (2006). A novel gene, Ami is expressed in vascular tissue in Xenopus laevis. *Gene Expr Patterns* **6**, 613-9.

Ion, A., Tartaglia, M., Song, X., Kalidas, K., van der Burgt, I., Shaw, A. C., Ming, J. E., Zampino, G., Zackai, E. H., Dean, J. C. et al. (2002). Absence of PTPN11 mutations in 28 cases of cardiofaciocutaneous (CFC) syndrome. *Hum Genet* **111**, 421-7.

Jiang, Y. and Evans, T. (1996). The Xenopus GATA-4/5/6 genes are associated with cardiac specification and can regulate cardiac-specific transcription during embryogenesis. *Dev Biol* **174**, 258-70.

Jiang, Z. S., Padua, R. R., Ju, H., Doble, B. W., Jin, Y., Hao, J., Cattini, P. A., Dixon, I. M. and Kardami, E. (2002). Acute protection of ischemic heart by FGF-2: involvement of FGF-2 receptors and protein kinase C. *Am J Physiol Heart Circ Physiol* **282**, H1071-80.

Jiang, Z. S., Srisakuldee, W., Soulet, F., Bouche, G. and Kardami, E. (2004). Non-angiogenic FGF-2 protects the ischemic heart from injury, in the presence or absence of reperfusion. *Cardiovasc Res* **62**, 154-66.

Kattman, S. J., Huber, T. L. and Keller, G. M. (2006). Multipotent flk-1+ cardiovascular progenitor cells give rise to the cardiomyocyte, endothelial, and vascular smooth muscle lineages. *Dev Cell* **11**, 723-32.

Kolker, S., Tajchman, U. and Weeks, D. L. (2000). Confocal Imaging of early heat development in Xenopus laevis. *Dev. Biol.* **218**, 64-73.

Kouskoff, V., Lacaud, G., Schwantz, S., Fehling, H. J. and Keller, G. (2005). Sequential development of hematopoietic and cardiac mesoderm during embryonic stem cell differentiation. *Proc Natl Acad Sci U S A* **102**, 13170-5.

Kupperman, E., An, S., Osborne, N., Waldron, S. and Stainier, D. Y. (2000). A sphingosine-1-phosphate receptor regulates cell migration during vertebrate heart development. *Nature* **406**, 192-5.

Lathrop, B., Thomas, K. and Glaser, L. (1985). Control of myogenic differentiation by fibroblast growth factor is mediated by position in the G1 phase of the cell cycle. *J Cell Biol* **101**, 2194-8.

Legius, E., Schrander-Stumpel, C., Schollen, E., Pulles-Heintzberger, C., Gewillig, M. and Fryns, J. P. (2002). PTPN11 mutations in LEOPARD syndrome. *J Med Genet* **39**, 571-4.

Li, L. and Vaessin, H. (2000). Pan-neural Prospero terminates cell proliferation during Drosophila neurogenesis. *Genes Dev* **14**, 147-51.

Lu, X., Borchers, A. G., Jolicoeur, C., Rayburn, H., Baker, J. C. and Tessier-Lavigne, M. (2004). PTK7/CCK-4 is a novel regulator of planar cell polarity in vertebrates. *Nature* **430**, 93-8.

Maheshwari, M., Belmont, J., Fernbach, S., Ho, T., Molinari, L., Yakub, I., Yu, F., Combes, A., Towbin, J., Craigen, W. J. et al. (2002). PTPN11 mutations in Noonan syndrome type I: detection of recurrent mutations in exons 3 and 13. *Hum Mutat* **20**, 298-304.

Mason, H. S., Latten, M. J., Godoy, L. D., Horowitz, B. and Kenyon, J. L. (2002). Modulation of Kv1.5 currents by protein kinase A, tyrosine kinase, and protein tyrosine phosphatase requires an intact cytoskeleton. *Mol Pharmacol* **61**, 285-93.

Mills, K. R., Kruep, D. and Saha, M. S. (1999). Elucidating the origins of the vascular system: a fate map of the vascular endothelial and red blood cell lineages in Xenopus laevis. *Dev Biol* **209**, 352-68.

Molkentin, J. D., Lin, Q., Duncan, S. A. and Olson, E. N. (1997). Requirement of the transcription factor GATA4 for heart tube formation and ventral morphogenesis. *Genes Dev* **11**, 1061-72.

Moody, S. A. (1987). Fates of the blastomeres of the 32-cell-stage Xenopus embryo. *Dev Biol* **122**, 300-19.

Moretti, A., Caron, L., Nakano, A., Lam, J. T., Bernshausen, A., Chen, Y., Qyang, Y., Bu, L., Sasaki, M., Martin-Puig, S. et al. (2006). Multipotent embryonic isl1+ progenitor cells lead to cardiac, smooth muscle, and endothelial cell diversification. *Cell* **127**, 1151-65.

Nguyen, L., Besson, A., Roberts, J. M. and Guillemot, F. (2006). Coupling cell cycle exit, neuronal differentiation and migration in cortical neurogenesis. *Cell Cycle* **5**, 2314-8.

Nieuwkoop, P. D. and Faber, J. (1975). Normal Table of *Xenopus laevis* (Daudin). Amsterdam: North Holland.

Noonan, J. and O'Connor, W. (1996). Noonan syndrome: a clinical description emphasizing the cardiac findings. *Acta Paediatr Jpn* **38**, 76-83.

Palmen, M., Daemen, M. J., De Windt, L. J., Willems, J., Dassen, W. R., Heeneman, S., Zimmermann, R., Van Bilsen, M. and Doevendans, P. A. (2004). Fibroblast growth factor-1 improves cardiac functional recovery and enhances cell survival after ischemia and reperfusion: a fibroblast growth factor receptor, protein kinase C, and tyrosine kinase-dependent mechanism. *J Am Coll Cardiol* **44**, 1113-23.

Parmacek, M. S. and Epstein, J. A. (2005). Pursuing cardiac progenitors: regeneration redux. *Cell* **120**, 295-8.

Pasumarthi, K. B. and Field, L. J. (2002). Cardiomyocyte cell cycle regulation. *Circ Res* **90**, 1044-54.

Pawson, T. (1994). Tyrosine kinase signalling pathways. *Princess Takamatsu Symp* **24**, 303-22.

Qu, C. K. (2000). The SHP-2 tyrosine phosphatase: signaling mechanisms and biological functions. *Cell Res* **10**, 279-88.

Raffin, M., Leong, L. M., Rones, M. S., Sparrow, D., Mohun, T. and Mercola, M. (2000). Subdivision of the cardiac Nkx2.5 expression domain into myogenic and nonmyogenic compartments. *Dev Biol* **218**, 326-40.

Reiter, J. F., Alexander, J., Rodaway, A., Yelon, D., Patient, R., Holder, N. and Stainier, D. Y. (1999). Gata5 is required for the development of the heart and endoderm in zebrafish. *Genes Dev* **13**, 2983-95.

Saga, Y., Miyagawa-Tomita, S., Takagi, A., Kitajima, S., Miyazaki, J. and Inoue, T. (1999). MesP1 is expressed in the heart precursor cells and required for the formation of a single heart tube. *Development* **126**, 3437-47.

Sater, A. K. and Jacobson, A. G. (1989). The specification of heart mesoderm occurs during gastrulation in Xenopus laevis. *Development* **105**, 821-30.

Schollen, E., Matthijs, G., Gewillig, M., Fryns, J. P. and Legius, E. (2003). PTPN11 mutation in a large family with Noonan syndrome and dizygous twinning. *Eur J Hum Genet* **11**, 85-8.

Smith, J. C. and Slack, J. M. W. (1983). Dorsalization and neural induction: properties of the organizer in *Xenopus laevis*. *J. Embryol. Exp. Morph.* **78**, 299-317.

Srivastava, D. (2006). Making or breaking the heart: from lineage determination to morphogenesis. *Cell* **126**, 1037-48.

Tang, T. L., Freeman, R. M., Jr., O'Reilly, A. M., Neel, B. G. and Sokol, S. Y. (1995). The SH2-containing protein-tyrosine phosphatase SH-PTP2 is required upstream of MAP kinase for early Xenopus development. *Cell* **80**, 473-83.

Tartaglia, M., Kalidas, K., Shaw, A., Song, X., Musat, D. L., van der Burgt, I., Brunner, H. G., Bertola, D. R., Crosby, A., Ion, A. et al. (2002). PTPN11 mutations in Noonan syndrome: molecular spectrum, genotype-phenotype correlation, and phenotypic heterogeneity. *Am J Hum Genet* **70**, 1555-63.

Tartaglia, M., Mehler, E. L., Goldberg, R., Zampino, G., Brunner, H. G., Kremer, H., van der Burgt, I., Crosby, A. H., Ion, A., Jeffery, S. et al. (2001). Mutations in PTPN11, encoding the protein tyrosine phosphatase SHP-2, cause Noonan syndrome. *Nat Genet* **29**, 465-8.

Tonissen, K. F., Drysdale, T. A., Lints, T. J., Harvey, R. P. and Krieg, P. A. (1994). XNkx-2.5, a Xenopus gene related to Nkx-2.5 and tinman: evidence for a conserved role in cardiac development. *Dev. Biol.* **162**, 325-328.

Trinh, L. A. and Stainier, D. Y. (2004). Fibronectin regulates epithelial organization during myocardial migration in zebrafish. *Dev Cell* **6**, 371-82.

van den Hoff, M. J., Kruithof, B. P. and Moorman, A. F. (2004). Making more heart muscle. *Bioessays* **26**, 248-61.

Van Vactor, D., O'Reilly, A. M. and Neel, B. G. (1998). Genetic analysis of protein tyrosine phosphatases. *Curr Opin Genet Dev* **8**, 112-26.

Vernon, A. E. and Philpott, A. (2003). A single cdk inhibitor, p27Xic1, functions beyond cell cycle regulation to promote muscle differentiation in Xenopus. *Development* **130**, 71-83.

Walsh, K. and Perlman, H. (1997). Cell cycle exit upon myogenic differentiation. *Curr Opin Genet Dev* **7**, 597-602.

Warkman, A. S. and Krieg, P. A. (2006). Xenopus as a model system for vertebrate heart development. *Semin Cell Dev Biol*.

Wu, S. M., Fujiwara, Y., Cibulsky, S. M., Clapham, D. E., Lien, C. L., Schultheiss, T. M. and Orkin, S. H. (2006). Developmental origin of a bipotential myocardial and smooth muscle cell precursor in the mammalian heart. *Cell* **127**, 1137-50.

Yang, W., Klaman, L. D., Chen, B., Araki, T., Harada, H., Thomas, S. M., George, E. L. and Neel, B. G. (2006). An Shp2/SFK/Ras/Erk Signaling Pathway Controls Trophoblast Stem Cell Survival. *Developmental Cell* **10**, 317-327.

Yuan, L., Yu, W. M. and Qu, C. K. (2003). DNA damage-induced G2/M checkpoint in SV40 large T antigen-immortalized embryonic fibroblast cells requires SHP-2 tyrosine phosphatase. *J Biol Chem* **278**, 42812-20.

Yuan, L., Yu, W. M., Xu, M. and Qu, C. K. (2005). SHP-2 phosphatase regulates DNA damage-induced apoptosis and G2/M arrest in catalytically dependent and independent manners, respectively. *J Biol Chem* **280**, 42701-6.

Zhang, J., Somani, A. K. and Siminovitch, K. A. (2000). Roles of the SHP-1 tyrosine phosphatase in the negative regulation of cell signalling. *Semin Immunol* **12**, 361-78.

CHAPTER 6

Conclusions and Future Directions

The tissue-specific regulation of cell proliferation plays a crucial role in organogenesis during development. However, the mechanisms by which this is achieved are not yet well understood. The work presented in this dissertation begins to address this problem in the developing heart by 1) examining the requirement for the transcription factor TBX5 in cardiac morphogenesis, and identifying a role for TBX5 in promoting cardiac cell cycle progression; and 2) characterizing the requirement for the protein tyrosine phosphatase SHP2 in the maintenance of proliferating cardiac progenitors during early cardiac development.

Cardiac cell cycle progression and morphogenesis

In Chapters 2 and 3, I describe the morphological abnormalities that arise in the developing heart as the result of depletion of the T-box transcription factors TBX5 and TBX20. We observed that in embryos lacking TBX5 or TBX20, the hearts are reduced in size and contain fewer cardiac cells. However, early cardiac genes, as well as markers of cardiac differentiation are expressed normally, indicating that cardiac precursors are properly specified and able to undergo terminal differentiation in the absence of TBX5 or TBX20. We have provided the first evidence that TBX20 is required for vertebrate heart

development, as well as showing that *Xenopus* embryos lacking TBX5 display a cardiac phenotype similar to that observed in the mouse (Bruneau et al., 2001), thus demonstrating that the function of TBX5 is conserved between vertebrates. The precise cellular functions of TBX5 and TBX20 have not been defined, however. Few direct transcriptional targets in the heart have been identified for either protein. Those that have been identified include *Atrial naturitic factor* (*ANF*) in the case of TBX5 (Bruneau et al., 2001); and *Tbx2* and possibly *N-myc* in the case of TBX20 (Cai et al., 2005).

The reduced number of cardiac cells that we observed both in hearts lacking TBX5 and TBX20 led us to hypothesize that these proteins are required for cell proliferation within the heart. A subsequent study of TBX20 performed in the mouse revealed that TBX20 promotes proliferation within the chamber myocardium by repressing *Tbx2* (Cai et al., 2005). TBX2 normally functions to inhibit cell cycle progression in the non-chamber myocardium by repressing *N-Myc*, a transcription factor that promotes cell proliferation within the heart. In addition to relieving repression of *N-myc* by TBX2, TBX20 has also been shown to activate transcription of *N-myc* in *in vitro* transcriptional assays, suggesting that *N-myc* may also be a target of TBX20. Thus, TBX20 acts as a positive regulator of cell cycle progression within the heart (Cai et al., 2005).

We have tested this hypothesis with respect to TBX5 in Chapter 4. Our detailed analysis of the defects resulting from depletion of TBX5 from *Xenopus* embryos has revealed that cardiac cells fail to progress through S phase of the cell cycle in the absence of TBX5. This suggests that, like TBX20, TBX5 promotes cardiac cell proliferation in the specific regions of the heart where it is expressed. In this way, TBX5 is required to establish of proper cardiac morphology during development. In addition, we have also shown that

depletion of TBX5 leads to a mis-regulation in the timing of cardiac differentiation, which is also likely to contribute to the cardiac abnormalities observed in these embryos.

Mutations to *Tbx5* in humans have been associated with the congenital heart disorder Holt-Oram Syndrome (Basson et al., 1997; Li et al., 1997). The identification of a requirement for TBX5 in cardiac cell cycle progression can therefore provide important insight into the cellular basis for this human disease. However, the precise molecular mechanism by which TBX5 functions to promote cell proliferation within the developing heart awaits characterization.

The maintenance of proliferating progenitor cells during early cardiogenesis

A mechanism by which proliferating cardiac progenitor cells are maintained in the developing heart is explored in Chapter 5. While it is known that cardiac progenitor cells are induced and maintained during early development by signals including members of the FGF, BMP, and WNT families (Zaffran and Frasch, 2002), the exact requirement for these signals, especially in promoting the survival of cardiac progenitor cells, has not been well established. In this work, we show that the activity SHP-2, a protein tyrosine phosphatase that functions downstream of receptor tyrosine kinases such as FGFR (Reviewed in (Ostman et al., 2006)), is required for the survival of cardiac progenitor cells.

We have found that treatment of cardiac explants with the SHP-2 inhibitor NSC-87877 beginning at the early neurula stage (stage 22) results in the progressive down-regulation of early cardiac markers, and a failure of cardiac differentiation due to programmed cell death. Treatment of cardiac explants with the SHP-2 inhibitor beginning at the late tailbud stage (stage 29) however, results in a much less severe cardiac phenotype,

with cardiac tissue able to undergo terminal differentiation. Examination of cardiac cell proliferation revealed that the mitotic index in SHP-2 inhibited explants from stage 29 is reduced to approximately half of that observed in controls, indicating that proliferating cardiac cells require SHP-2 for their maintenance.

At early stages of vertebrate heart development, nearly all cardiac cells are proliferating (Pasumarthi and Field, 2002), and these cells undergo programmed cell death in the absence of SHP-2 activity. As cardiomyocytes begin to undergo differentiation, an increasing number of cells exit the cell cycle. Thus, when cardiac explants are treated with the SHP-2 inhibitor beginning at stage 29, a much smaller subset of cells is affected than when treatment begins at stage 22. This suggests that SHP-2 signaling is required specifically for the survival of proliferating cardiac cells. We further show that SHP-2 likely functions primarily downstream of FGF signaling to promote cardiac cell survival.

The identification of factors required for the expansion and survival of proliferating cardiac progenitor cells is of considerable importance both to our understanding of cardiac development, as well as to the generation of therapies for human cardiac diseases during adulthood. Recently, several populations of multipotent cardiac progenitor cells have been identified, in both embryonic and neonatal mammalian hearts. The culture of these cells following isolation from the heart requires the presence of growth factors, as the cells must be cultured in the presence of other cardiac cells or in dense clonal colonies in order to survive and proliferate (Laugwitz et al., 2005; Moretti et al., 2006; Wu et al., 2006). The nature of the required growth factors has not been determined, however, our experiments point to a requirement for FGF/SHP-2/MAPK signaling in the survival of proliferating cardiac cells.

Future Directions

TBX5 and heart development

A goal of this project in the immediate future is to further characterize the pathway in which TBX5 functions to regulate the cardiac cell cycle in *Xenopus*. We hypothesize that TBX5 is required for cell cycle progression non cell-autonomously. To address this, we will inject *Xenopus* embryos in one of two blastomeres at the two-cell stage with the TBX5 Morpholinos and fluorescent dextran. This will allow us to determine if only the cardiac cells directly depleted of TBX5 undergo reduced cell proliferation, or whether proliferation is also reduced in cardiac cells not depleted of TBX5. If the effect is non-cell autonomous, this will imply that the requirement for TBX5 in cardiac cell proliferation is indirect, with TBX5 perhaps acting upstream of growth factors to promote cell cycle progression. If the requirement for TBX5 is cell autonomous, this would imply that TBX5 might directly regulate the transcription of genes required for G1/S transition, such as D and E cyclins, or Cdks 2, 4, and 6, within the developing heart.

Ultimately, the goal of this project is to identify direct transcriptional targets for TBX5. In this way, we hope to gain further insight into the requirement for TBX5 in cell cycle progression, as well as to identify additional cellular requirements for TBX5. Currently, a number of promising approaches towards this goal are being undertaken by others in the lab. These include the purification of TBX5 protein to produce an antibody, and the development of a proteomics-based screen to identify cardiac-specific binding partners of TBX5. The production of an antibody will allow us to perform chromatin immunoprecipitation to identify *in vivo* sites at which TBX5 is bound to the DNA. With the

sequencing of the *Xenopus tropicalis* genome, genes located in reasonable proximity to these binding sites can be further examined as potential transcriptional targets of TBX5.

As the specificity of many transcription factors is regulated, at least in part, by interaction with different binding partners, it is also of critical importance to identify additional proteins that interact with TBX5. Thus, we are also taking a proteomics-based approach to identify proteins that interact with TBX5 within the heart. His-tagged TBX5 purified in bacteria is bound to a nickel column, and lysate either from adult heart tissue, or *Xenopus tropicalis* embryos is then put over the column. TBX5 and any proteins bound to it are then eluted, and interacting proteins can be identified by mass spectroscopy. By identifying proteins that interact with TBX5 we can potentially identify additional cellular functions for TBX5, as well as gain further insight into the regulation of TBX5 during heart development.

Finally, we plan to identify upstream regulators of *Tbx5* expression. Our previous results have implied that expression of *Tbx5* is itself dependent on the cell cycle. Inhibiting the cell cycle using either aphidicolin or colchicine results in loss of expression of *Tbx5* and other early cardiac genes, but does not affect cardiac differentiation. We therefore hypothesize that, in addition to the role of TBX5 in positively regulating cell cycle progression in the heart, expression of *Tbx5* is in turn regulated by the signaling pathways that control cell proliferation. To test this, we have cloned the promoter region of *Tbx5*, and are presently taking a transgenic approach to identify the minimal region of the *Tbx5* promoter sufficient to drive expression of a GFP transgene within the developing *Xenopus* heart. Once we identify this minimal promoter element, we will make use of available databases and genome sequences to identify putative transcription factor binding sites in this

element that are evolutionarily conserved. We can then mutate these binding sites to determine whether they are required for expression of the Tbx5::GFP transgene *in vivo*. In addition, we will also perform transcriptional assays to determine whether the transcription factors that bind to these sites can drive expression of a Tbx5::luciferase reporter *in vitro*. Initially, we will focus our analysis of putative upstream regulators of *Tbx5* on transcription factors known to regulate cell cycle progression.

Growth factors required for cardiac progenitor survival and expansion

Having identified a requirement for the protein tyrosine phosphatase SHP-2 in the survival of cardiac progenitor cells, we next plan to further characterize the pathway(s) in which SHP-2 functions during early heart development. While we have shown that SHP-2 functions downstream of the FGF pathway to regulate cardiac cell survival, we hypothesize that SHP-2 may be regulated by additional upstream pathways at different stage of development. Previous studies have shown that both the phosphorylation of SHP-2 at its C terminus, and its interaction with specific scaffolding and adaptor molecules are characteristic of the particular receptor tyrosine kinase functioning upstream of SHP-2. For example, SHP-2 is phosphorylated at Y542 and Y580 downstream of FGF and PDGF signaling, but not downstream EGF or IGF (Araki et al., 2004). In addition, SHP-2 interacts with the adaptor protein FRS-2 only downstream of FGFR and IGFR activation (Delahaye et al., 2000; Kontaridis et al., 2002; Xu et al., 1998). Thus, by studying the phosphorylation status of SHP-2, and also which binding partners it associates with, we can gain information about which pathways are acting upstream of SHP-2 in a particular cell type. We have shown that SHP-2 is phosphorylated at Y542 and Y580 and that it interacts with FRS-2 during early

cardiac looping stages of heart development. We therefore plan to assess both the phosphorylation state of SHP-2 and interaction with FRS-2 throughout the course of cardiac development, to begin to determine whether SHP-2 might be regulated differently, or activated downstream of different pathways as heart development progresses.

Another approach to characterizing the pathway or pathways in which SHP-2 functions to promote cardiac cell survival is to perform an expression screen to identify factors that are able to compensate for the loss of SHP-2 activity. To do this, pooled RNAs will be generated from a neurula stage cDNA library, and injected into one-cell stage embryos. Explants will then be cut from these embryos at the mid-neurula stage, and cultured in the presence of the SHP-2 inhibitor NSC-87877. The use of a line of cardiac actin::GFP transgenic frogs enables us to rapidly assess whether a particular RNA pool can rescue the failure of cardiac differentiation that results from SHP-2 inhibition. In this way, we can identify proteins required downstream of SHP-2 for the survival cardiac cells. This will allow us to obtain critical insight into the molecular mechanisms by which the maintenance and proliferation of cardiac progenitor cells are regulated during development.

References

Araki, T., Mohi, M. G., Ismat, F. A., Bronson, R. T., Williams, I. R., Kutok, J. L., Yang, W., Pao, L. I., Gilliland, D. G., Epstein, J. A. et al. (2004). Mouse model of Noonan syndrome reveals cell type- and gene dosage-dependent effects of Ptpn11 mutation. *Nat Med* **10**, 849-57.

Basson, C. T., Bachinsky, D. R., Lin, R. C., Levi, T., Elkins, J. A., Soults, J., Grayzel, D., Kroumpouzou, E., Traill, T. A., Leblanc-Straceski, J. et al. (1997). Mutations in human TBX5 [corrected] cause limb and cardiac malformation in Holt-Oram syndrome. *Nat Genet* **15**, 30-5.

Bruneau, B. G., Nemer, G., Schmitt, J. P., Charron, F., Robitaille, L., Caron, S., Conner, D. A., Gessler, M., Nemer, M., Seidman, C. E. et al. (2001). A murine model of Holt-Oram syndrome defines roles of the T-box transcription factor Tbx5 in cardiogenesis and disease. *Cell* **106**, 709-21.

Cai, C. L., Zhou, W., Yang, L., Bu, L., Qyang, Y., Zhang, X., Li, X., Rosenfeld, M. G., Chen, J. and Evans, S. (2005). T-box genes coordinate regional rates of proliferation and regional specification during cardiogenesis. *Development* **132**, 2475-87.

Delahaye, L., Rocchi, S. and Van Obberghen, E. (2000). Potential involvement of FRS2 in insulin signaling. *Endocrinology* **141**, 621-8.

Kontaridis, M. I., Liu, X., Zhang, L. and Bennett, A. M. (2002). Role of SHP-2 in fibroblast growth factor receptor-mediated suppression of myogenesis in C2C12 myoblasts. *Mol Cell Biol* **22**, 3875-91.

Laugwitz, K. L., Moretti, A., Lam, J., Gruber, P., Chen, Y., Woodard, S., Lin, L. Z., Cai, C. L., Lu, M. M., Reth, M. et al. (2005). Postnatal isl1+ cardioblasts enter fully differentiated cardiomyocyte lineages. *Nature* **433**, 647-53.

Li, Q. Y., Newbury-Ecob, R. A., Terrett, J. A., Wilson, D. I., Curtis, A. R., Yi, C. H., Gebuhr, T., Bullen, P. J., Robson, S. C., Strachan, T. et al. (1997). Holt-Oram syndrome is caused by mutations in TBX5, a member of the Brachyury (T) gene family. *Nat Genet* **15**, 21-9.

Moretti, A., Caron, L., Nakano, A., Lam, J. T., Bernshausen, A., Chen, Y., Qyang, Y., Bu, L., Sasaki, M., Martin-Puig, S. et al. (2006). Multipotent embryonic isl1+ progenitor cells lead to cardiac, smooth muscle, and endothelial cell diversification. *Cell* **127**, 1151-65.

Ostman, A., Hellberg, C. and Bohmer, F. D. (2006). Protein-tyrosine phosphatases and cancer. *Nat Rev Cancer* **6**, 307-20.

Pasumarthi, K. B. and Field, L. J. (2002). Cardiomyocyte cell cycle regulation. *Circ Res* **90**, 1044-54.
Wu, S. M., Fujiwara, Y., Cibulsky, S. M., Clapham, D. E., Lien, C. L., Schultheiss, T. M. and Orkin, S. H. (2006). Developmental origin of a bipotential myocardial and smooth muscle cell precursor in the mammalian heart. *Cell* **127**, 1137-50.

Xu, H., Lee, K. W. and Goldfarb, M. (1998). Novel recognition motif on fibroblast growth factor receptor mediates direct association and activation of SNT adapter proteins. *J Biol Chem* **273**, 17987-90.

Zaffran, S. and Frasch, M. (2002). Early signals in cardiac development. *Circ Res* **91**, 457-69.